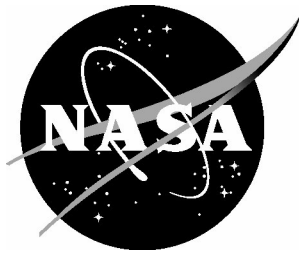


NASA/CR-2014-218284
NIA Report No. 2014-0619



Finite Element Analysis of Composite Joint Configurations With Gaps and Overlaps

Ronald Krueger
National Institute of Aerospace, Hampton, Virginia

NASA STI Program . . . in Profile

Since its founding, NASA has been dedicated to the advancement of aeronautics and space science. The NASA scientific and technical information (STI) program plays a key part in helping NASA maintain this important role.

The NASA STI program operates under the auspices of the Agency Chief Information Officer. It collects, organizes, provides for archiving, and disseminates NASA's STI. The NASA STI program provides access to the NASA Aeronautics and Space Database and its public interface, the NASA Technical Report Server, thus providing one of the largest collections of aeronautical and space science STI in the world. Results are published in both non-NASA channels and by NASA in the NASA STI Report Series, which includes the following report types:

- **TECHNICAL PUBLICATION.** Reports of completed research or a major significant phase of research that present the results of NASA Programs and include extensive data or theoretical analysis. Includes compilations of significant scientific and technical data and information deemed to be of continuing reference value. NASA counterpart of peer-reviewed formal professional papers, but having less stringent limitations on manuscript length and extent of graphic presentations.
- **TECHNICAL MEMORANDUM.** Scientific and technical findings that are preliminary or of specialized interest, e.g., quick release reports, working papers, and bibliographies that contain minimal annotation. Does not contain extensive analysis.
- **CONTRACTOR REPORT.** Scientific and technical findings by NASA-sponsored contractors and grantees.

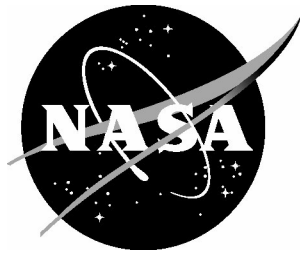
- **CONFERENCE PUBLICATION.** Collected papers from scientific and technical conferences, symposia, seminars, or other meetings sponsored or co-sponsored by NASA.
- **SPECIAL PUBLICATION.** Scientific, technical, or historical information from NASA programs, projects, and missions, often concerned with subjects having substantial public interest.
- **TECHNICAL TRANSLATION.** English-language translations of foreign scientific and technical material pertinent to NASA's mission.

Specialized services also include organizing and publishing research results, distributing specialized research announcements and feeds, providing information desk and personal search support, and enabling data exchange services.

For more information about the NASA STI program, see the following:

- Access the NASA STI program home page at <http://www.sti.nasa.gov>
- E-mail your question to help@sti.nasa.gov
- Fax your question to the NASA STI Information Desk at 443-757-5803
- Phone the NASA STI Information Desk at 443-757-5802
- Write to:
STI Information Desk
NASA Center for AeroSpace Information
7115 Standard Drive
Hanover, MD 21076-1320

NASA/CR-2014-218284
NIA Report No. 2014-0619



Analysis of Joint Configurations With Gaps and Overlaps

Ronald Krueger
National Institute of Aerospace, Hampton, Virginia

National Aeronautics and
Space Administration

Langley Research Center
Hampton, Virginia 23681-2199

Prepared for Langley Research Center
under Contract NNL09AA00A

June 2014

Trade names and trademarks are used in this report for identification only. Their usage does not constitute an official endorsement, either expressed or implied, by the National Aeronautics and Space Administration.

Available from:

NASA Center for AeroSpace Information
7115 Standard Drive
Hanover, MD 21076-1320
443-757-5802

FINITE ELEMENT ANALYSIS OF COMPOSITE JOINT CONFIGURATIONS WITH GAPS AND OVERLAPS

Ronald Krueger*

National Institute of Aerospace
NASA Langley Research Center, Hampton, VA, USA

ABSTRACT

The goal of the current study is to identify scenarios for which thermal and moisture effects become significant in the loading of a composite structure. In the current work, a simple configuration was defined, and material properties were selected. A Fortran routine was created to automate the mesh generation process. The routine was used to create the models for the initial mesh refinement study. A combination of element length and width suitable for further studies was identified. Also, the effect of the overlap length and gap length on computed shear and through-thickness stresses along the bondline of the joints was studied for the mechanical load case. Further, the influence of neighboring gaps and overlaps on these joint stresses was studied and was found to be negligible. The results suggest that for an initial study it is sufficient to focus on one configuration with fixed overlap and gap lengths to study the effects of mechanical, thermal and moisture loading and combinations thereof on computed joint stresses.

NOMENCLATURE

c	Length of resin gap in joint
E_{ii}	Young's modulus
G_{ij}	Shear modulus
G_{Ic}	Mode I fracture toughness
G_{IIc}	Mode II fracture toughness
h	Ply thickness
t	Model/specimen thickness
T_g	Glass transition temperature
T_0	Stress free temperature
$T_{0,dry}$	Stress free temperature, dry
$T_{0,wet}$	Stress free temperature, wet
α_i	Coefficient of thermal expansion
β_i	Coefficient of moisture expansion (swelling coeff.)
δ	Length of overlap in joint
γ_{ij}	Shear strains

* R. Krueger, National Institute of Aerospace, 100 Exploration Way, Hampton, VA, 23666. This work was performed at the Durability, Damage Tolerance and Reliability Branch, MS 188E, NASA Langley Research Center, Hampton, VA, 23681, USA

ϵ_{ii}	Normal strains
η	Exponent of B-K failure criterion
ν_{ij}	Poisson's ratio
ρ	Density (specific weight)
σ_{ii}	Normal stresses
τ_{ij}	Shear stresses

BACKGROUND

Environmental factors that affect the performance of composite laminates include temperature, moisture content and hygrothermal history. Early studies showed that residual stress relaxation due to hygrothermal history altered the static mechanical strain necessary to cause matrix cracking in experiments [1]. Depending on material type and hygrothermal history, this effect was shown to either increase or decrease the resistance to matrix cracking. Matrix crack growth in laminates subjected to creep load and severe environments may require the development of viscoelastic failure criteria [1]. The viscoelastic response of laminated composites under the influence of mechanical and hygrothermal loads was studied analytically [2]. Application of the analysis included the effect of residual thermal stress relaxation upon creep in laminated composite plates under mechanically applied loads [3]. Generalized plane-strain finite elements were also formulated using linear viscoelastic theory. Analyses of changes in interlaminar stresses at the free edge of multidirectional laminates subjected to cyclic load conditions indicated that several variables can affect peak amplitude in interlaminar stresses and cycle-to-cycle variations in stress state. These influencing parameters were determined to be frequency, stress ratio, relative dwell time and environment [4].

PROBLEM OVERVIEW

An overview of a scenario where combined mechanical and thermal load effects become significant was discussed in detail in reference 1 and is presented in Figure 1. For the pure elastic case, the transverse residual stress in the ply is tensile and the stresses increase as the temperature drops from the stress free temperature $T_{0,dry}$ to an ambient value (see dashed red line along path ① → ②). During moisture absorption, the transverse residual stress drops and may become compression (see dashed red line along path ②). An increase in temperature will increase the compressive stress (see dashed black line along path ③). The stress increases during moisture desorption (see dashed black line along path ④) and the cycle starts from the beginning (see dashed red line along path ①). A stress relaxation, however, may occur caused by accelerated viscoelastic effects due to an increase in temperature and moisture content (see solid red line along path ③'). As the temperature drops, the tensile transverse residual stress continues to increase beyond the original residual tensile stress (see solid red line path along ⑤) [1]. For the viscoelastic case, therefore, the presence of the thermal load could make the stresses worse due to the effect of the previous creep.

These combined thermal and moisture effects may become significant in the loading of a composite fuselage structure where several individual components are connected with longitudinal joints, as shown in Figure 2. Since airframe manufacturers have recently become interested in joint configurations, which may be designed with multiple overlaps and resin gaps as shown in Figure 3, it has become important to understand the stresses at the bondline. Overlap length, δ , and resin gap size, c , shown in Figure 3a may also vary. As the overlap length, δ , approaches zero ($\delta \rightarrow 0$) the design resembles the traditional splice joint, as shown in Figure 3b.

The current study, therefore aims at identifying scenarios where thermal and moisture effects become significant in the loading of a composite structure. Linear and geometrically non-linear finite element analyses of simple and more complex examples are required first, to study the single and combined effects of mechanical, thermal and hygral loading on the computed strains and stresses. The results from this initial study of simple specimens and load scenarios will be used as guidance to define the next steps. These next steps may include additional analysis of more complex specimens under different load combinations and more advanced viscoelastic analysis, as well as testing.

The focus of the present work was to study the effect of overlap length and gap length on shear and through-thickness stresses along the bondline of staggered overlap joints using linear and geometrically non-linear finite element analyses. First, the material properties obtained from the literature are discussed. Second, the selected specimen configuration is introduced. Third, the finite element analysis is described, including a Fortran routine that was created to quickly generate two- and three-dimensional models of different configurations of interest. Fourth, the results of an initial mesh refinement study are discussed for the mechanical load case. Fifth, the effects of the overlap length and gap length on computed shear and through-thickness stresses at the bondline are examined. A summary and outlook for future steps are provided. The description of the Fortran routine and the required user input, as well as an Abaqus/Standard[®] input deck, are given in the appendix.

MATERIAL DATA

For the current study, material data for carbon/epoxy IM7/8552 were used since it is a commonly used material in the aerospace industry. Elastic constants, cure temperature and hygrothermal expansion coefficients for this material were collected from data available in the open literature [5-20]. Details about the data gathered are discussed in appendix A. A recent discussion indicated that the stress free temperature may actually be higher than published T_g values [21, 22]. However, this may be process dependent and may require a separate investigation and separate material characterization. Additional material characterization may also become necessary to generate constants required as input data for viscoelastic finite element analysis.

SELECTED CONFIGURATION

A simple configuration to study the effects of overlap (δ) and gap (c) lengths on overlap stresses is shown in Figure 4. This configuration represents the idealized local section of an overlap bounded by adjacent plies representative of the center section of a specimen. It is based on prior experience with similar analyses [21, 22]. For this simple configuration, a layup of $[45, 90, -45, 0]_S$ was considered, where the center 0° plies were overlapped [23]. An overlap length, δ , varying between 6.35 mm and 63.5 mm and a gap size, c , varying between 1.27 mm and 12.7 mm were proposed [23]. These dimensions are of interest to the aerospace industry based on manufacturing considerations for advanced tooling and hand-layup tolerances [22-23]. For modeling purposes, boundary conditions were considered such that the section is constrained at one end ($u=v=0$) and displacements ($u=const.$) are applied at the other, thereby approximating tensile loading commonly applied to such joints. This model was used first to perform a mesh refinement study to determine the degree of refinement adequate to capture the stress gradients in the overlap region as discussed later. Second, an investigation of the effects of changing the dimensions δ and c in the range

mentioned above were investigated. Two-dimensional plane-strain models were used first for linear and geometrically non-linear finite element analysis.

A more complex configuration with 16 plies $[45, 90, -45, 0]_{2s}$ and several staggered overlaps and gaps is shown in Figure 5. This configuration may be investigated at a later point including three-dimensional finite element analysis as well as specimen manufacturing and testing. Details of the specimen configuration such as layup, length and width would be defined after a successful study of the simple configuration shown in Figure 4.

ANALYSIS

Finite element modeling

The commercial finite element software Abaqus/Standard[®] [24] was used to analyze the mechanical load cases and is capable of handling the thermal, moisture and combined load cases as well. For the current study only two-dimensional analyses were performed using higher order plane-stress CPS8 solid elements to model the specimen.

For more advanced analysis, a quasi-static procedure in Abaqus/Standard[®] may be used to analyze viscoelastic material and two-layer viscoplastic material behavior. The quasi-static procedure can also be used to analyze quasi-static creep and swelling problems, which occur over fairly long time periods (rate-dependent plasticity: creep and swelling).

Fortran routine for automatic mesh generation

A FORTRAN routine was developed that will automatically create an Abaqus/Standard[®] [24] input deck (.inp file) and thus simplify the variation in dimensions and mesh size for specimen types of interest. Specimen dimensions and material data including ply orientation and stacking sequence are provided by the user in a simple data file that is read by the routine at the beginning of the execution. Gaps are modeled by using the resin material properties in the respective regions of the finite element mesh. Examples of two-dimensional models of specimen types that can be created are shown in Figure 6. The mesh density in the thickness direction and locally in the length direction can easily be changed, which allows for mesh refinement and convergence studies. Different geometries of interest can also be generated such as a single lap-shear specimen shown in Figure 6b - 6d or a double lap-shear specimen as shown in Figure 6e. By changing the Abaqus/Standard[®] element type and specifying additional input parameters for the third dimension, the meshes shown in Figures 7 can easily be created. An example mesh for the single lap-shear specimen is shown in Figure 7a. In addition to changing the mesh density in the thickness direction and locally in the length direction, the routine also allows mesh refinement across the width of the specimen as shown in Figure 7b for the example of a double lap-shear specimen. The desired input for mechanical loads and boundary conditions can also be generated automatically as shown in Figure 8. An example of the prescribed displacements and fixed boundary conditions is shown in Figure 8a. Appropriate Abaqus/Standard[®] input for the thermal and moisture distributions, which are represented as fields, can also be generated. Currently only constant fields over the entire domain, as shown in Figures 8b and c, can be automatically generated. The details of the routine and a brief guide on its use are provided in appendix B. An example for user input is also provided together with a Abaqus/Standard[®] input file that was created using the routine.

Generalized plane-strain approach

Several assumptions are possible when using two-dimensional finite element models. A plane-stress model enforces the out-of-plane *stresses* to be zero ($\sigma_{zz}=\tau_{xz}=\tau_{yz}=0$) and allows the displacement to be the free parameter. The plane-strain model, on the other hand, enforces the out-of-plane *strains* to be zero ($\epsilon_{zz}=\gamma_{xz}=\gamma_{yz}=0$), which excessively constrains the plies. The effect is most marked for 45° plies because of their high in-plane Poisson's ratio, while it is small for 0° and 90° plies. Hence, the two dimensional plane-stress and plane-strain conditions may serve as upper and lower limits compared to the three-dimensional solution [25].

A different approach to account for three-dimensional width effects was suggested in reference 26 such that modified material properties are entered in a two-dimensional model to create a generalized plane-strain case. The generalized plane-strain case is regarded as an intermediate state between plane-strain and plane-stress, and assumes that the out-of-plane normal strain $\epsilon_{zz}=-\nu_L\epsilon_{xx}$, where ν_L is the laminate Poisson's ratio, and the shear strain $\gamma_{xz}=\gamma_{yz}=0$. With these assumptions, ply stiffnesses were calculated for each ply angle in the specimen and entered as material properties for the two-dimensional plane-stress models. Calculated properties are listed in Table II.

Application of load and boundary conditions

The load and boundary conditions shown in Figures 4 and 8 were used to simulate a region that is part of a larger section but would also mimic the condition of a test specimen clamped in hydraulic grips with applied constant displacement. The displacement was applied to the model such that the specimen was subjected to an axial tensile strain $\epsilon_{xx}=0.01$. It was planned to apply a constant temperature over the entire specimen (as shown in Figure 8b) and use the difference between cure and room temperature ($\Delta T=157$ K) as input. For the moisture loading, a constant moisture distribution over the specimen was assumed (as shown in Figure 8c) to avoid the calculation of moisture diffusion through the thickness at this point. A literature study suggests that 1% increase in mass or weight due to moisture absorption is a reasonable assumption to simulate a saturated condition in the specimen [27-28].

Current finite element model

The configuration selected earlier (shown in Figure 4a) was used for mesh refinement studies. For this first set of analyses, an overlap length of $\delta=25.4$ mm and a gap length of $c=2.54$ mm were chosen. Abaqus/Standard® plane-stress CPS8 solid elements were used to model a section that was $3\delta=76.2$ mm long, as shown in Figure 9a. A local displacement $u=0.762$ mm (0.03") was applied at the left edge of the model to simulate an axial strain $\epsilon_{xx}=0.01$ in the section, modeled as shown in Figure 9b. The right edges of the section were fixed as shown in Figure 9c. The detail of the area of interest is shown in Figure 10 where the gap is modeled as a region $c=2.54$ mm (0.1") with resin properties. The element length, Δx , shown in Figure 10b was varied during the refinement study. The paths defined in Abaqus/Standard® along which the stresses were computed (results shown later) were also included in Figure 10b (light blue lines). Due to a change in material properties, the computed stresses differ from one side of the path to the other when crossing the interface between plies. Therefore, stresses had to be computed for both sides of an interface for the same path, as shown in Figures 10c and d.

The mesh refinement study was performed to determine the mesh required for subsequent analysis. Meshes were refined locally in the length and thickness directions as shown in Figure 11. A selection of local meshes used in the area of interest are shown in Figure 11. The element length Δx

was varied between $\Delta x=0.847\text{mm}$ for the initial coarse mesh, shown in Figure 11b, and $\Delta x=0.026\text{mm}$ for the most refined mesh, shown in Figure 11e. Simultaneously, the element height Δy was varied between $\Delta y=0.15\text{mm}$ (one ply thickness) for the initial coarse mesh shown in Figure 11b and $\Delta y=0.025\text{mm}$ for the most refined mesh, shown in Figure 11e.

The element length and height combinations modeled were:

- $\Delta x=0.847\text{mm}$, $\Delta y=0.15\text{mm}$ – Figure 11b
- $\Delta x=0.423\text{mm}$, $\Delta y=0.075\text{mm}$ – Figure 11c
- $\Delta x=0.212\text{mm}$, $\Delta y=0.05\text{mm}$
- $\Delta x=0.106\text{mm}$, $\Delta y=0.0375\text{mm}$ – Figure 11d
- $\Delta x=0.053\text{mm}$, $\Delta y=0.03\text{mm}$
- $\Delta x=0.026\text{mm}$, $\Delta y=0.025\text{mm}$ – Figure 11e

Based on the results of the mesh refinement study (discussed in the next section) element dimensions $\Delta x=0.026\text{mm}$ and $\Delta y=0.025\text{mm}$ were chosen for the remainder of the study. To determine the effects of overlap length, δ , and a gap length, c , three additional configurations were studied:

- $\delta=25.4\text{ mm}$, $c=1.27\text{ mm}$
- $\delta=25.4\text{ mm}$, $c=12.7\text{ mm}$
- $\delta=6.35\text{ mm}$, $c=2.54\text{ mm}$

Another model was created to simulate the case of multiple overlaps and gaps. The overlap length of $\delta=25.4\text{ mm}$ and a gap length of $c=2.54$ were held fixed but two additional overlaps and gaps were added to the configuration as shown in Figure 12 to study if the presence of neighboring overlaps and gaps had a major effect on the results calculated for the initial 0° overlap in the center. A minimal influence of neighboring overlaps and gaps would indicate that, for a preliminary study, it is sufficient to study the effects of mechanical, thermal and moisture load on a simple configuration with one overlap, as shown in Figure 4a.

ANALYSIS RESULTS

Mesh refinement study

Computed deformation

The deformed finite element model is shown in Figure 13 for an applied displacement $u=0.762\text{ mm}$ which was used to simulate an axial tensile strain $\epsilon_{xx}=0.01$. The deformation of the entire section is shown in Figure 13a where the undeformed outline is depicted as a dashed line. The local deformations shown in Figures 13b to 13e correspond to the refined meshes shown previously in Figures 11b to 11e. The results suggest that a refinement through the thickness may also be required to capture the local deformation in the -45° ply above the resin region.

Computed stresses

Stresses were plotted along the pre-defined paths shown in Figure 10. Due to a change in material properties, the computed stresses differ on the sides of the path when crossing the interface between plies. Therefore, stresses were always plotted for both sides of an interface for the same path. For

the current study, the focus is on the shear stresses τ_{xy} and the through-thickness stresses σ_{yy} plotted on both interfaces along path 2. Path 2 was selected because the axial load, which is carried in the individual 0° plies, is transferred via shear along the overlap and therefore high stresses are expected in this region. However, further investigation is necessary to determine whether the stress along paths 1 and 3 could become critical under certain load conditions [21, 22].

The computed shear stresses τ_{xy} and through-thickness stresses σ_{yy} along path 2 are plotted in Figures 14 through 17. The results indicate that refined meshes are required to fully capture the steep stress gradient in the vicinity of the overlap. The zone of computed high stresses and gradients is small and extends to about 2.5 to 3 mm on either side of the juncture of the resin zone and the terminated 0° ply ($x=2.54$ mm). Farther away from this location, coarser meshes yield the same results as fine meshes. Shear stresses τ_{xy} quickly drop to zero as expected, as shown in Figures 14 and 16. The through-thickness stresses σ_{yy} reach a constant value outside this region, as shown in Figures 15 and 17. Based on these results, element dimensions $\Delta x=0.026$ mm and $\Delta y=0.025$ mm were chosen for the remainder of the study for the resin gap and the zone of peak stresses. Larger elements were used in the area where constant stresses were observed. For the current study, only trends were monitored and computed stress values were not compared to any failure stress as suggested in references 21 and 22.

Computed stresses for linear and geometric non-linear analysis

A comparison between stresses computed from geometrically non-linear analysis and results obtained from linear analysis are shown in Figures 18 through 21. Except for the through-thickness stresses, σ_{yy} , along the upper interface of path 2 (shown in Figure 19), the results follow the same trend and are in excellent agreement. The through-thickness stresses σ_{yy} in the top 0° ply computed from the geometrically non-linear analysis decrease close to the 0° ply/resin boundary (green crosses) while the results from linear analysis sharply increase (red Xs). Away from the 0° ply/resin boundary, both results are in excellent agreement with each other. This discrepancy requires further investigation. However, based on the excellent agreement at all other locations, it was decided to use linear analysis for the remainder of the study since it allows simple superposition of results.

Effects of overlap and gap lengths on computed bondline stresses

To determine the effects of overlap length, δ , and gap length, c , additional configurations were analyzed. The individual results for computed shear stresses τ_{xy} and through-thickness stresses σ_{yy} along path 2 are plotted in Figures 22 through 37. The left edge of the resin pocket was chosen as the $x=0$ location for all plots as above. The results confirm that to the right of the 0° ply/resin boundary and to the left of the 45° ply/resin boundary ($x<0$) the computed shear stresses τ_{xy} decrease to zero and the through-thickness stresses σ_{yy} reach a constant value over a short distance, x . The study therefore focused on the results at the zone near the 0° ply/resin boundary where the computed stresses have the highest values, as suggested in references 21 and 22.

A comparison between stresses from all configurations is shown in Figures 38 through 41. The 0° ply/resin boundary was chosen as the $x=0$ location for the plots so that all stress profiles could be combined in one graph for comparison. The computed shear stresses τ_{xy} shown in Figures 38 and 40 are in excellent agreement for all configurations considered. Varying the overlap length, δ , and gap length, c , did not affect the results. The computed through-thickness stresses σ_{yy} plotted in Figures 39 and 41 exhibit some sensitivity, in particular for the small values of the overlap length, δ . For the short overlap length, some transverse deflection of the specimen was observed which may

cause the difference in computed through-thickness stresses σ_{yy} . This difference requires further investigation. Nevertheless, the results suggest that for an initial study, it is sufficient to focus on one configuration with a fixed overlap length, δ , and a gap length, c , to study the effects of mechanical, thermal and moisture loading and combinations thereof which is in agreement with previous findings [21, 22].

SUMMARY

The objective of the current study was to identify scenarios in which thermal and moisture effects become significant in the loading of a composite structure. In the current work, a simple configuration was defined, and material properties were selected. A Fortran routine was created to automate the mesh generation process. The routine was used to create the models for the initial mesh refinement study. A combination of element length and width suitable for further studies was identified. Also the effect of the overlap length and gap length on computed stresses at the overlap interface and resin gap was studied for the mechanical load case. Further, the influence of neighboring gaps and overlaps on the results was studied and was found to be negligible. The results suggest that for an initial study, it is sufficient to focus on one configuration with a fixed overlap length and a gap length to study the effects of mechanical, thermal and moisture loading and combinations thereof on overlap stresses. A user guide and example input values, as well as a listing of an Abaqus/Standard[®] input file, are provided in the appendix.

FUTURE STEPS

With a configuration selected, the mesh refinement study complete, and a critical area identified, the study now needs to focus on identifying scenarios where thermal and moisture effects become significant in the loading of a composite structure. Linear and geometrically non-linear finite element analyses need to be carried out to study the effects of

1. Mechanical load only
2. Thermal load only
3. Moisture only
4. Combination of mechanical load + moisture
5. Combination of mechanical load + thermal load
6. Combination of thermal load + moisture
7. Combination of all three load cases

Depending on the results of the initial analyses, more advanced analyses may be required. These analyses may include

- Viscoelastic analysis to determine where the stress can be additive
- Time dependent material properties
- More complex example geometries
- Specific structural geometries and load histories that have been identified to be a potential problem.

The specimen configurations to be manufactured and tested, as well as the test matrix, should be decided upon after the successful completion of the proposed analyses.

ACKNOWLEDGEMENTS

This work was performed under Interagency Agreement IA1-1093, DTFACT-10-X-00009 between the Federal Aviation Administration and the National Aeronautics and Space Administration. Lynn Pham (FAA) served as the technical monitor.

The author would like to thank James Reeder, Isabelle Paris and D.M. Hoyt for their input and valuable discussions.

REFERENCES

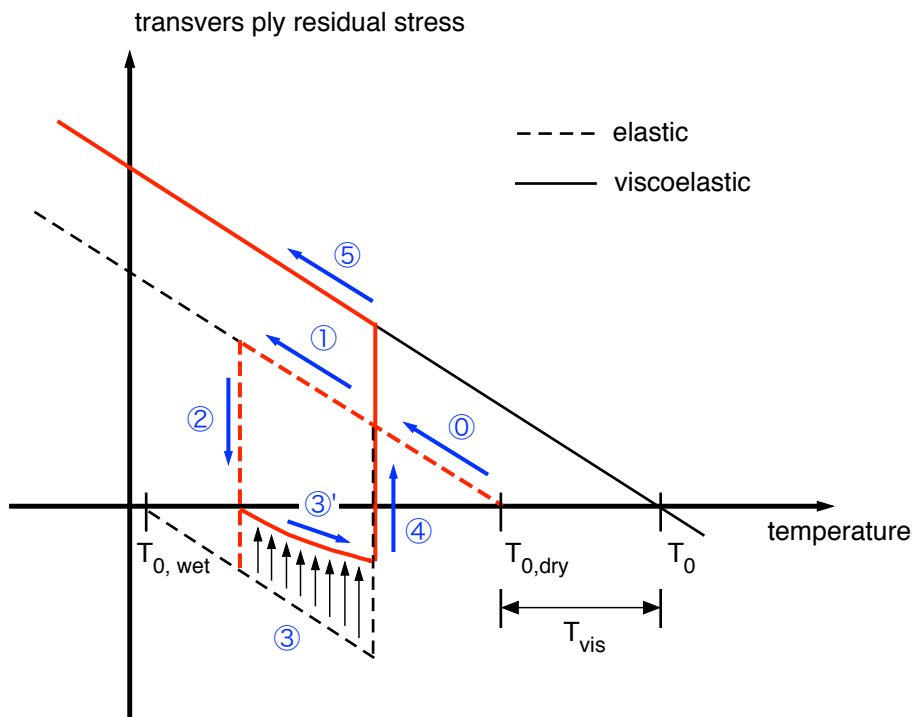
- [1] R. J. ROTHSCILDS, L. B. ILCEWICZ, P. NORDIN, and S. H. APPLGATE, "The Effect of Hygrothermal Histories on Matrix Cracking in Fiber Reinforced Laminates," *Journal of Engineering Materials and Technology*, Vol. 110, pp. 158-168, 1988.
- [2] K. Y. LIN and S. YI, "Analysis of Interlaminar Stresses in Viscoelastic Composites," *International Journal of Solids and Structures*, Vol. 27, pp. 929-945, 1991.
- [3] D. L. FLAGGS and F. W. CROSSMAN, "Analysis of the Viscoelastic Response of Composite Laminates During Hygrothermal Exposure," *Journal of Composite Materials*, Vol. 15, pp. 21-40, 1981.
- [4] K. Y. LIN, I. H. HWANG, and L. B. ILCEWICZ, "History Dependent Free Edge Stresses in Composites," in *Composite Material Design and Characterization*, pp. 517-526.
- [5] R. KRUEGER, J. G. RATCLIFFE, and P. J. MINGUET, "Analysis of Composite Panel-Stiffener Debonding Using A Shell/3D Modeling Technique," Hampton, VA, NASA/CR-2007-214879, 2007.
- [6] R. KRUEGER, "Application of Benchmark Examples to Assess the Single and Mixed-Mode Static Delamination Propagation Capabilities in ANSYS," NASA/CR-2012-217588, 2012.
- [7] P. P. CAMANHO, P. MIAMI, and C. G. DAVILA, "Prediction of Size Effects in Notched Laminates Using Continuum Damage Mechanics," *Composites Science and Technology*, vol. 67, pp. 2715-2727, 2007.
- [8] KADDOUR, HINTON, LI, SMITH, "Instructions to Contributions of the Third World-Wide Failure Exercise (WWFE-III), Part (A)," February 2008.
- [9] *Mil-Hdbk-17F*, Vol. 2, 2002. (Hexcel IM7/8552 Prepreg, IM7G 12k/8552 UD tape)
- [10] Hexel Data Sheet, HexPly[®] 8852 (Hexcel HexPly[®] 8852 UD Carbon Prepreg, IM7 fiber)
- [11] *Polymer Matrix Composites: Material Properties, Composite Materials Handbook (CMH-17), Volume 2*, 2012. (Hexcel IM7/8552 Prepreg, IM7G 12k/8552 UD tape)
- [12] Hexcel 8552, IM7 Unidirectional Prepreg, 190gsm & 35% RC – Qualification Material Property Data Report, NIAR – Wichita State University, CAM-RP-2009-015 Rev A, 2011.
- [13] Hexcel 8552 IM7 Unidirectional Prepreg, 190gsm & 35% RC – Qualification Statistical Analysis Report, NIAR – Wichita State University, CAM-RP-2009-028 Rev N/C, 2011.
- [14] STEVEN HALLET, personal communication (most likely generic carbon/epoxy data).
- [15] ABDUL ARAFAT, personal communication (AS4/8552 carbon/epoxy data).
- [16] T. K. O'BRIEN, I. S. RAJU, and D. P. GARBER, "Residual Thermal and Moisture Influences on the Strain Energy Release Rate Analysis of Edge Delaminations," *Journal of Composites Technology & Research*, Vol. 8, pp. 37-47, 1986.
- [17] T. K. O'BRIEN, "Residual Thermal and Moisture Influences on the Analysis of Local Delaminations," *Journal of Composites Technology & Research*, Vol. 14, pp. 86-94, 1992.
- [18] S. W. TSAI, *Theory of Composite Design*, Think Composites, 1992.
- [19] S. W. TSAI and H. T. HAHN, *Introduction to Composite Materials*, Technomic Publishing Co., Inc., 1980.
- [20] OSULaminates, Java Application for laminated plate theory analysis, written and documented by John A. Nairn, Version 2.1, 2007.
- [21] D.M. HOYT, NSE Composites, personal communication.
- [22] I.L. PARIS, Bombardier, personal communication.
- [23] L. ILCEWICZ, FAA, personal communication.
- [24] Abaqus/Standard[®] 6.12 User's Manual, Dassault Systèmes Simulia Corporation, Providence, RI, USA, 2012.
- [25] R. KRUEGER, I. L. PARIS, T. K. O'BRIEN, and P. J. MINGUET, "Comparison of 2D Finite Element Modeling Assumptions with Results from 3D Analysis for Composite Skin-Stiffener Debonding," *Composite Structures*, vol. 57, pp. 161-168, 2002.
- [26] D. M. HOYT, S. H. WARD, and P. J. MINGUET, "Strength and Fatigue Life Modeling of Bonded Joints in Composite Structure," *Journal of Composite Technology and Research*, vol. 24, pp. 190-210, 2002.
- [27] D. S. CAIRNS and D. F. ADAMS, "Moisture and Thermal Expansion of Composite Materials," University of Wyoming UWME-DR-101-104-1, 1981.
- [28] *Polymer Matrix Composites: Guidelines for Characterization of Structural Materials, Composite Materials Handbook (CMH-17) Volume 1*, SAE International, 2012

TABLE I. MATERIAL PROPERTIES USED FOR CURRENT STUDY

IM7/8552 Unidirectional Graphite/Epoxy Prepreg fiber volume approximately 60%, ply thickness $h=0.15$ mm		
$E_{11} = 161$ GPa	$E_{22} = 11.38$ GPa	$E_{33} = 11.38$ GPa
$\nu_{12} = 0.32$	$\nu_{13} = 0.32$	$\nu_{23} = 0.45$
$G_{12} = 5.2$ GPa	$G_{13} = 5.2$ GPa	$G_{23} = 3.9$ GPa
Glass transition temperature		
$T_{g,dry} = 177$ °C	$T_{g,wet} = 143$ °C	
Coefficients of thermal expansion		
$\alpha_1 = -9 \cdot 10^{-7}$ 1/°C	$\alpha_2 = 2.88 \cdot 10^{-5}$ 1/°C	$\alpha_3 = 2.88 \cdot 10^{-5}$ 1/°C
Coefficients of moisture expansion		
$\beta_1 = 0.0$ 1/%M	$\beta_2 = 3310 \cdot 10^{-6}$ 1/%M	

TABLE II. MATERIAL PROPERTIES USED FOR 2D FE ANALYSES

IM7/8552 Unidirectional Graphite/Epoxy Prepreg, ply thickness $h=0.15$ mm Input properties calculated using Minguet's generalized plane-strain approach [27]		
0° - ply		
$E_{11} = 161$ GPa	$E_{22} = 14.39$ GPa	$G_{12} = 5.2$ GPa
$\nu_{12} = 0.467$		
90° - ply		
$E_{11} = 9.81$ GPa	$E_{22} = 12.42$ GPa	$G_{12} = 3.9$ GPa
$\nu_{12} = 0.461$		
$\pm 45^\circ$ - ply		
$E_{11} = 32.4$ GPa	$E_{22} = 13.8$ GPa	$G_{12} = 4.55$ GPa
$\nu_{12} = 0.464$		



- ① Initial transverse residual stress is tensile
- ① Transverse residual stress increases as temperature drops to an ambient value
- ② Transverse residual stress drops due to moisture absorption and becomes compressive
- ③ Compressive stress increases as temperatures increases
- ③' Stress relaxation caused by accelerated viscoelastic effects due to increase in temperature and moisture content
- ④ Desorption of moisture
- ⑤ A drop in temperature results in an increase in original tensile residual stress

Figure 1. A schematic diagram of viscoelastic changes in the stress free temperature due to environmental history [1].

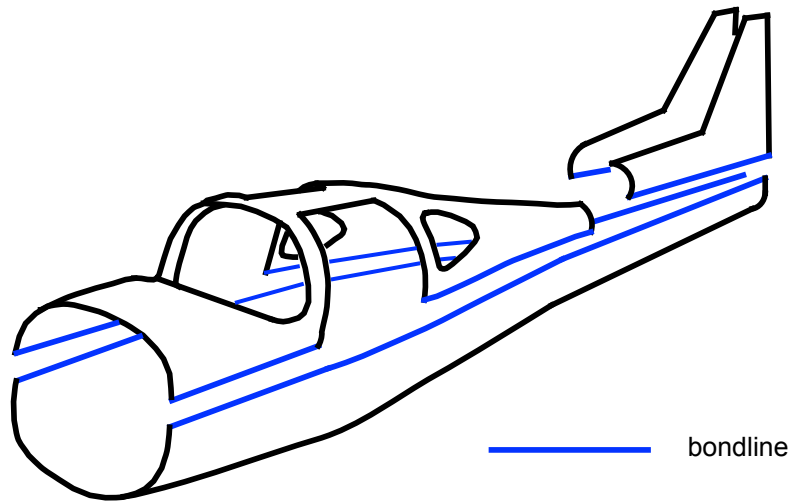
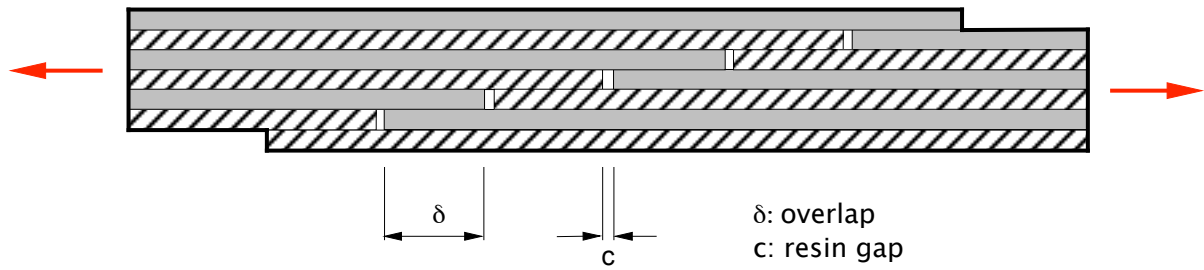
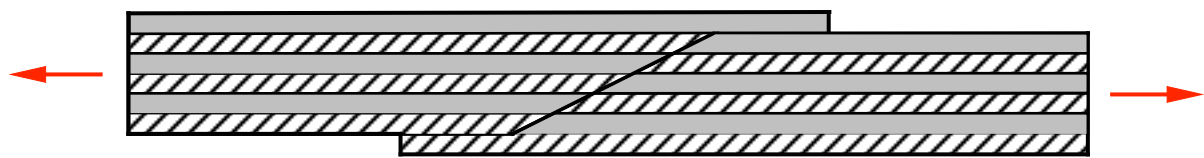


Figure 2. *Fuselage components with longitudinal joints.*



a. *Staggering of overlaps.*



as $\delta \rightarrow 0$, splice joint

b. *Splice joint.*

Figure 3. *Joint configurations with overlaps and gaps.*

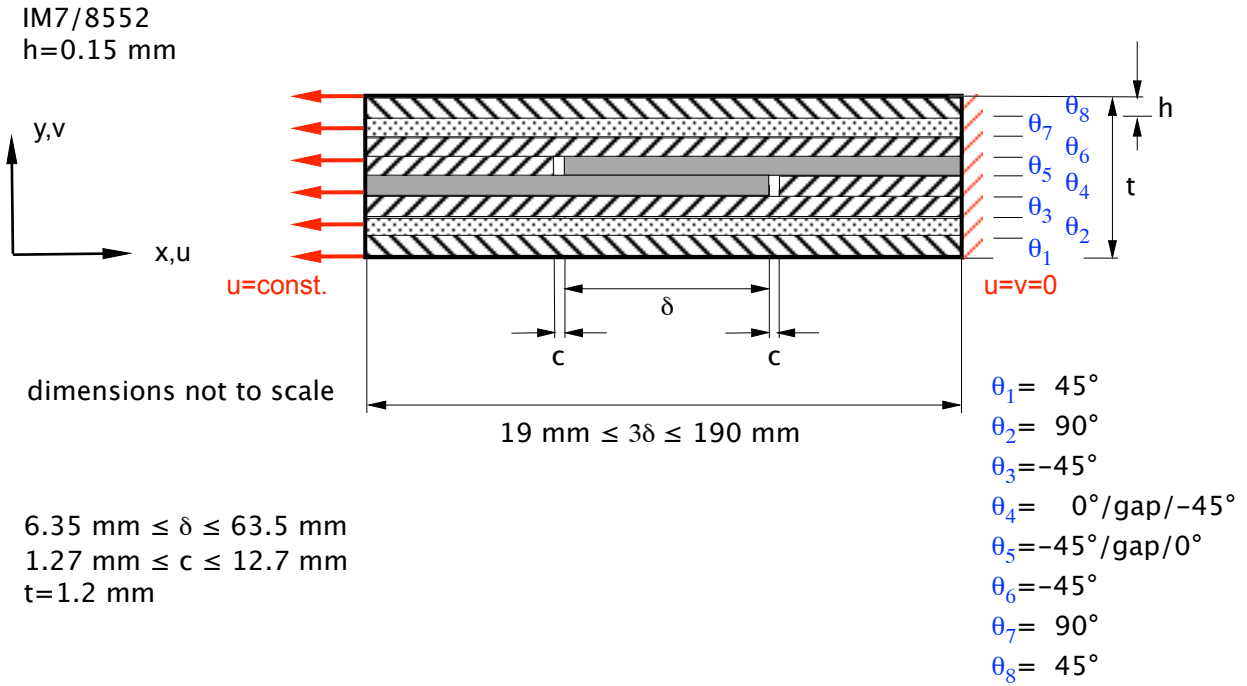


Figure 4. Simple configuration to study the effects of overlap and gap lengths and perform mesh refinement.

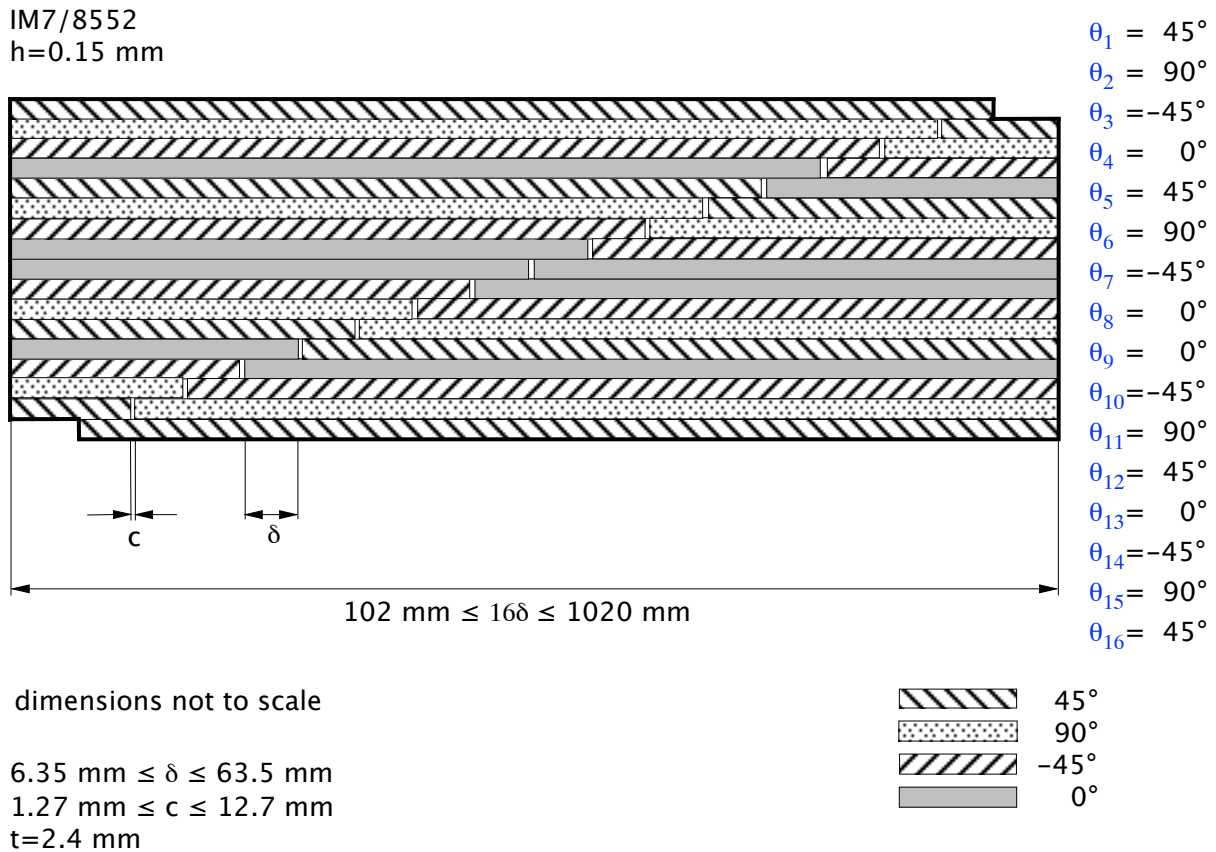
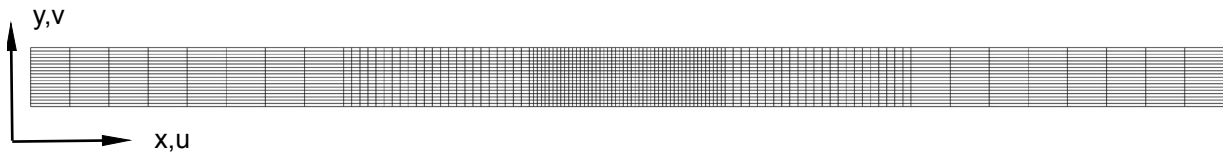
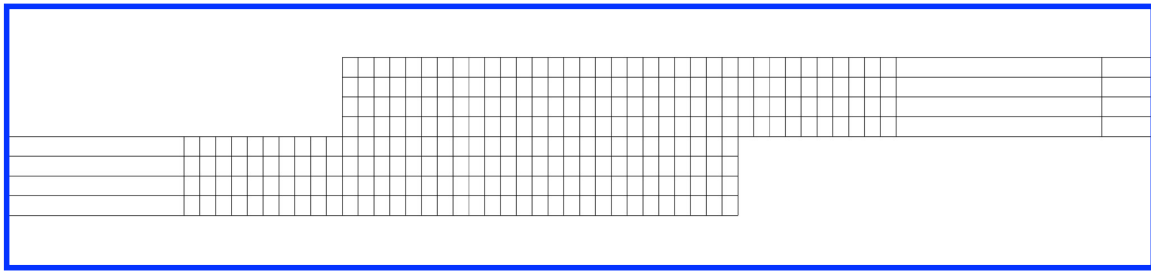
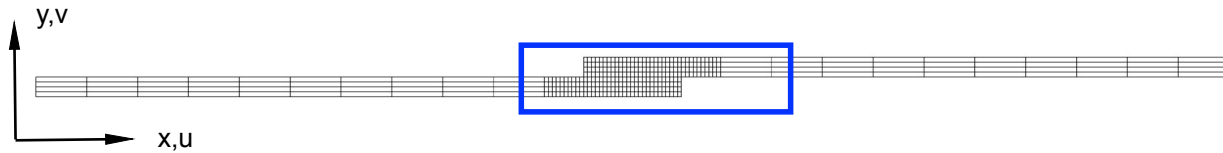


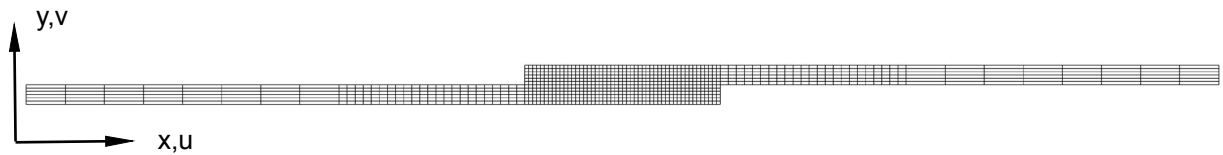
Figure 5. More complex configuration of staggered overlaps and gaps.



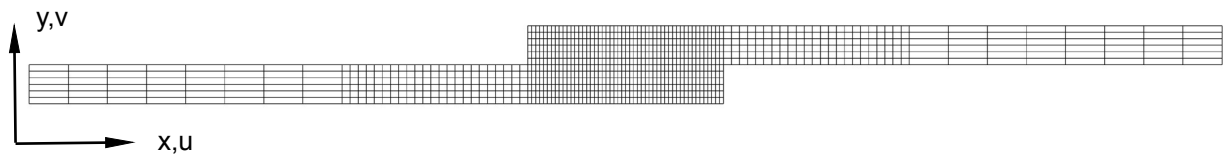
a. Mesh for initial study of configurations in Figures 4 and 5.



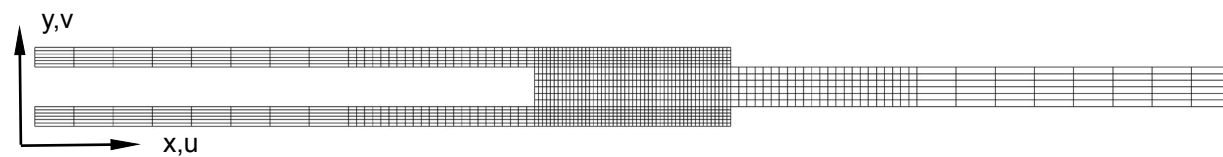
b. Single lap-shear specimen.



c. Single lap-shear specimen with increased overlap.

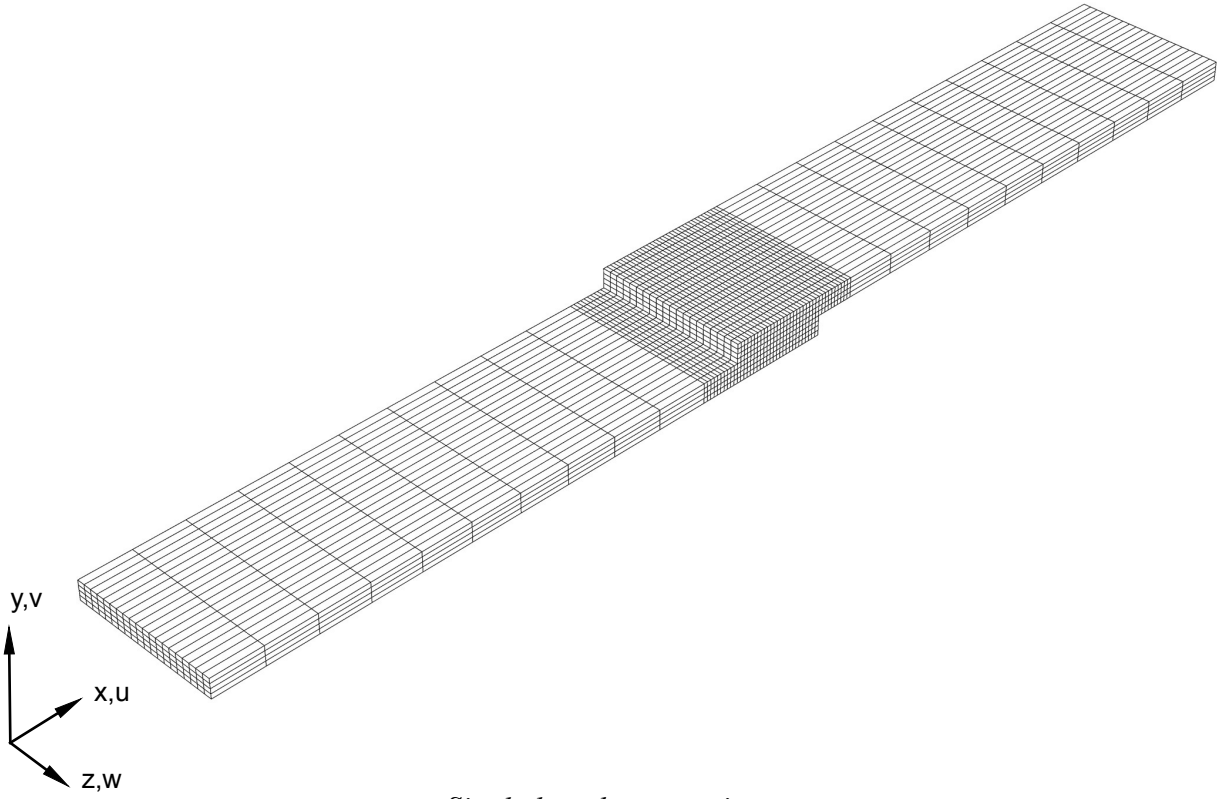


d. Single lap-shear specimen with increased arm thickness.

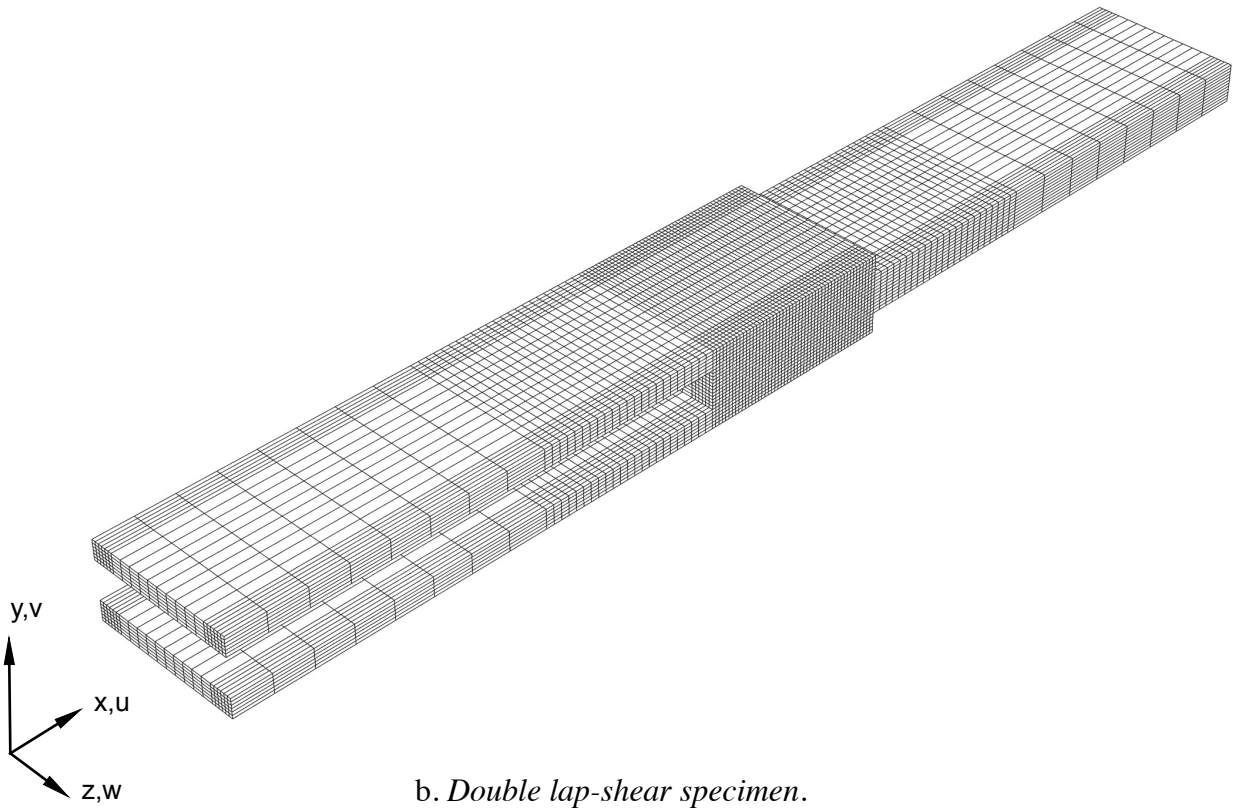


e. Double lap-shear specimen.

Figure 6. Two-dimensional finite element models created by FORTRAN routine.

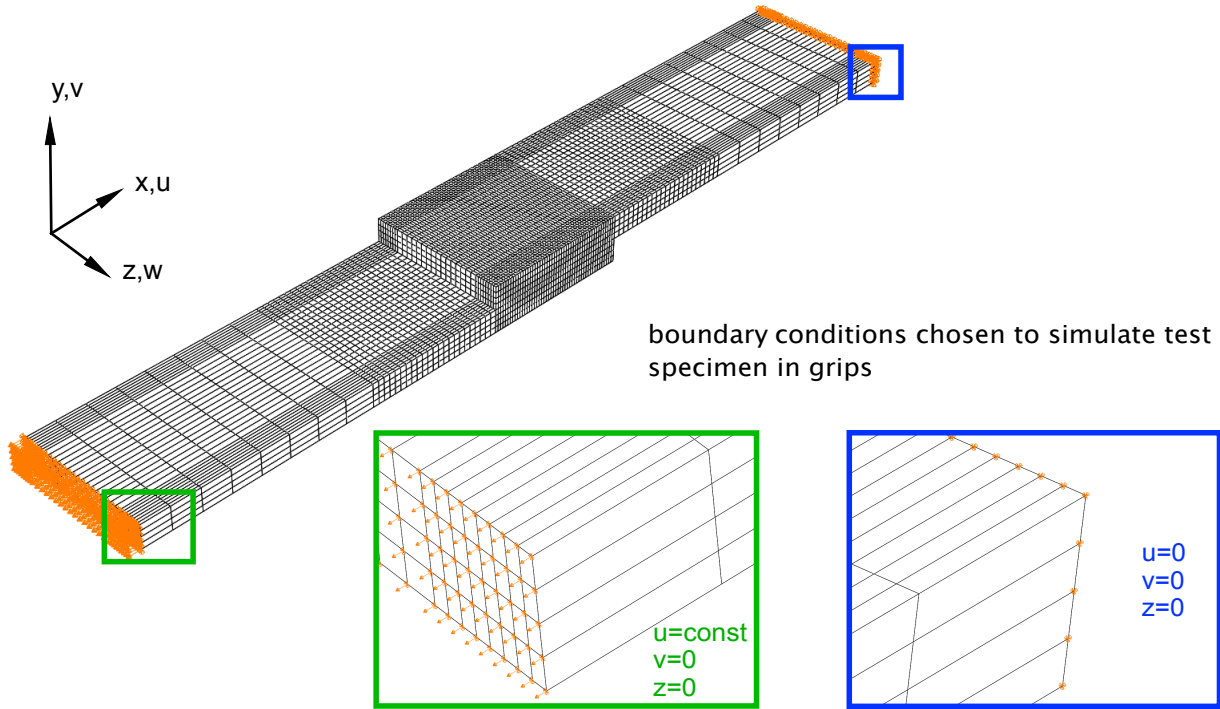


a. *Single lap-shear specimen.*

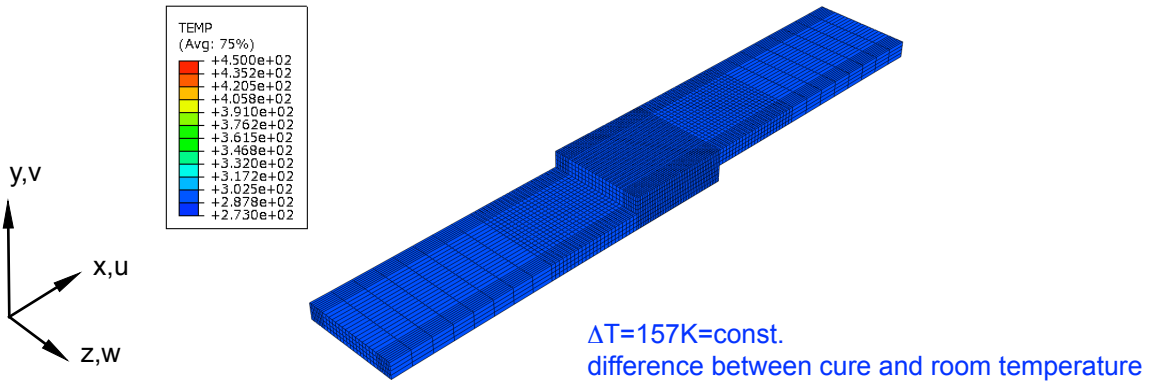


b. *Double lap-shear specimen.*

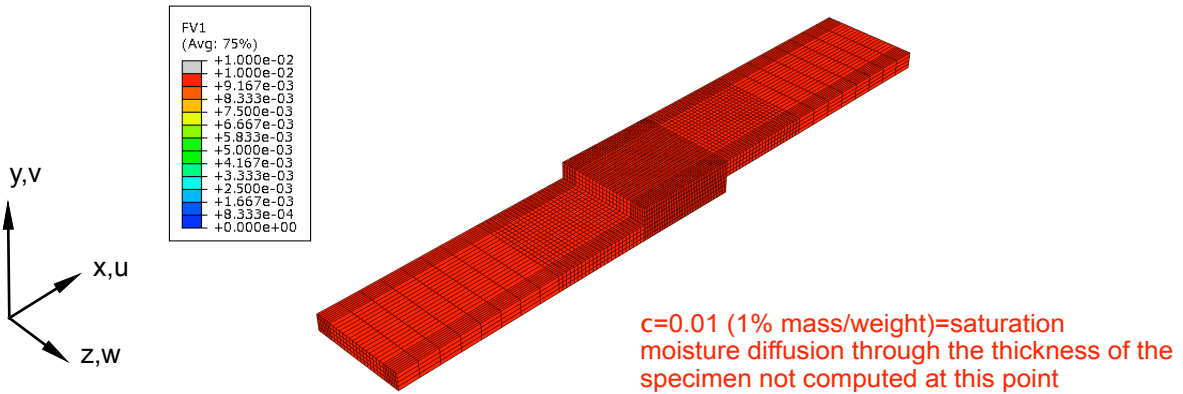
Figure 7. *Three-dimensional finite element model created by FORTRAN routine.*



a. Boundary conditions and mechanical load.

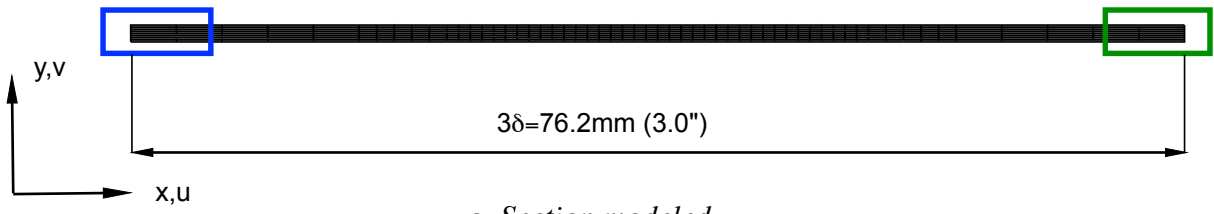


b. Thermal load case.

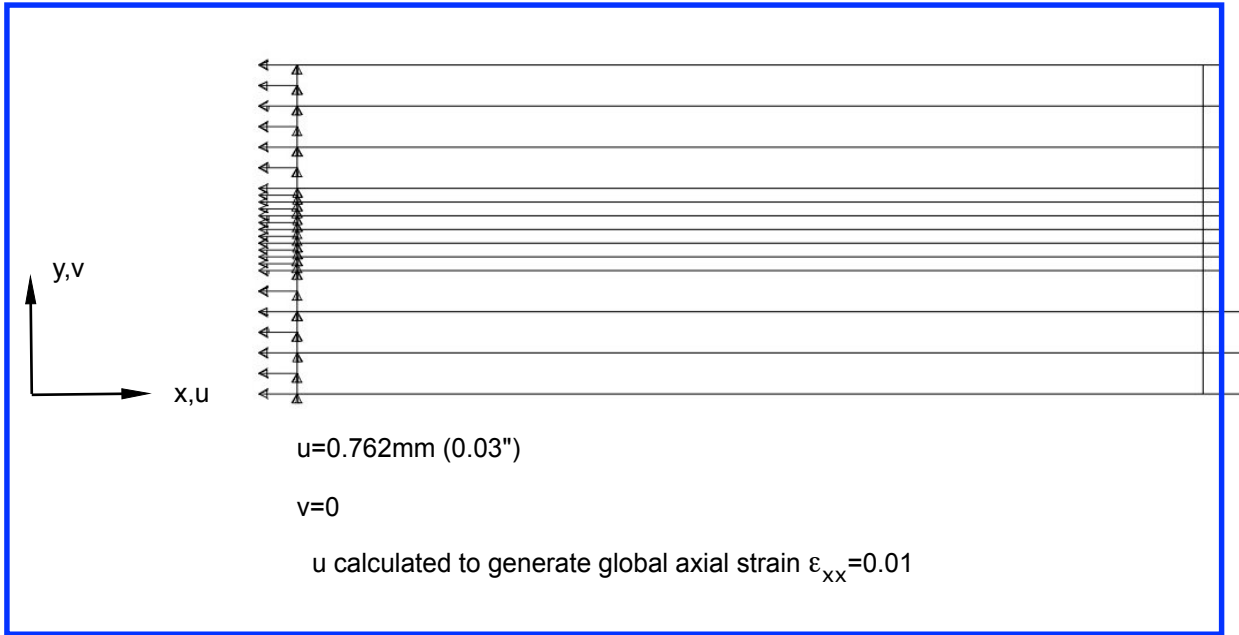


c. Moisture load case.

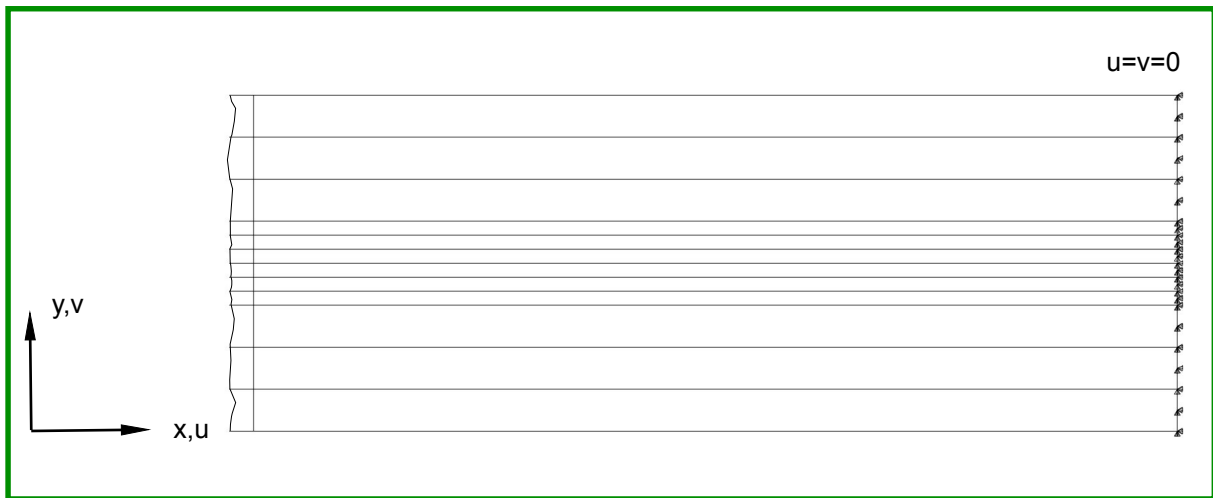
Figure 8. Load, boundary conditions and field input created by FORTRAN routine.



a. Section modeled.



b. Local detail of left edge and boundary condition.



c. Local detail of right edge and boundary condition.

Figure 9. Finite element model.

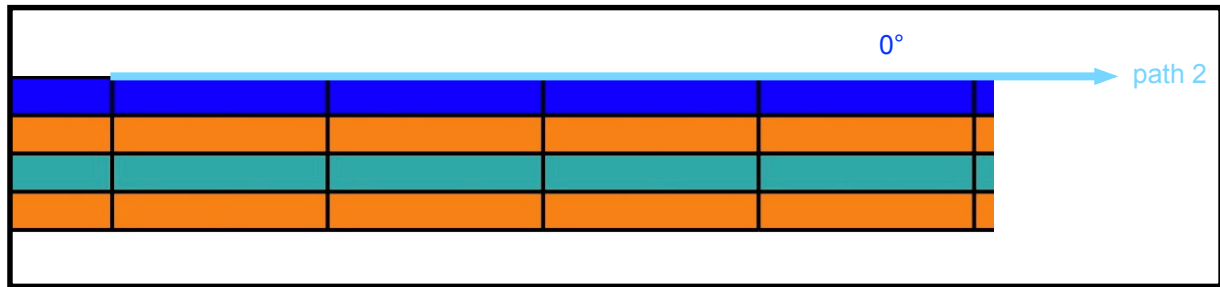
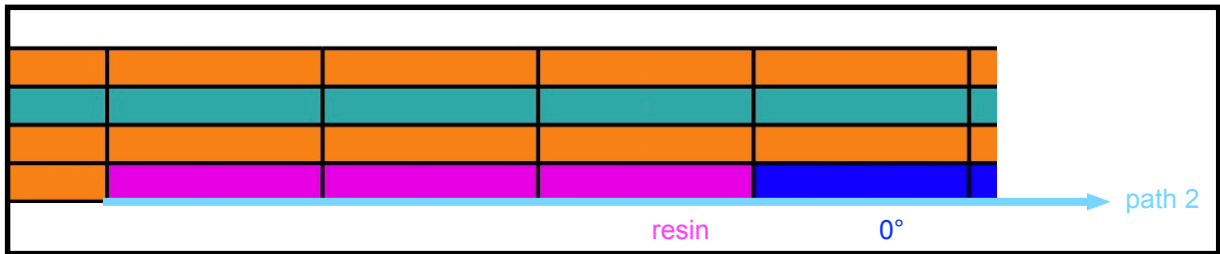
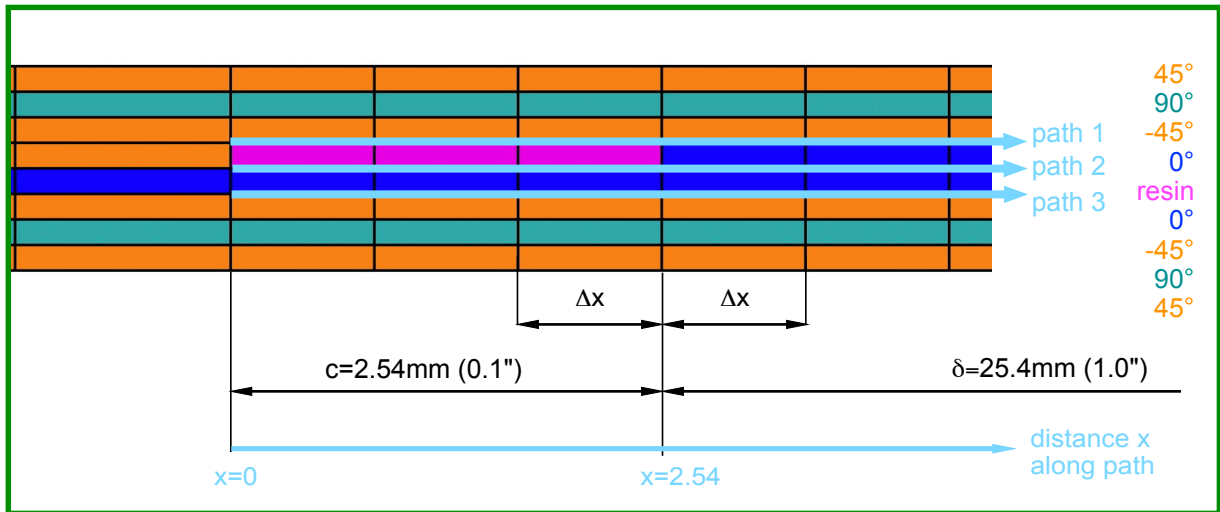
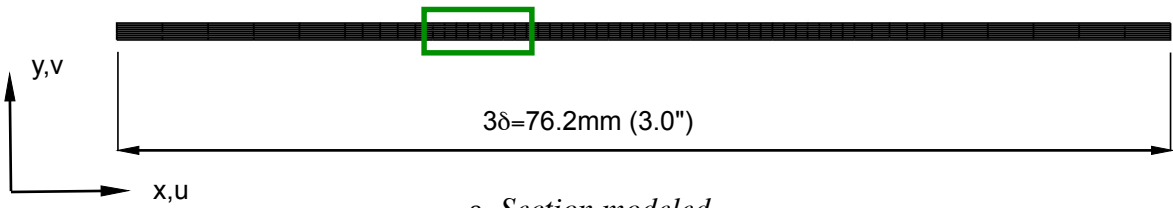


Figure 10. Definition of paths for stress plots.

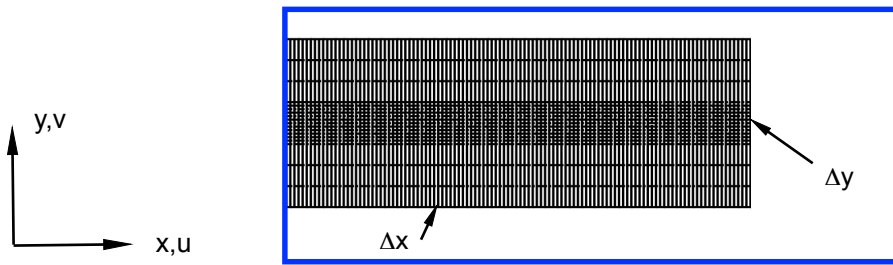
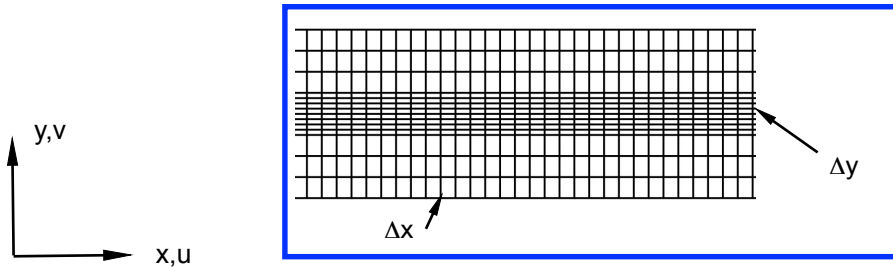
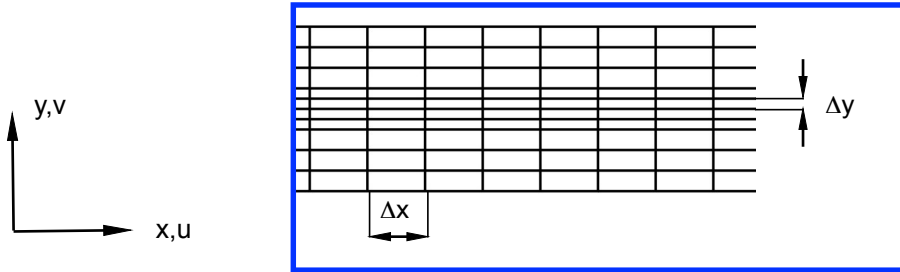
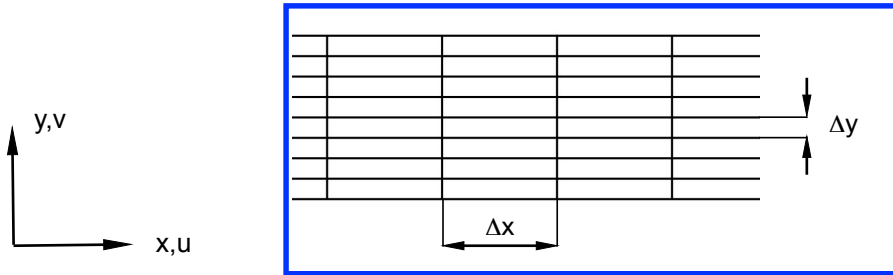
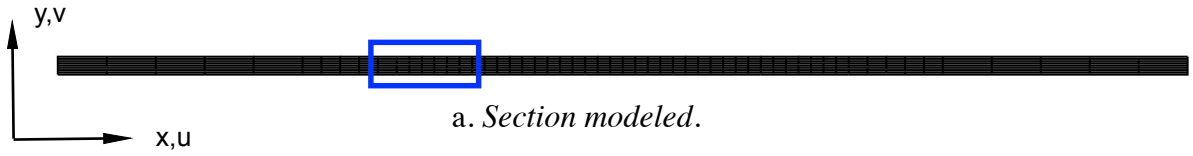


Figure 11. Finite element meshes used for mesh refinement study.

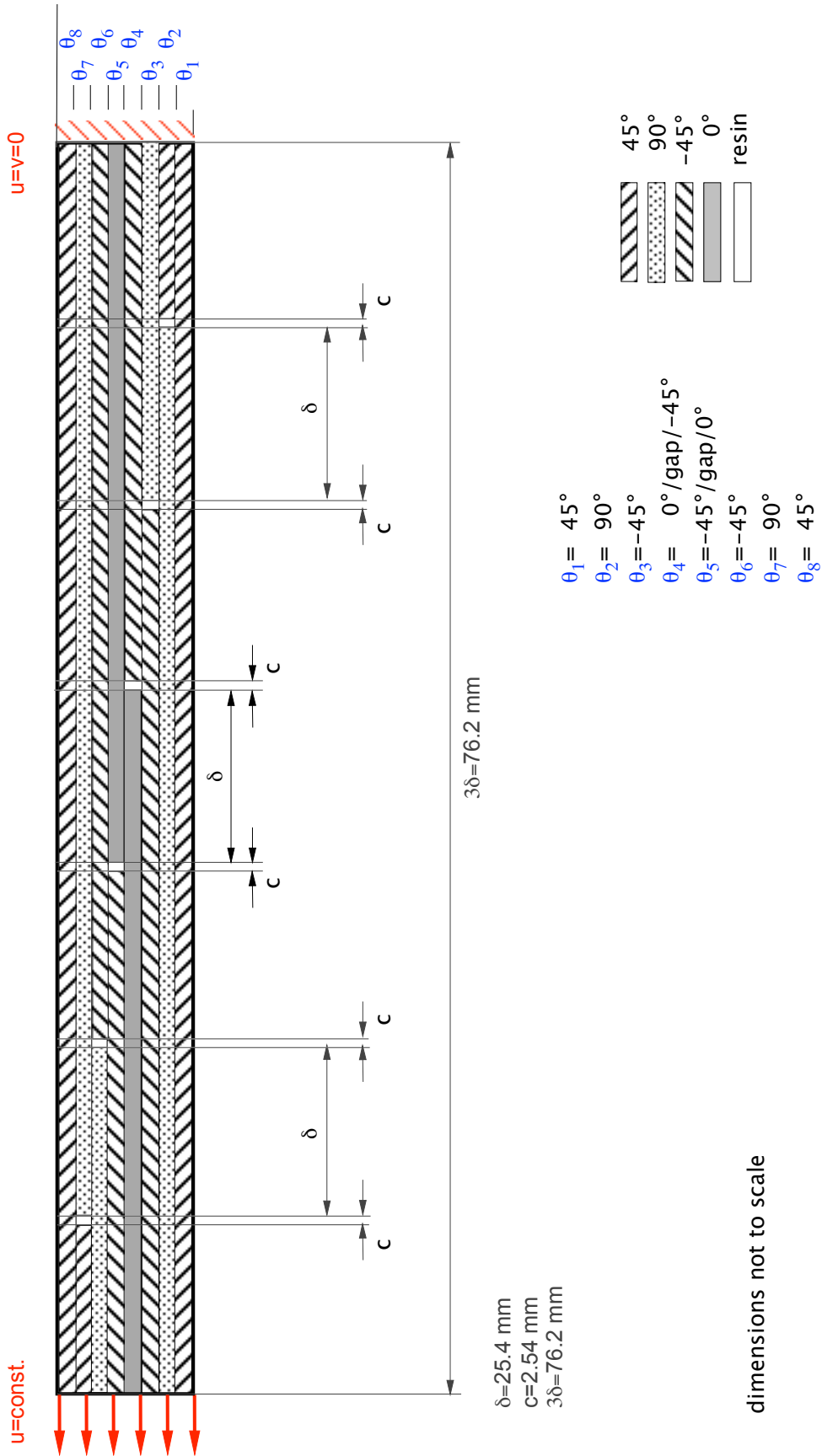
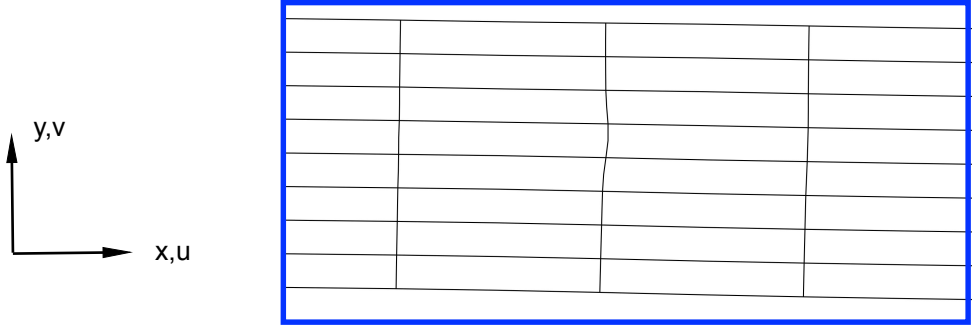
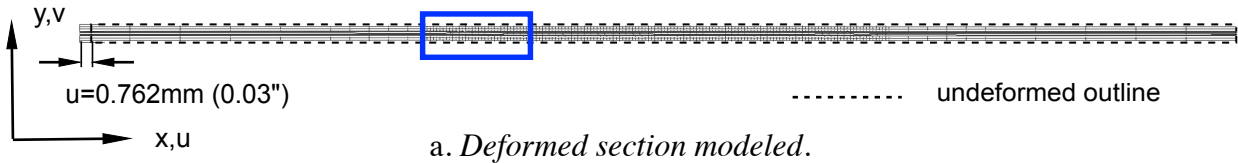
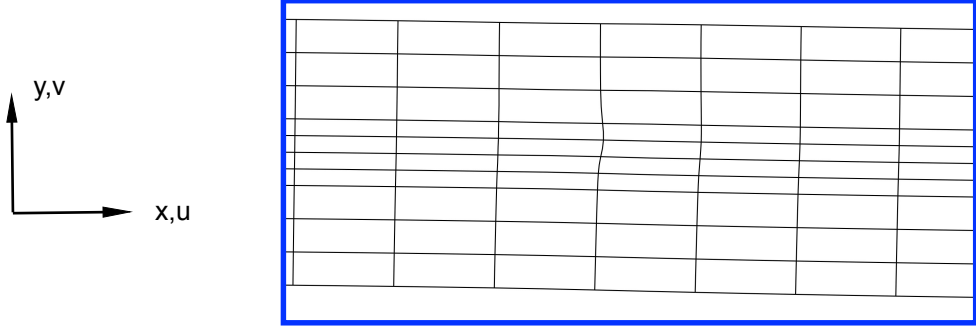


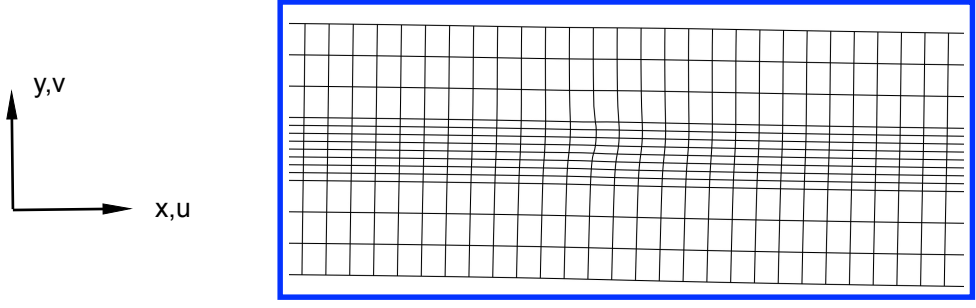
Figure 12. Specimen configuration with multiple overlaps.



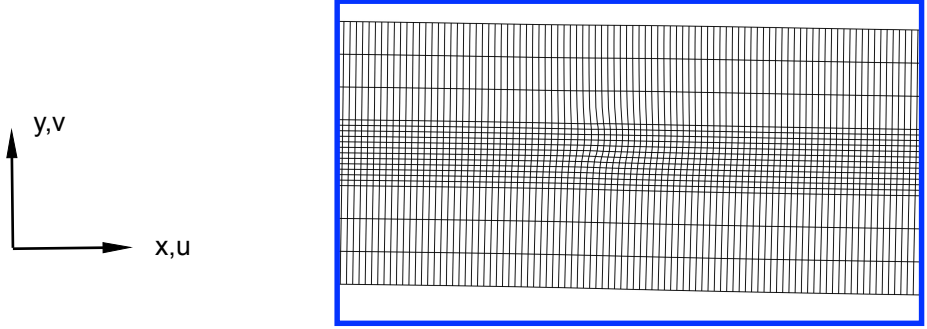
b. Local detail of deformed model for coarse mesh $\Delta x=0.847\text{mm}$.



c. Local detail of deformed model for $\Delta x=0.423\text{mm}$.



d. Local detail of deformed model for $\Delta x=0.106\text{mm}$.



e. Local detail of deformed model for refined mesh $\Delta x=0.026\text{mm}$.

Figure 13. Deformed finite element model.

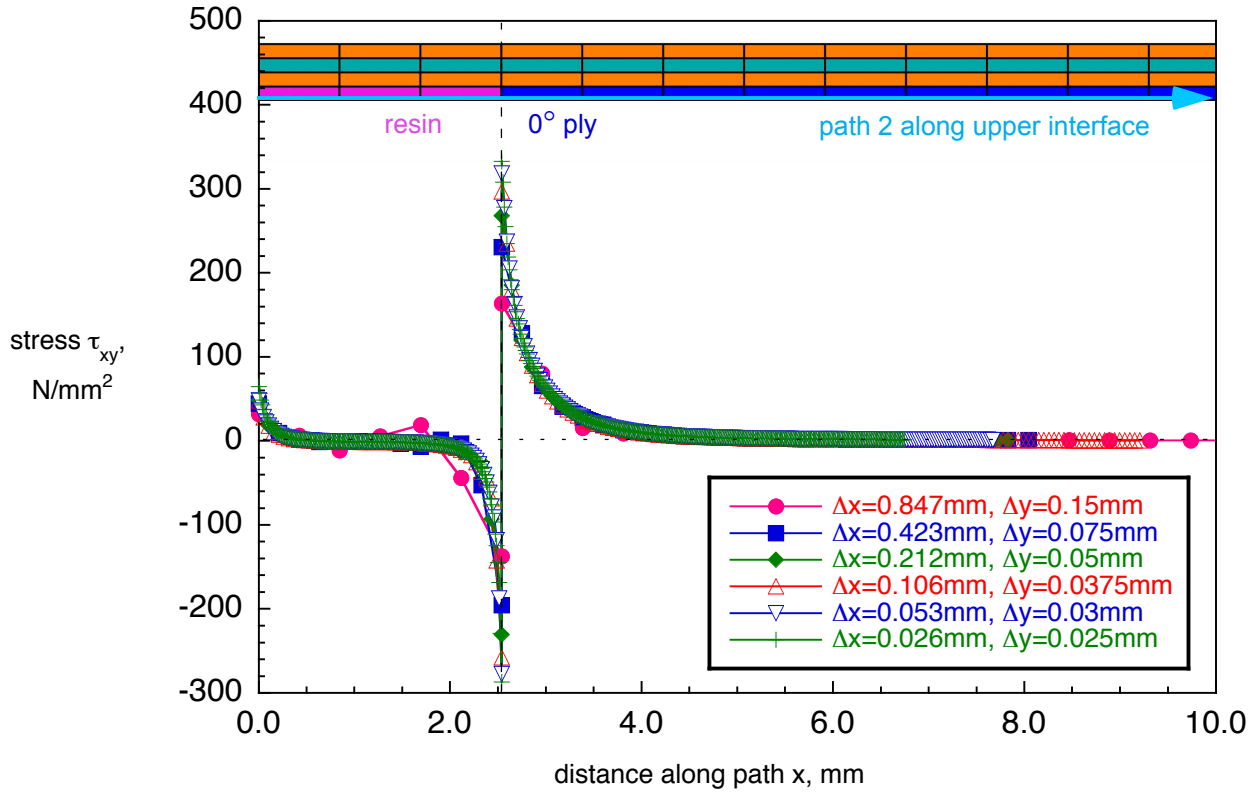


Figure 14. Stress τ_{xy} along path 2 in upper 0° ply interface for $\delta=25.4\text{mm}$, $c=2.54\text{mm}$.

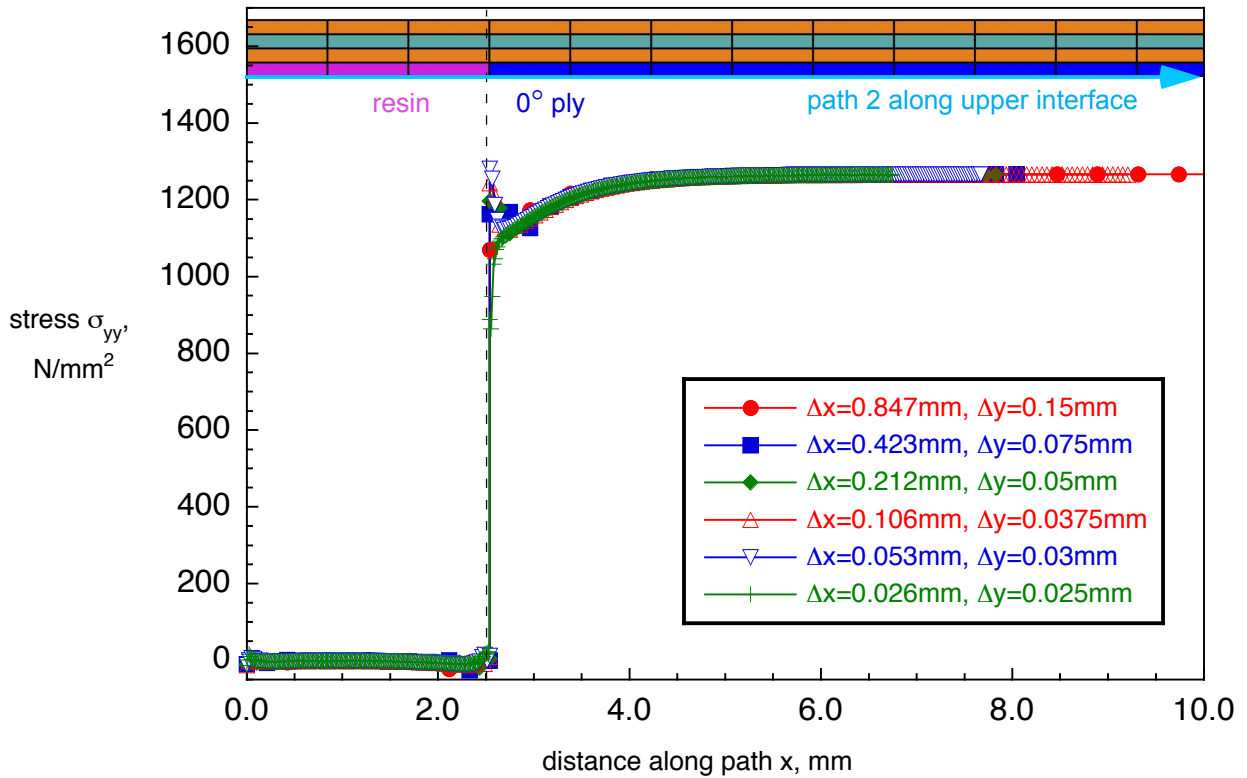


Figure 15. Stress σ_{yy} along path 2 in upper 0° ply interface for $\delta=25.4\text{mm}$, $c=2.54\text{mm}$.

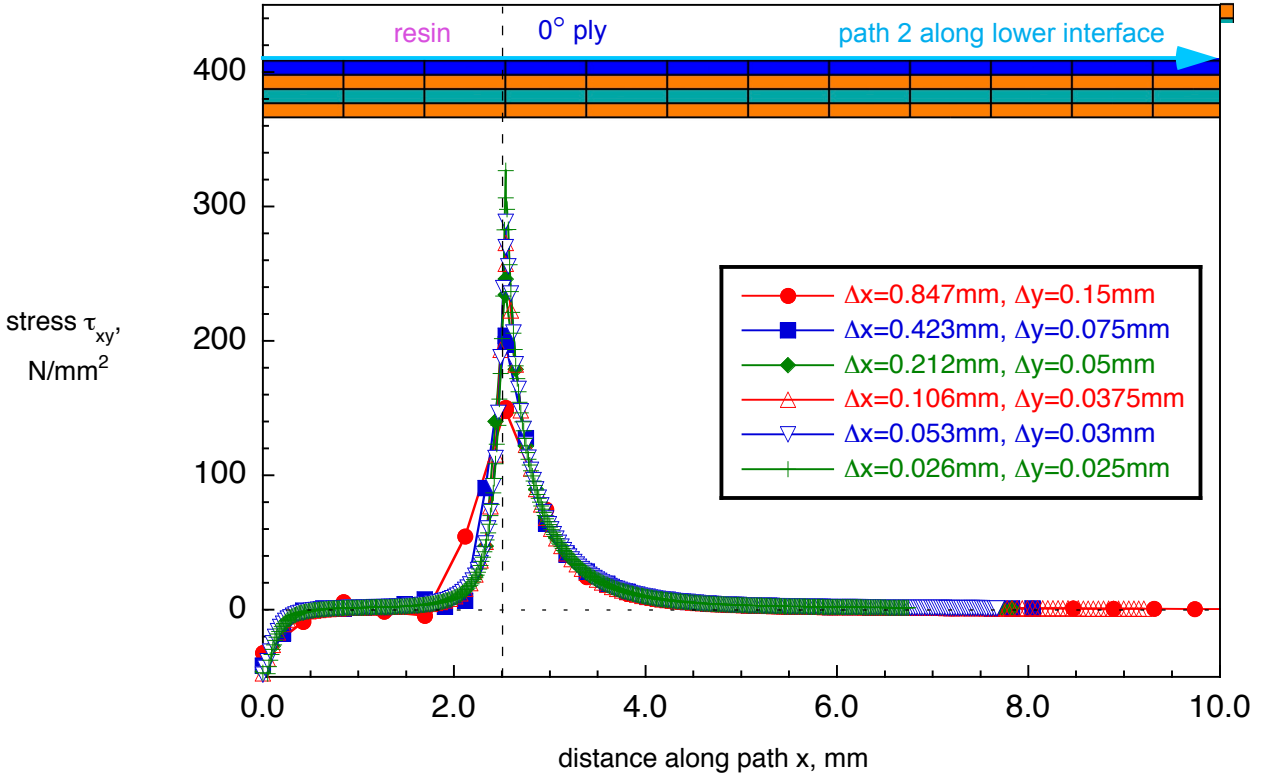


Figure 16. Stress τ_{xy} along path 2 in lower 0° ply interface for $\delta=25.4\text{mm}, c=2.54\text{mm}$.

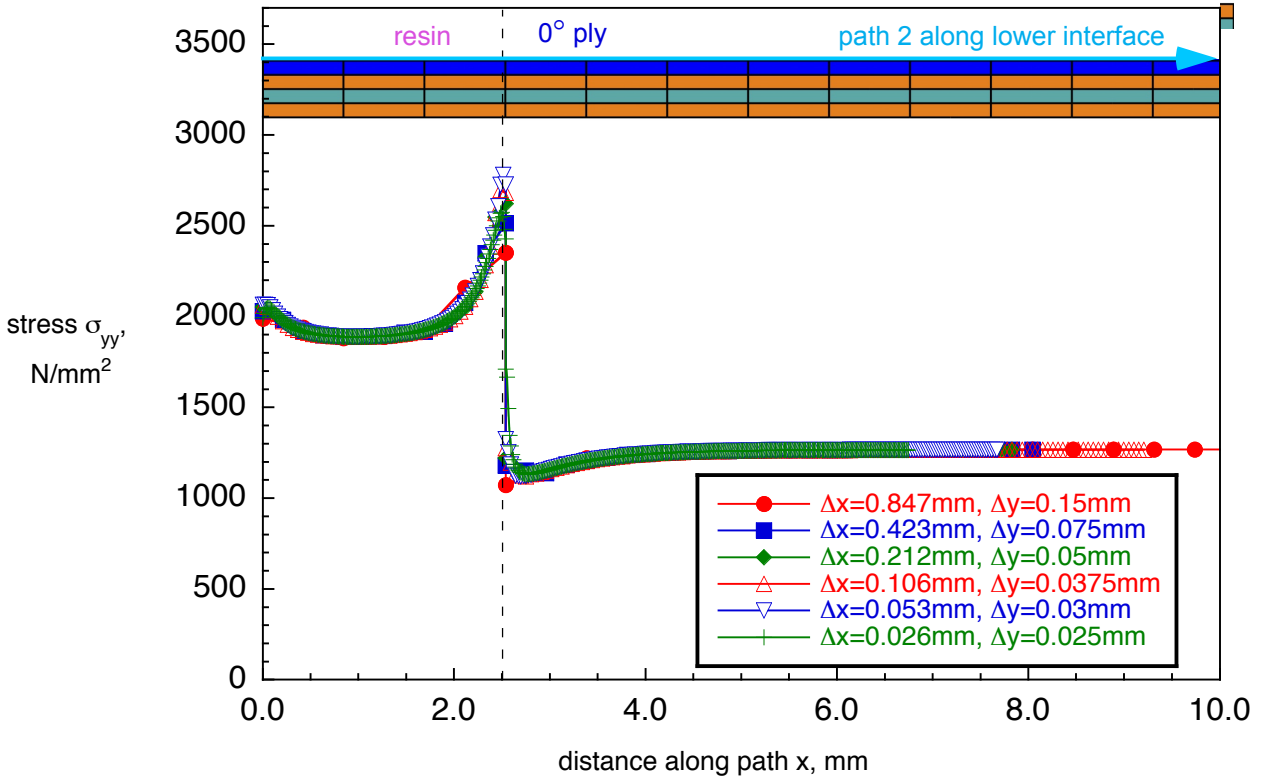


Figure 17. Stress σ_{yy} along path 2 in lower 0° ply interface for $\delta=25.4\text{mm}, c=2.54\text{mm}$.

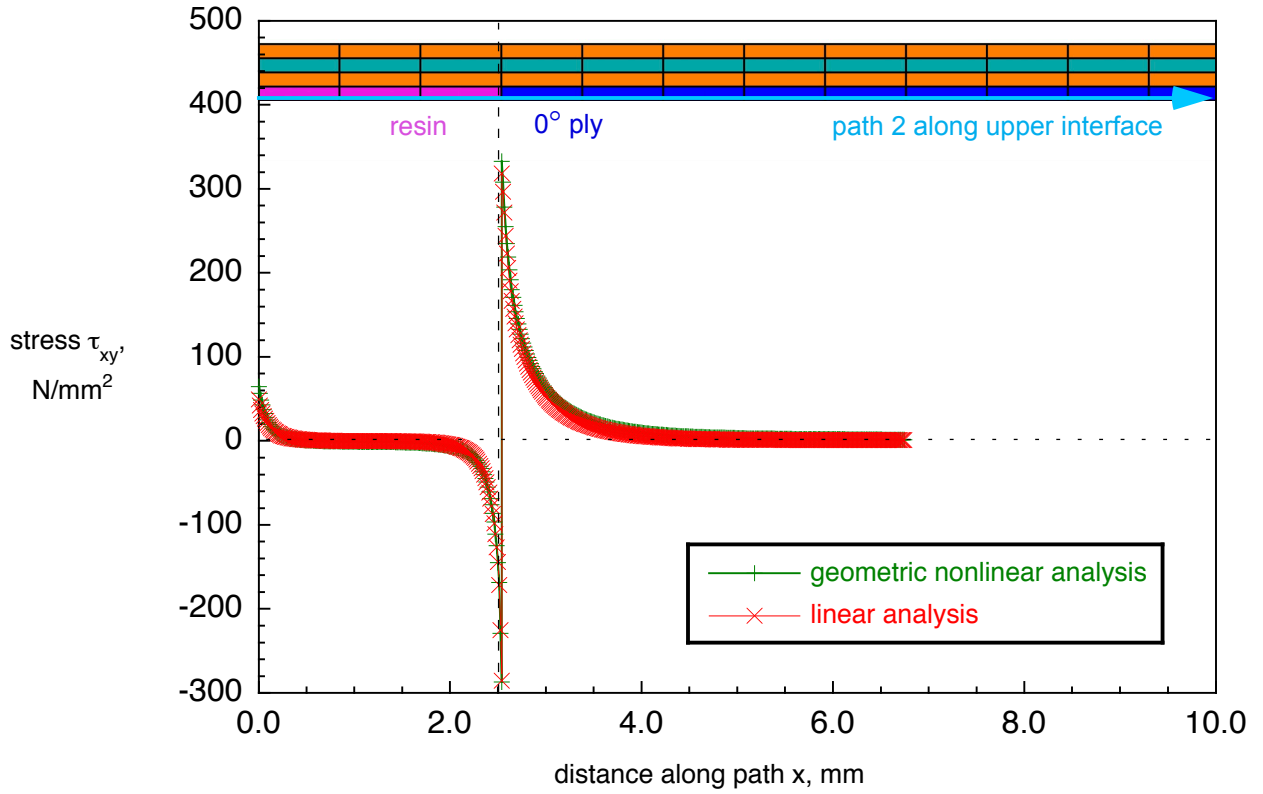


Figure 18. Stress τ_{xy} along path 2 in upper 0° ply interface for $\delta=25.4\text{mm}$, $c=2.54\text{mm}$.

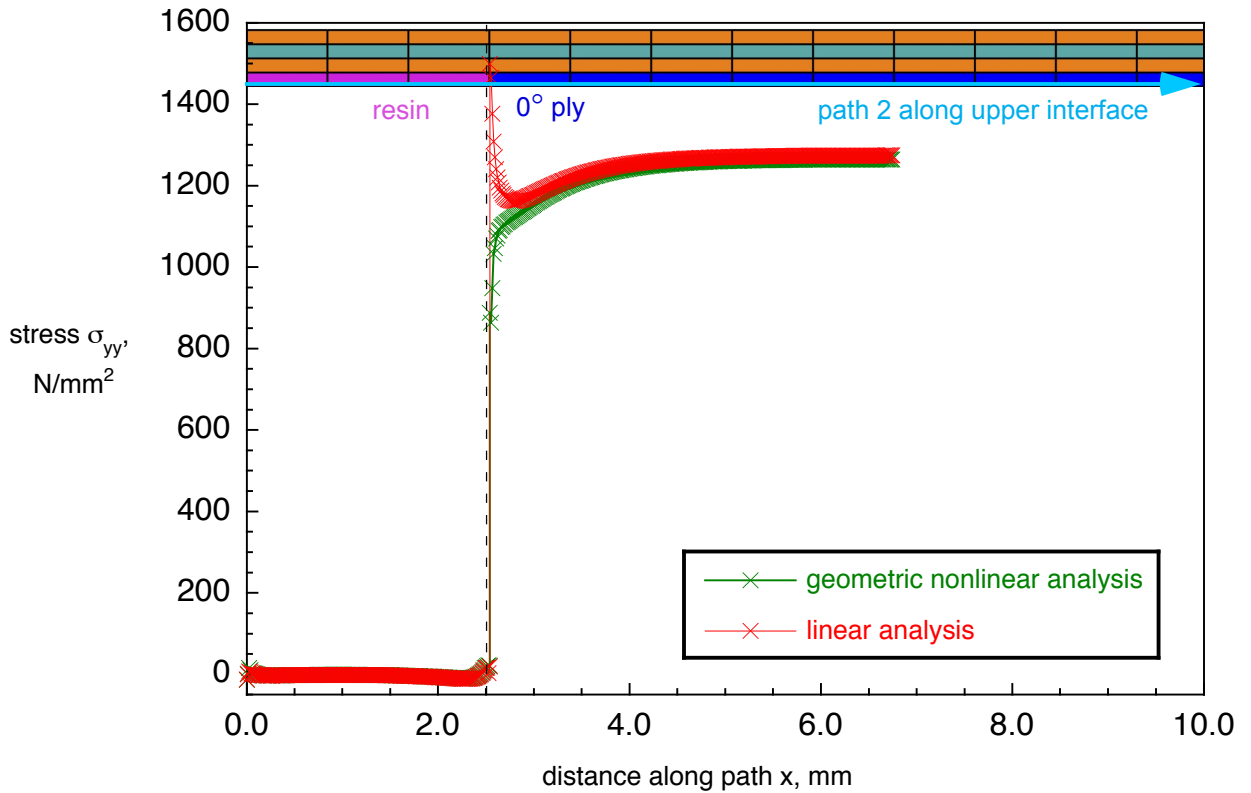


Figure 19. Stress σ_{yy} along path 2 in upper 0° ply interface for $\delta=25.4\text{mm}$, $c=2.54\text{mm}$.

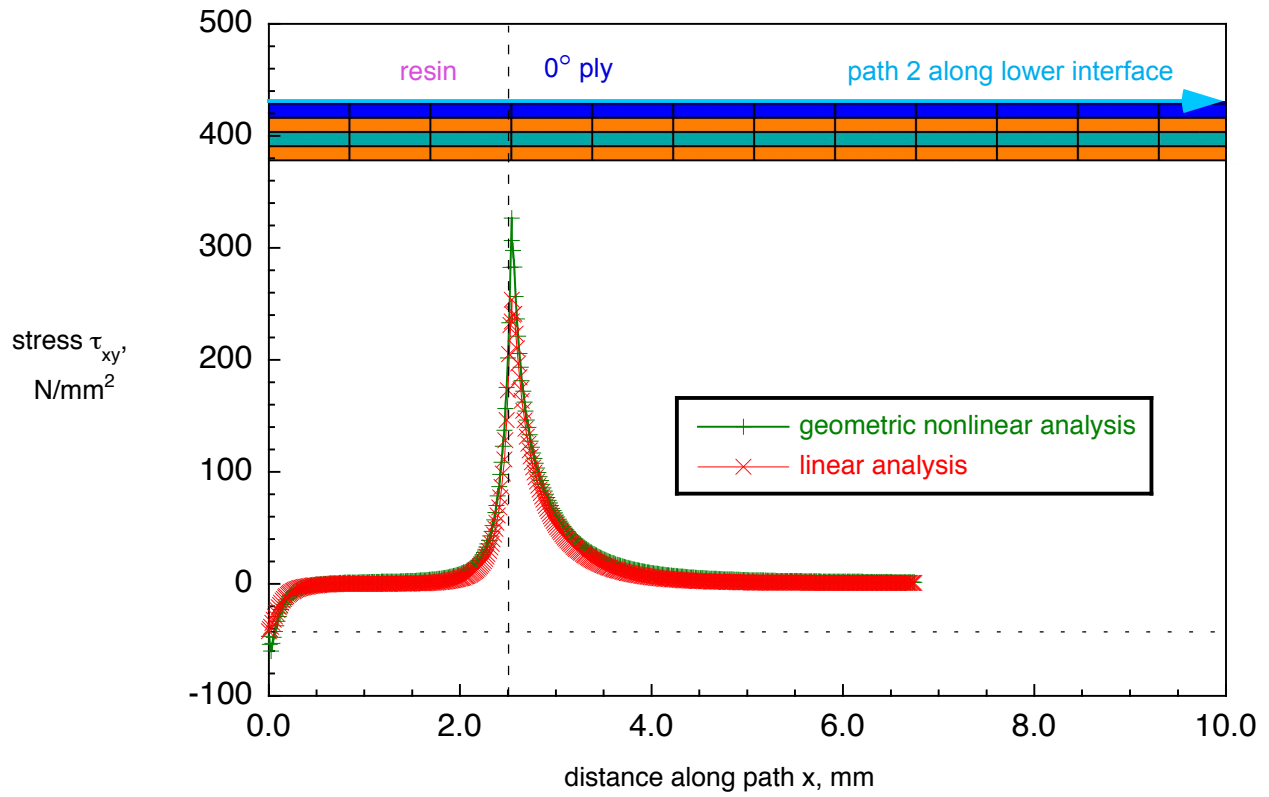


Figure 20. Stress τ_{xy} along path 2 in lower 0° ply interface for $\delta=25.4\text{mm}$, $c=2.54\text{mm}$.

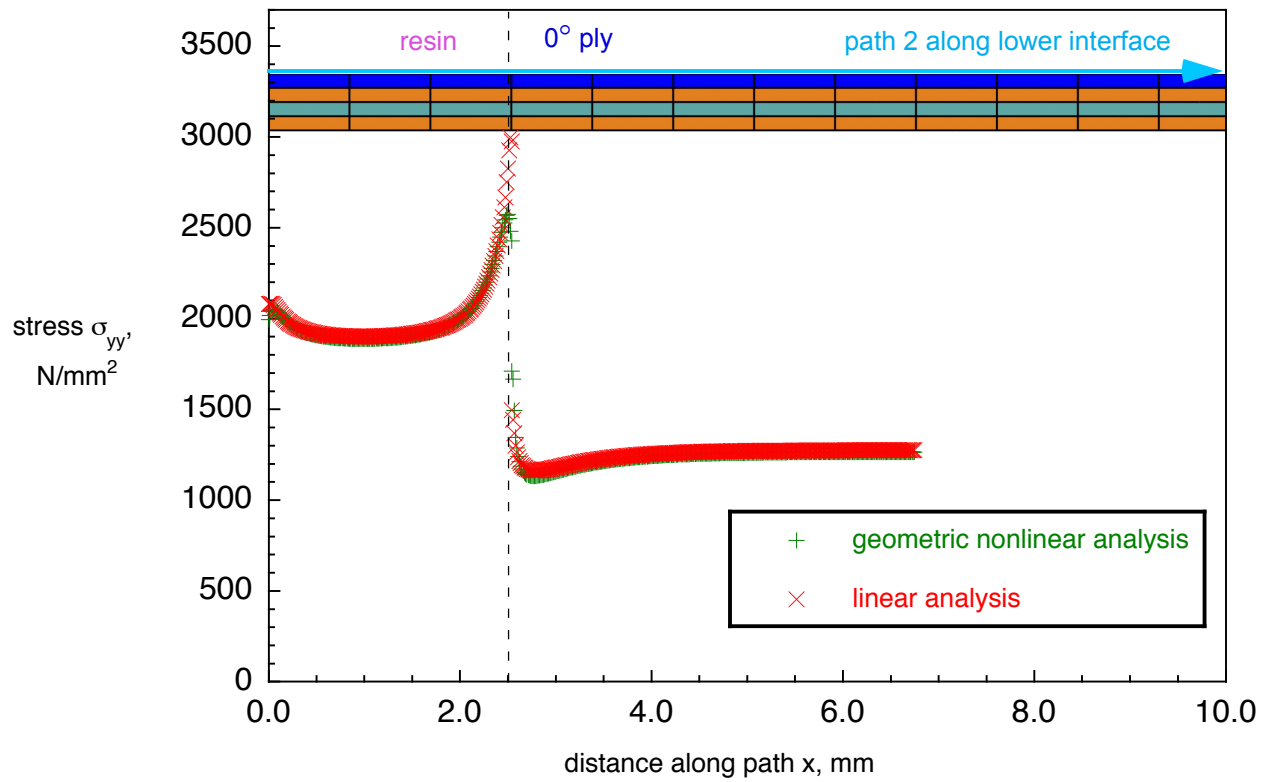


Figure 21. Stress σ_{yy} along path 2 in lower 0° ply interface for $\delta=25.4\text{mm}$, $c=2.54\text{mm}$.

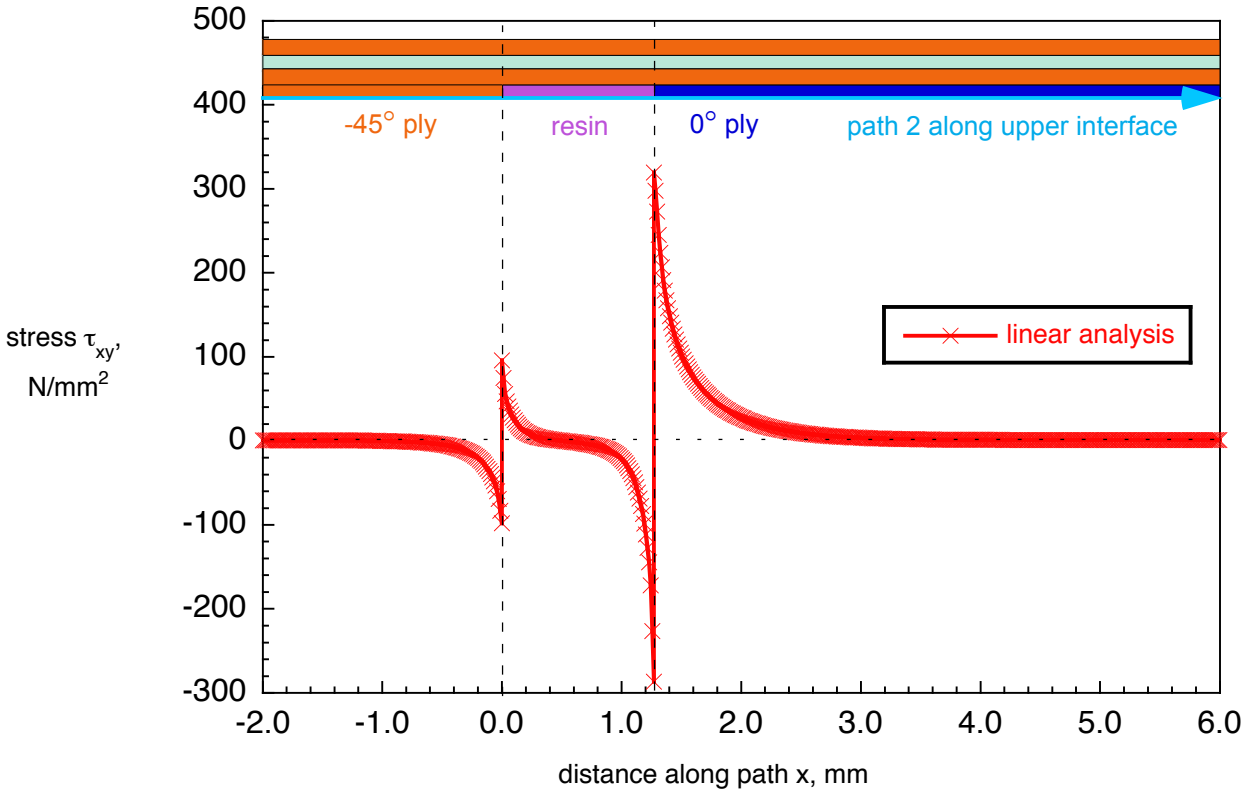


Figure 22. Stress τ_{xy} along path 2 in upper 0° ply interface for $\delta=25.4\text{mm}$, $c=1.27\text{mm}$.

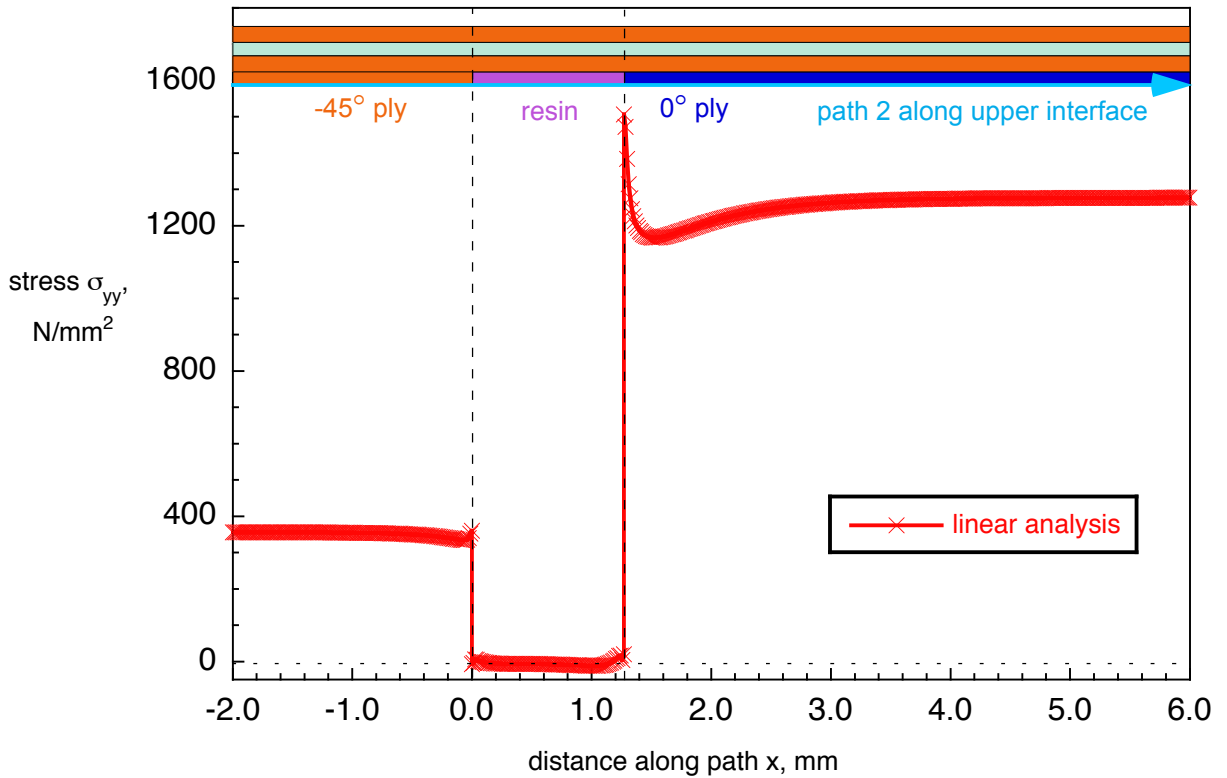


Figure 23. Stress σ_{yy} along path 2 in upper 0° ply interface for $\delta=25.4\text{mm}$, $c=1.27\text{mm}$.

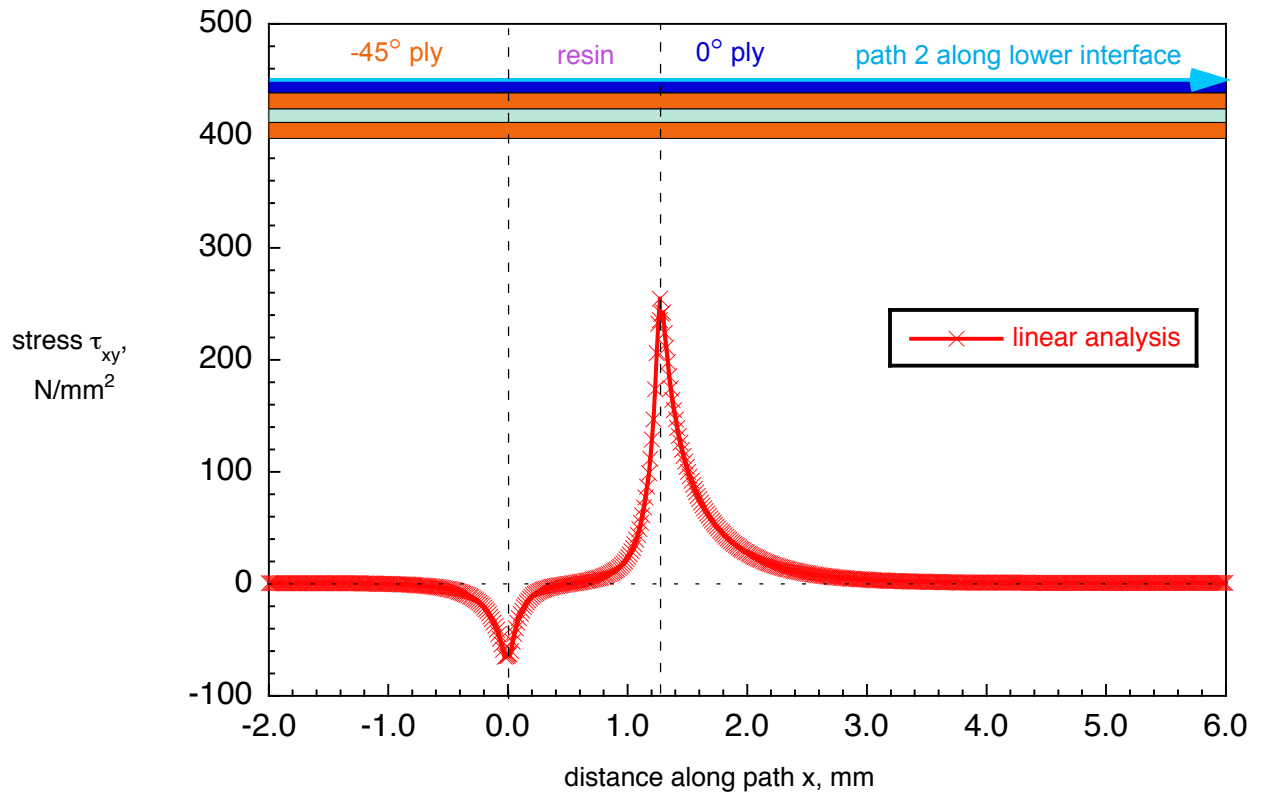


Figure 24. Stress τ_{xy} along path 2 in lower 0° ply interface for $\delta=25.4\text{mm}$, $c=1.27\text{mm}$.

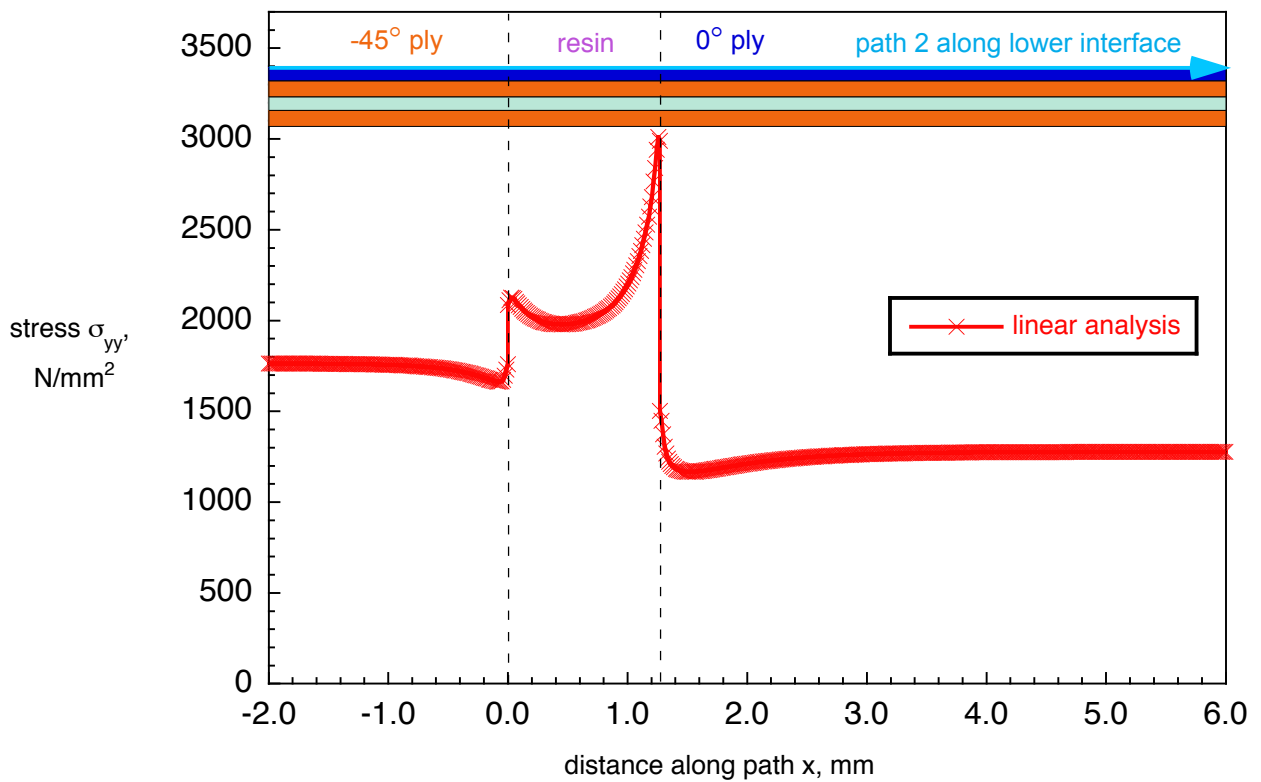


Figure 25. Stress σ_{yy} along path 2 in lower 0° ply interface for $\delta=25.4\text{mm}$, $c=1.27\text{mm}$.

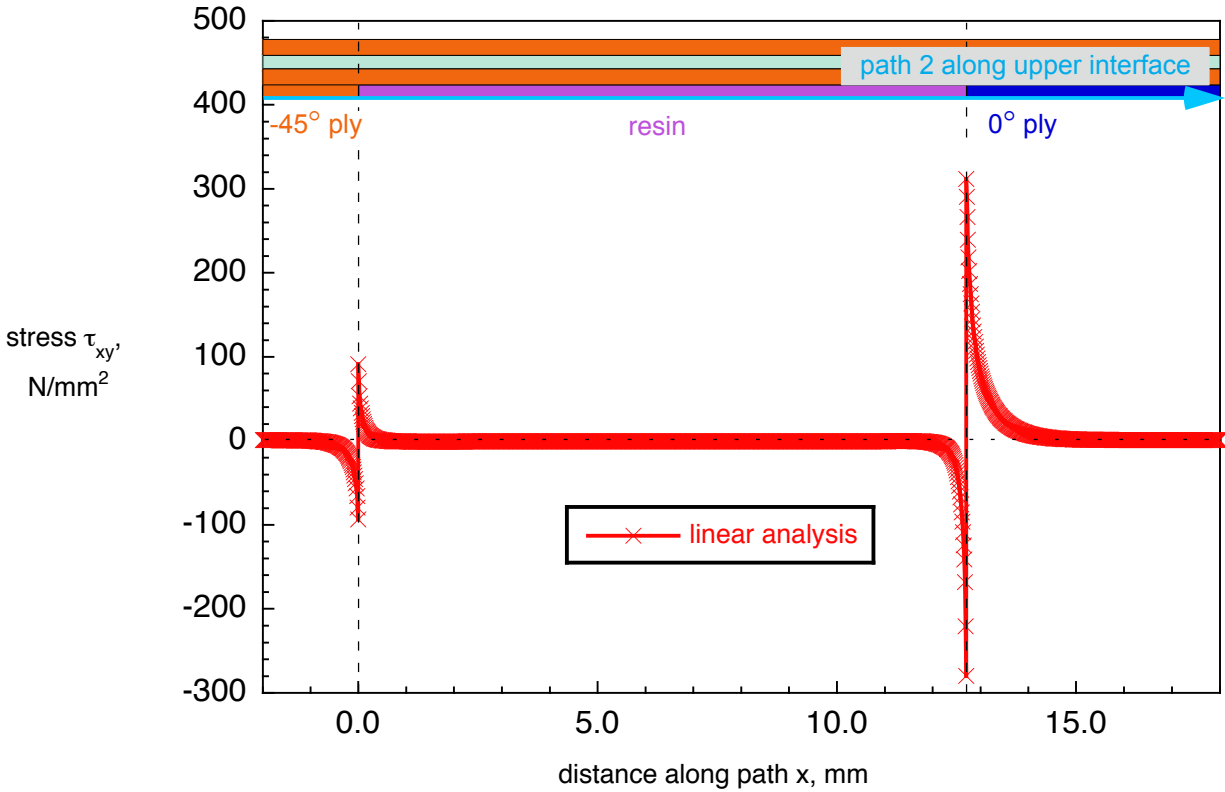


Figure 26. Stress τ_{xy} along path 2 in upper 0° ply interface for $\delta=25.4\text{mm}$, $c=12.7\text{mm}$.

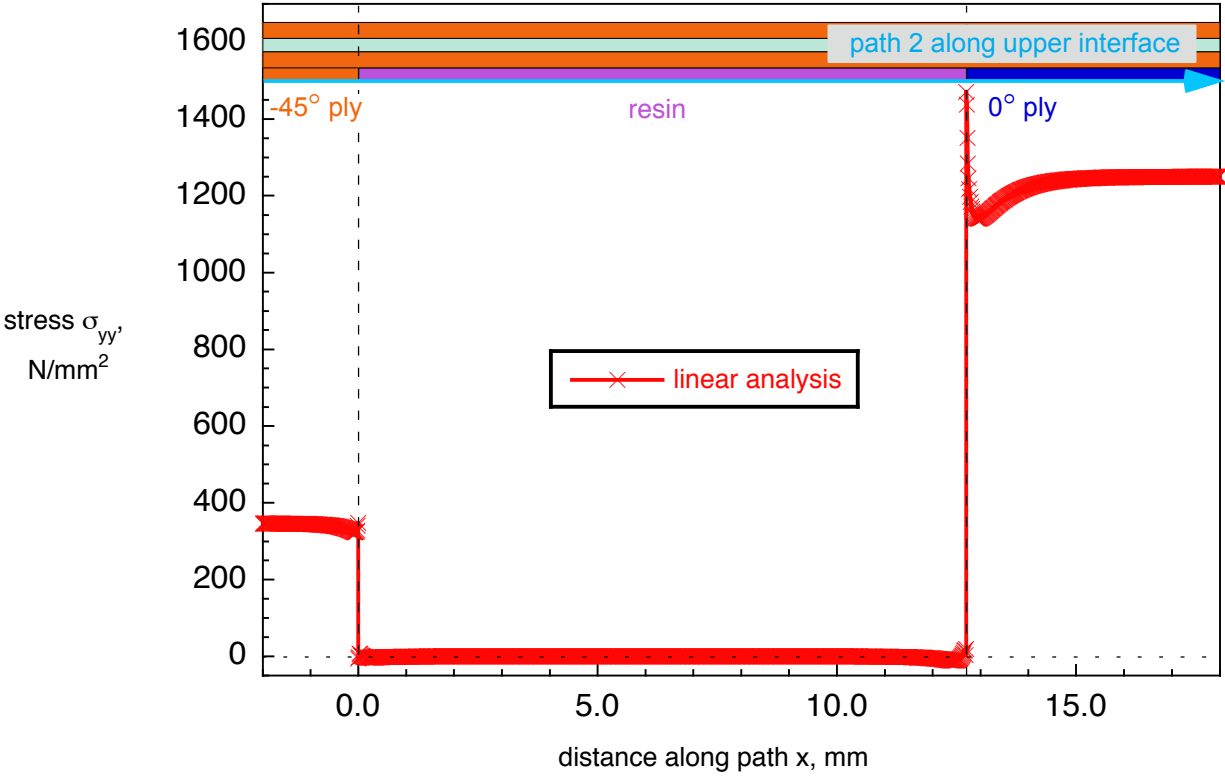


Figure 27. Stress σ_{yy} along path 2 in upper 0° ply interface for $\delta=25.4\text{mm}$, $c=12.7\text{mm}$.

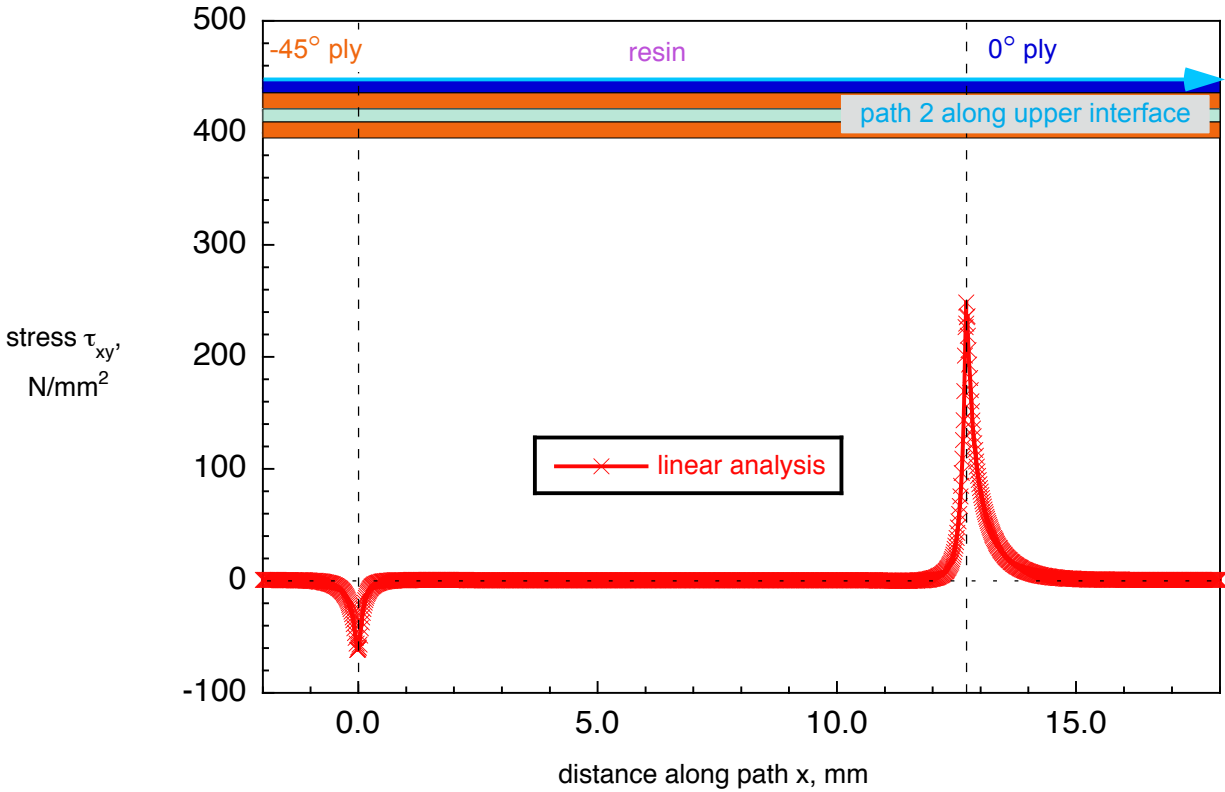


Figure 28. Stress τ_{xy} along path 2 in lower 0° ply interface for $\delta=25.4\text{mm}$, $c=12.7\text{mm}$.

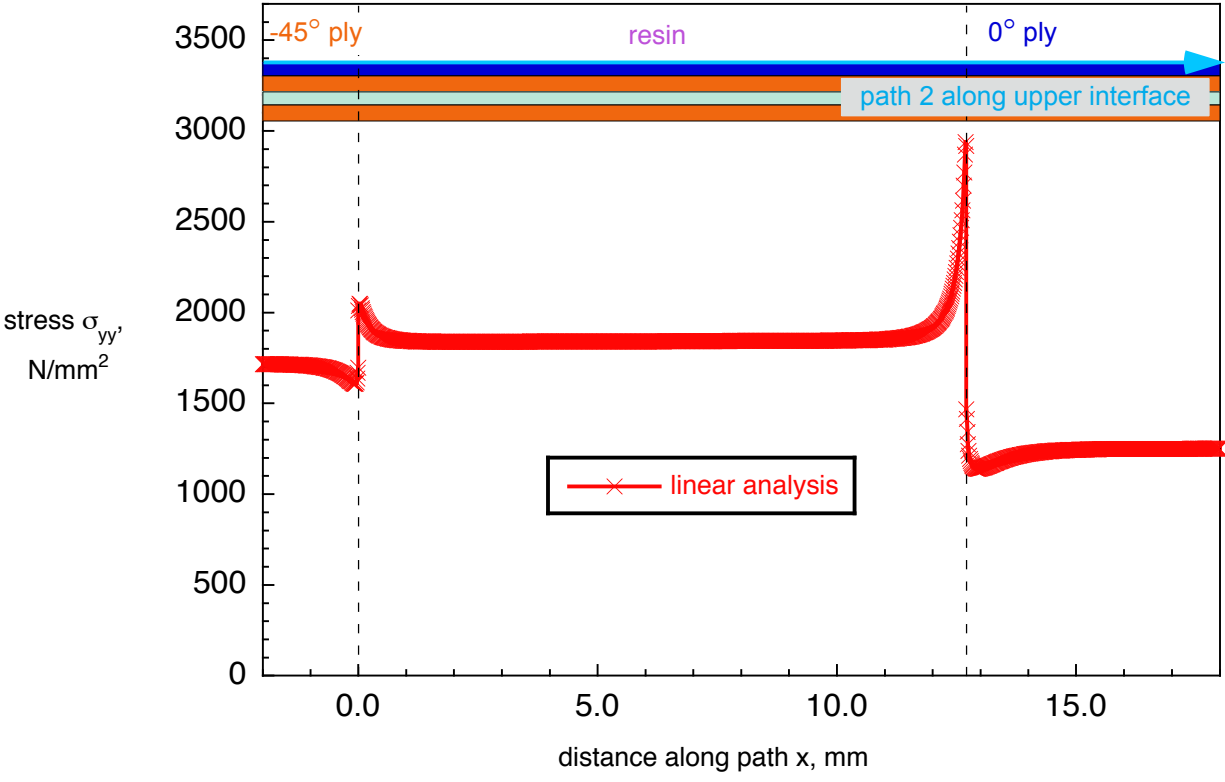


Figure 29. Stress σ_{yy} along path 2 in lower 0° ply interface for $\delta=25.4\text{mm}$, $c=12.7\text{mm}$.

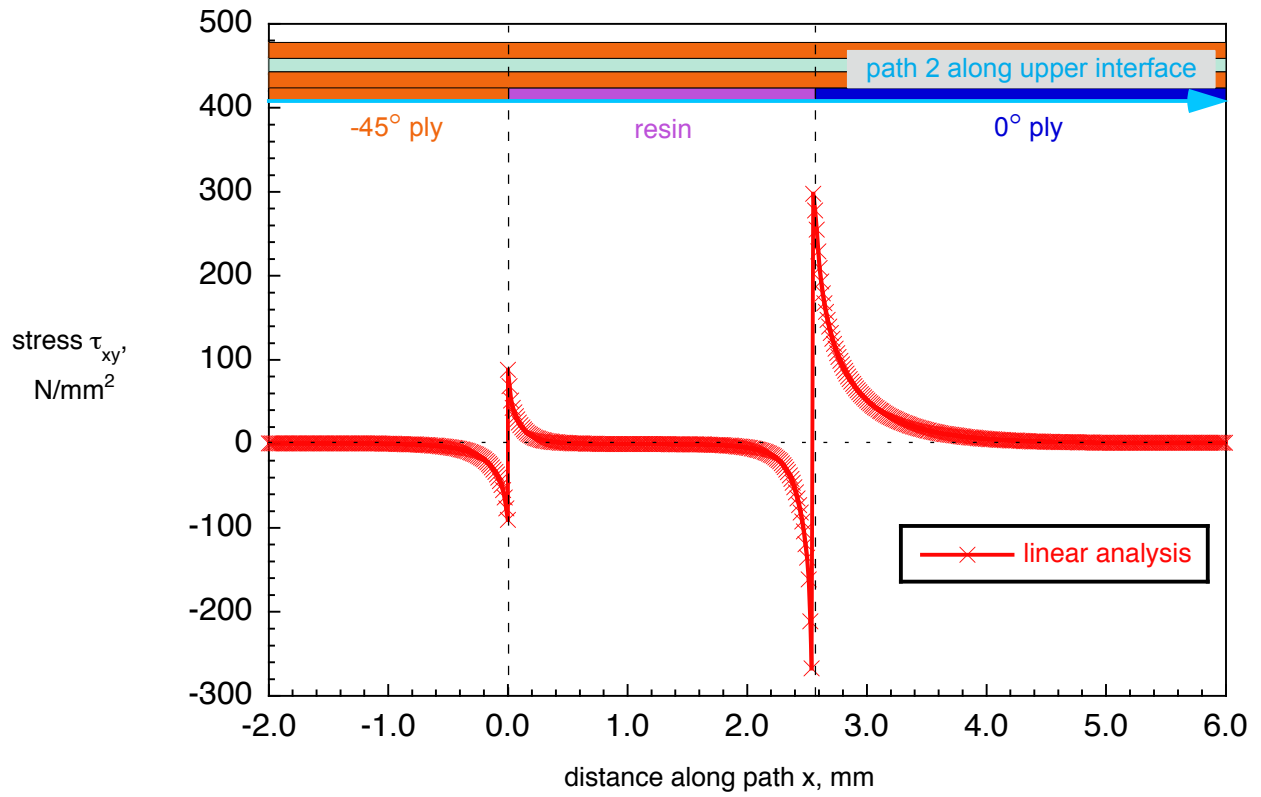


Figure 30. Stress τ_{xy} along path 2 in upper 0° ply interface for $\delta=6.35\text{mm}$, $c=2.54\text{mm}$.

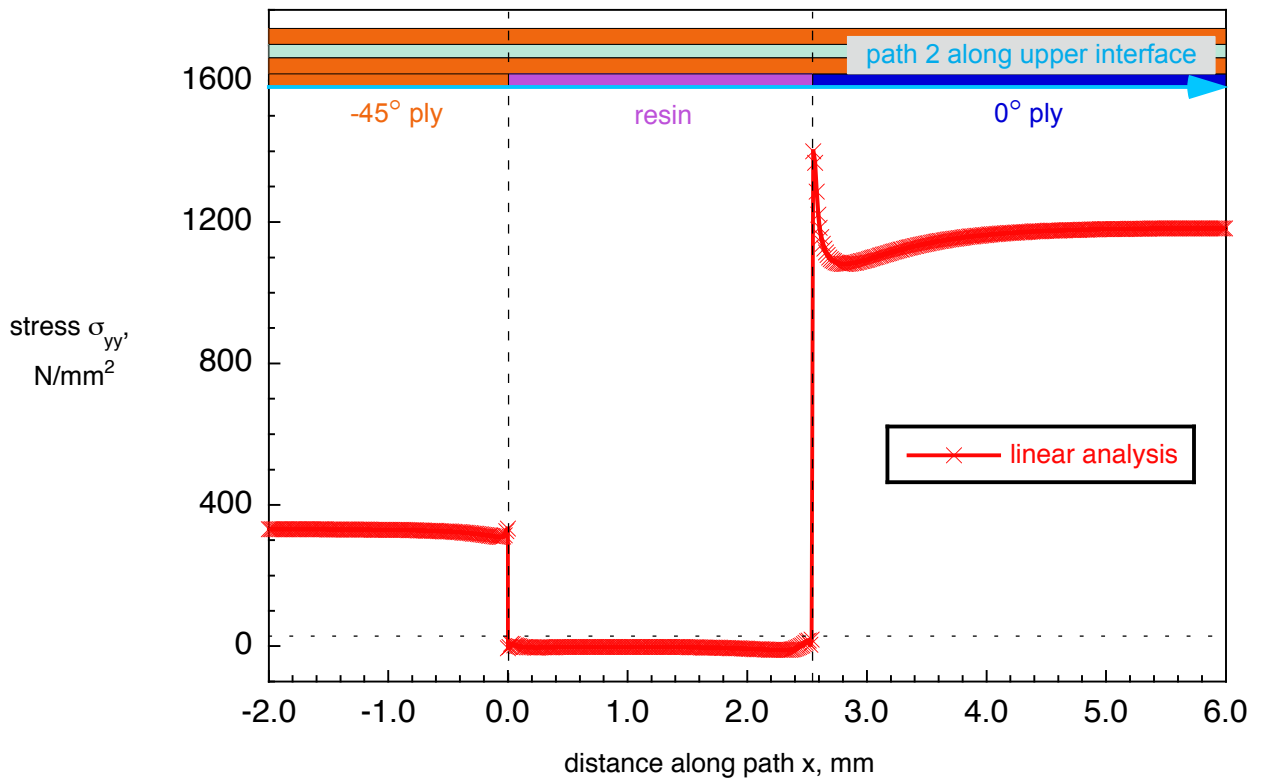


Figure 31. Stress σ_{yy} along path 2 in upper 0° ply interface for $\delta=6.35\text{mm}$, $c=2.54\text{mm}$.

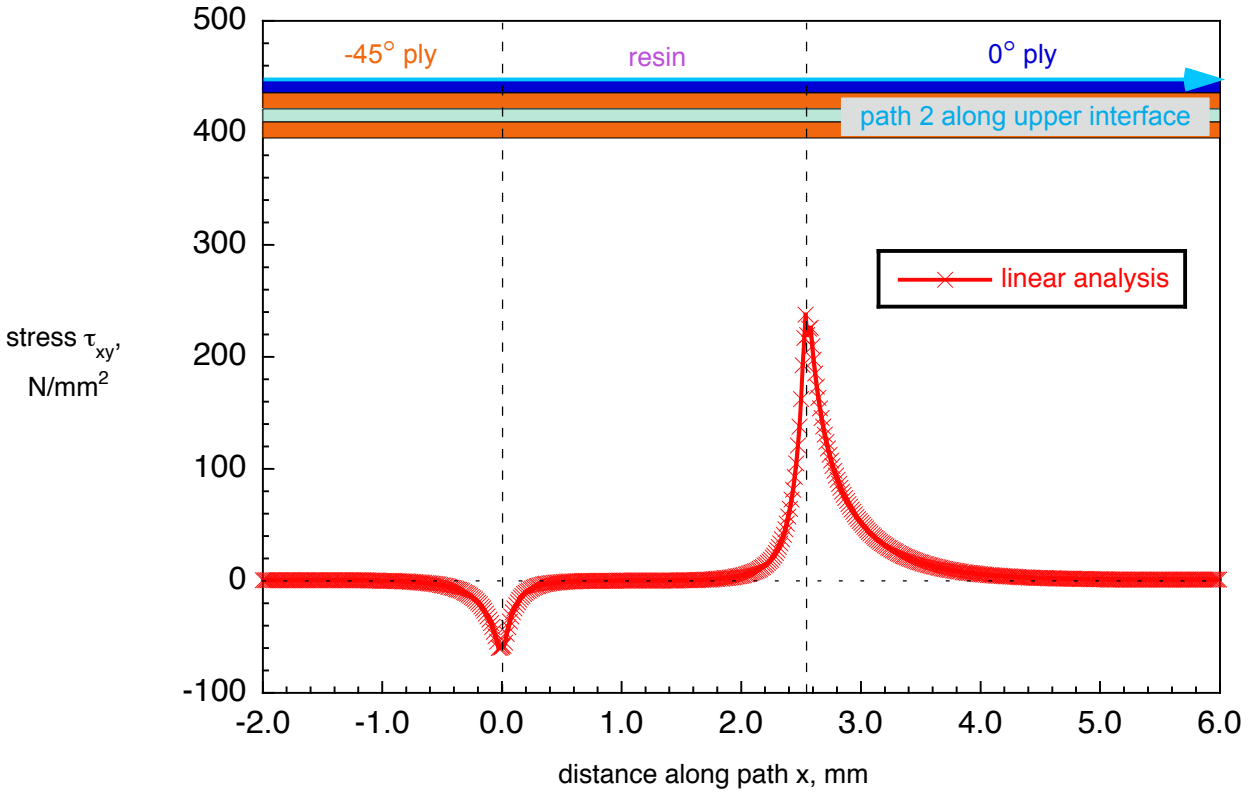


Figure 32. Stress τ_{xy} along path 2 in lower 0° ply interface for $\delta=6.35\text{mm}$, $c=2.54\text{mm}$.

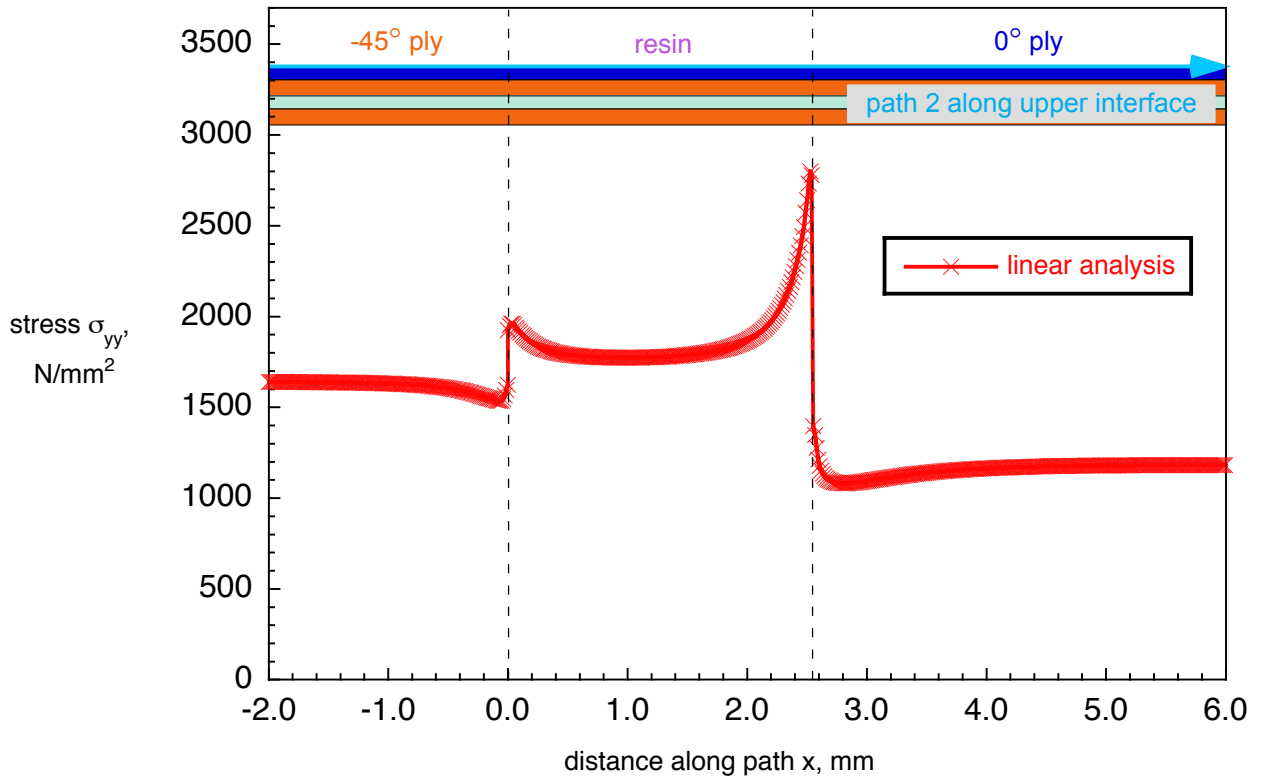


Figure 33. Stress σ_{yy} along path 2 in lower 0° ply interface for $\delta=6.35\text{mm}$, $c=2.54\text{mm}$.

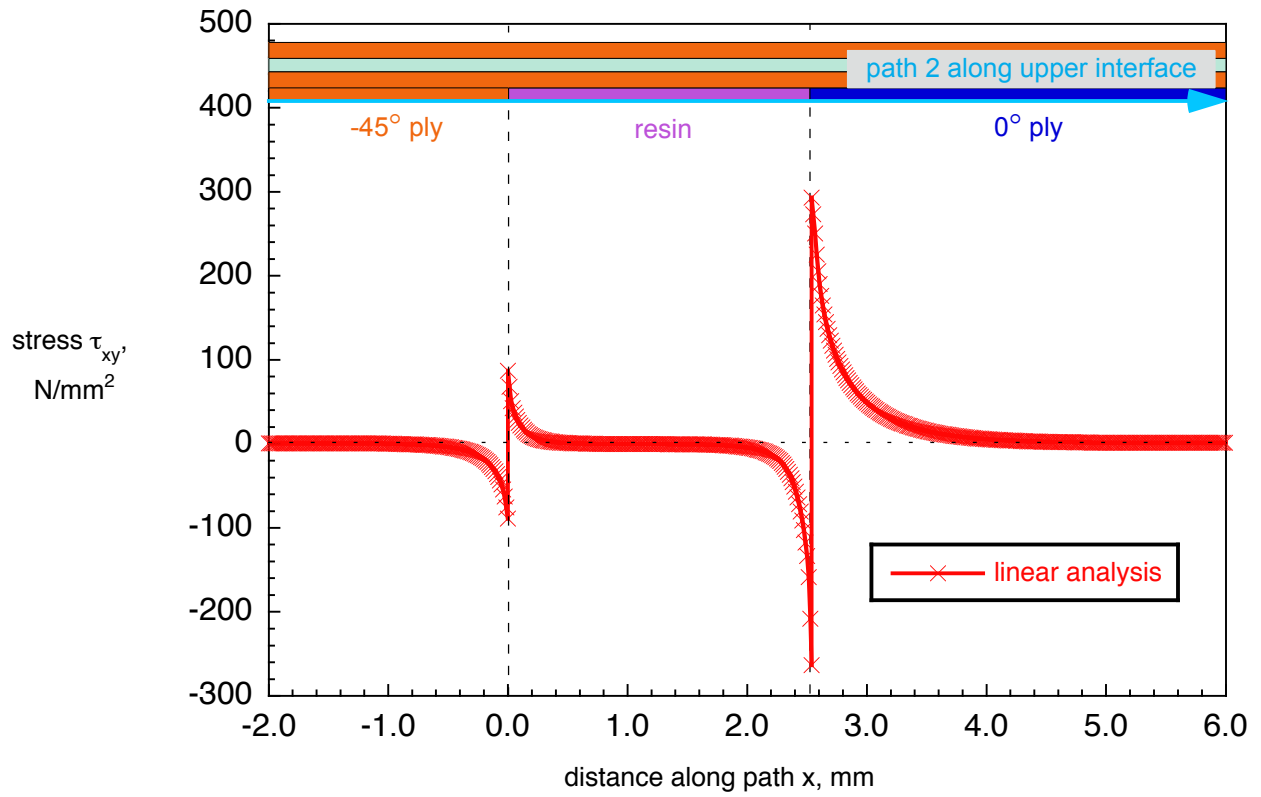


Figure 34. Stress τ_{xy} along path 2 in upper 0° ply interface for multiple overlaps.

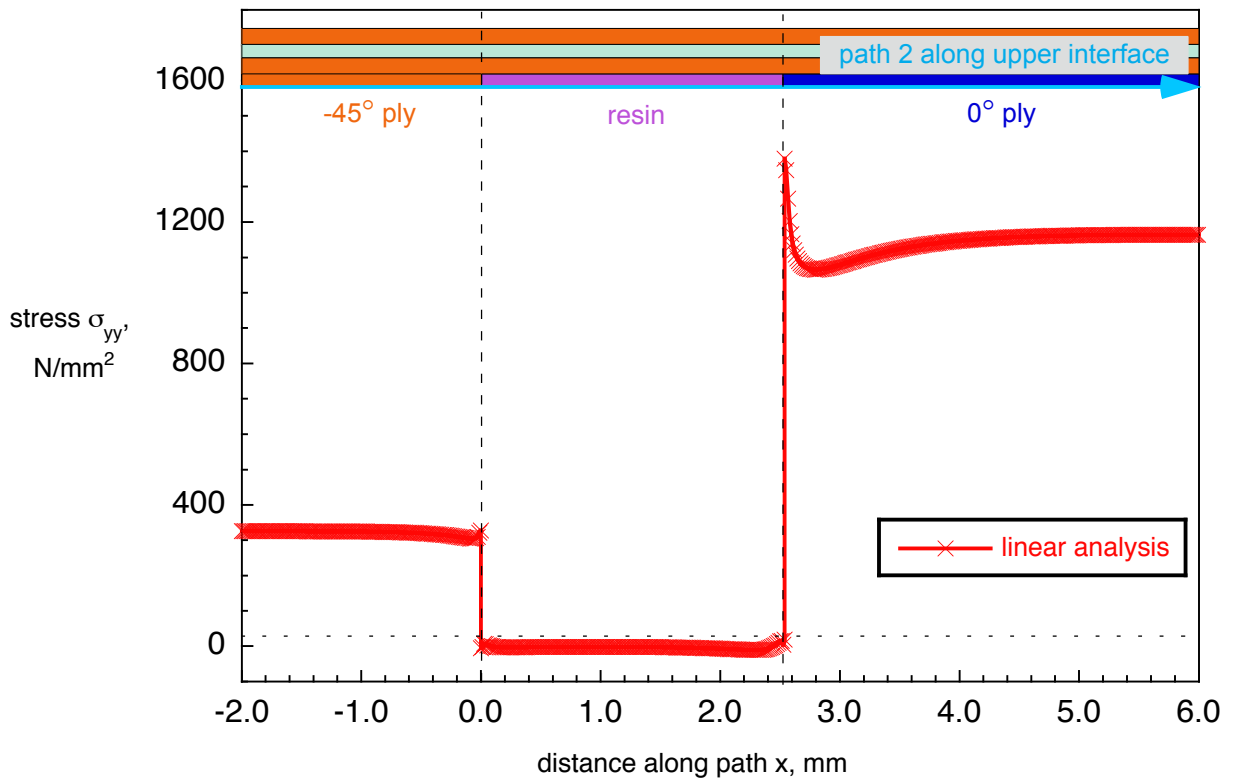


Figure 35. Stress σ_{yy} along path 2 in upper 0° ply interface for multiple overlaps.

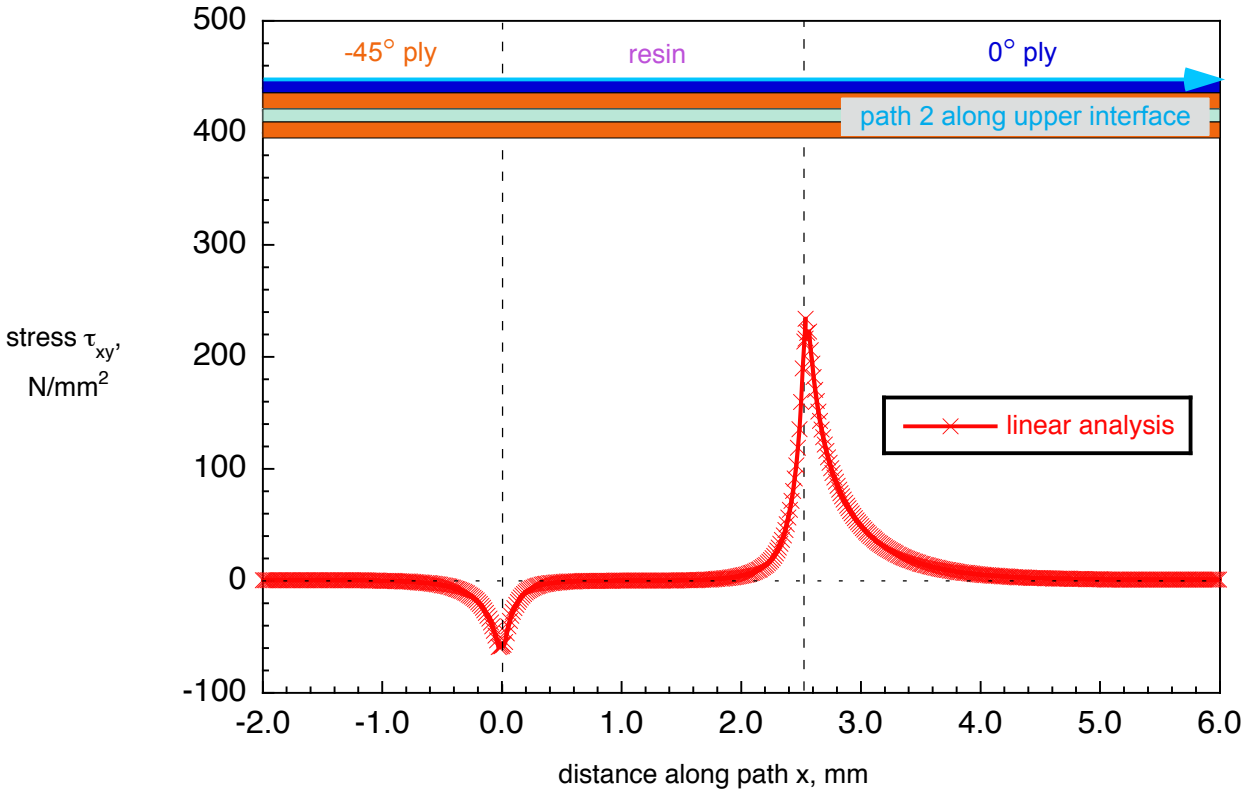


Figure 36. Stress τ_{xy} along path 2 in lower 0° ply interface for multiple overlaps.

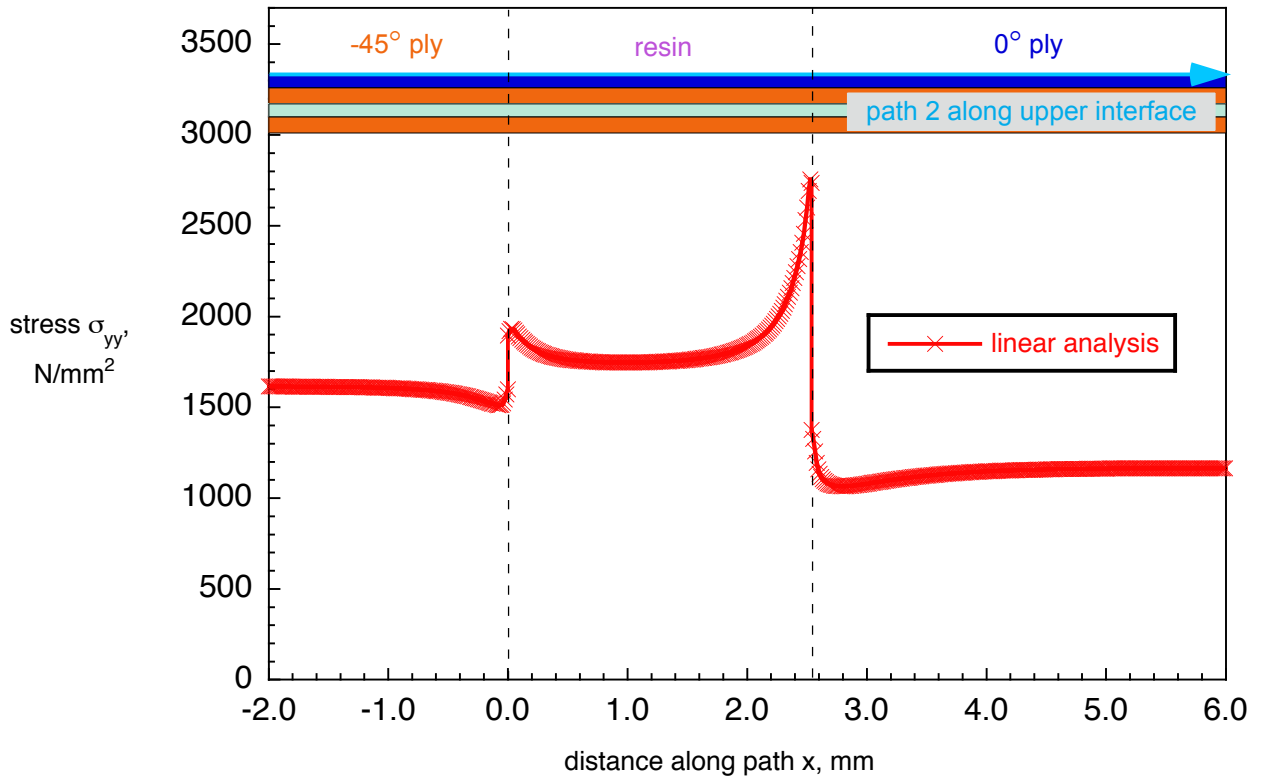


Figure 37. Stress σ_{yy} along path 2 in lower 0° ply interface for multiple overlaps.

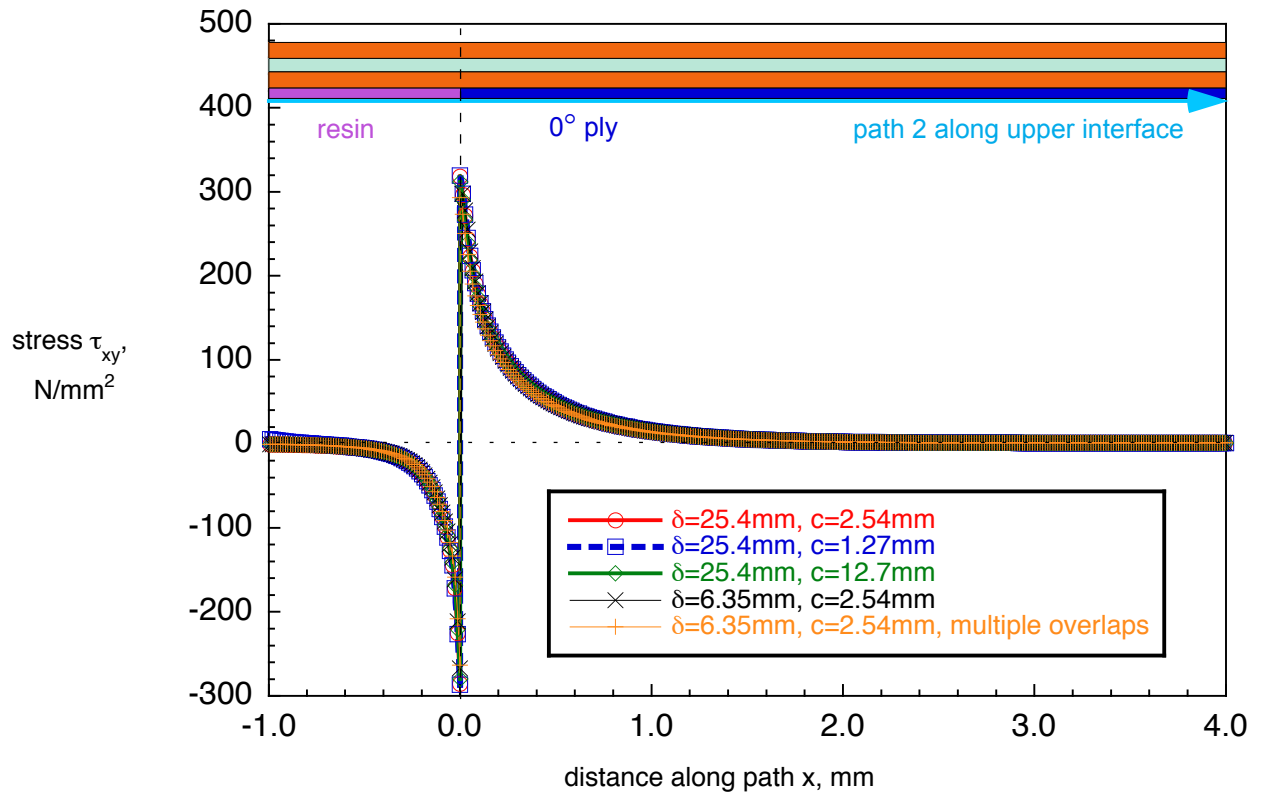


Figure 38. Stress τ_{xy} along path 2 in upper 0° ply interface for all configurations studied.

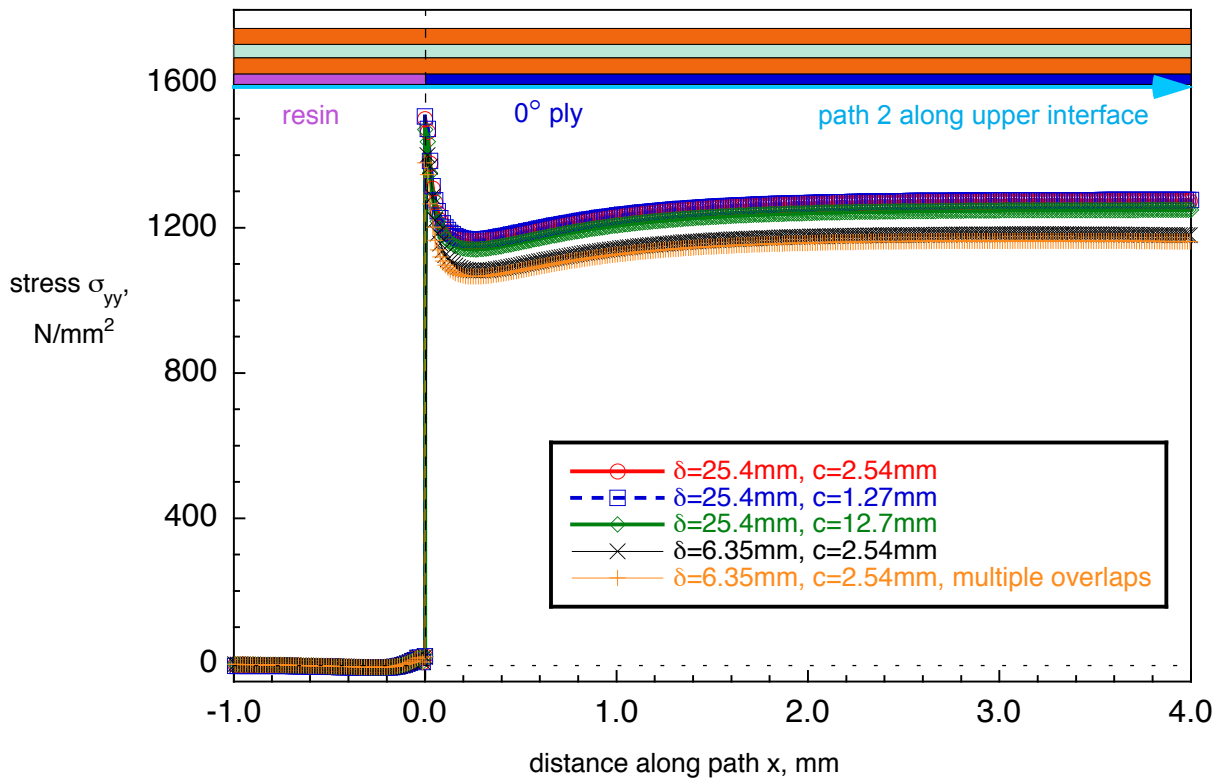


Figure 39. Stress σ_{yy} along path 2 in upper 0° ply interface for all configurations studied.

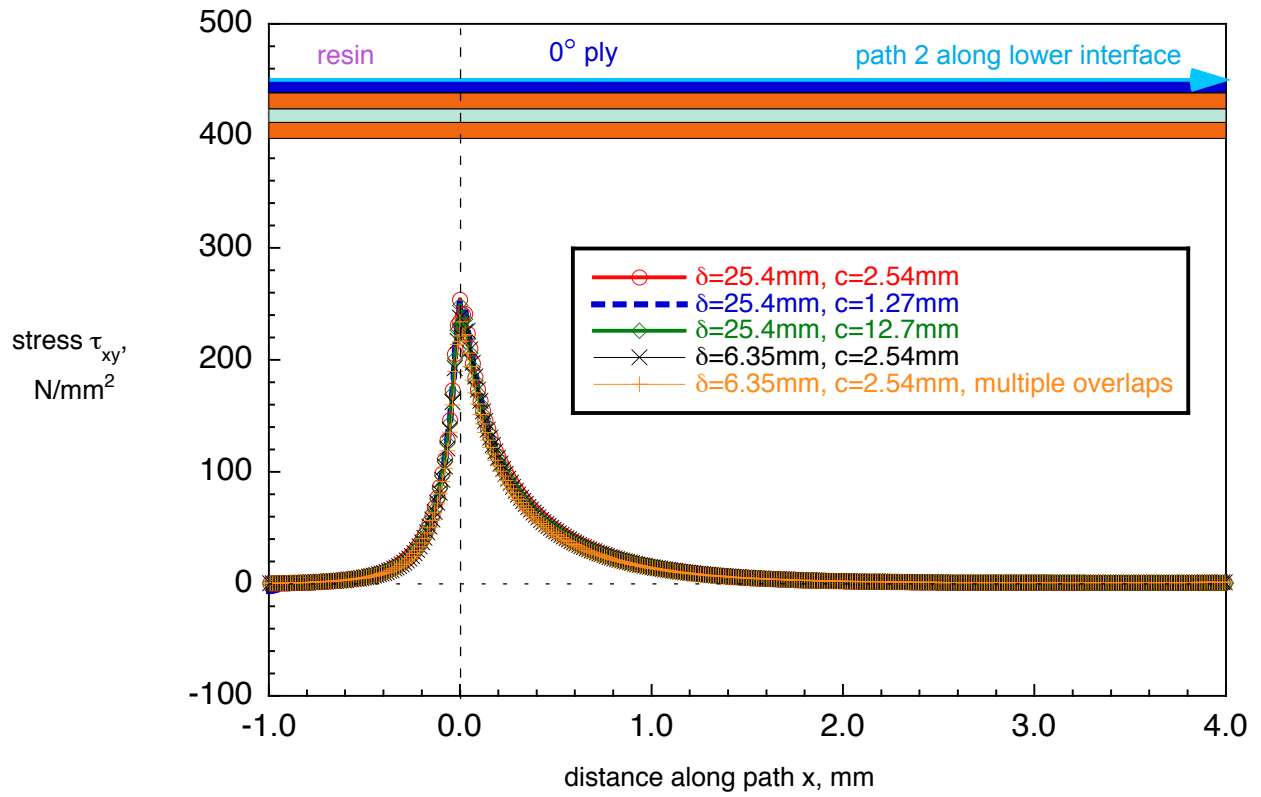


Figure 40. Stress τ_{xy} along path 2 in lower 0° ply interface for all configurations studied.

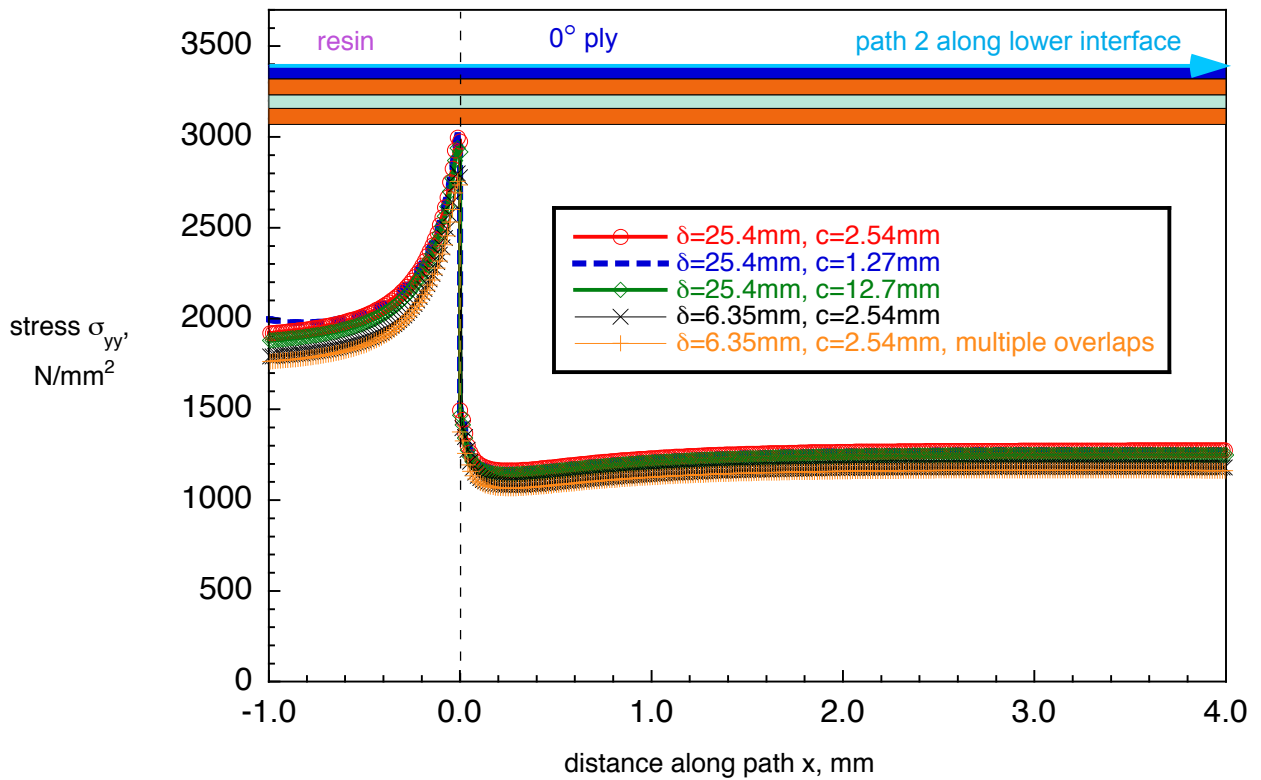


Figure 41. Stress σ_{yy} along path 2 in lower 0° ply interface for all configurations studied.

APPENDIX A: SELECTION OF MATERIAL DATA

A study was performed to gather material data published in the open literature. The goal was to obtain a complete set of input data for one material which could be used in a finite element analysis. The material set should include the ply thickness, h , the elastic moduli, E_{ii} , G_{ij} , and ν_{ij} , the glass transition temperature or stress free temperature, T_g , as well as the hygrothermal coefficients of expansion α_i and β_i . None of the sources queried [5-22] provided a full set of data for one material. The most complete data sets were found for IM7/8552 listed in Table A-I. The data in the last column (boldface blue font) were selected for the current study. The pooled data are listed in the right column of Table A-I (boldface blue) and are identical to the values shown in Table I. Data for other materials are listed in Tables A-II through A-IV for completeness. The coefficients for moisture expansion, β_i , for IM7/8552 could not be found in the open literature. Therefore, the data for IM7/8551-7 listed in Table A-IV were used together with the T_g for that material (highlighted in boldface blue) and included in the right column of Table A-I to make up a complete set of input data.

TABLE A-I. MATERIAL PROPERTIES FOR IM7/8552 FROM DIFFERENT SOURCES

Property	[5]	[6]	[7]	[8]	[9,11]	[9,11]	[10]	[12, 13]	Selected data
<i>Fiber Vol. %</i>			59.1	60	57.4	60.3	57.7	57.3	
<i>h [mm]</i>	0.15		0.125	0.125	0.185	0.152	0.131	0.183	0.15
<i>E₁₁ [GPa]</i>	150	161	171.4	165		162	164	162	161
<i>E₂₂ [GPa]</i>	10.7	11.38	9.08	9.00			12	8.97	11.38
<i>E₃₃ [GPa]</i>	10.7	11.38		9.00	9.3				11.38
<i>ν₁₂</i>	0.33	0.32	0.32	0.34		0.311		0.316	0.32
<i>ν₁₃</i>	0.33	0.32		0.34					0.32
<i>ν₂₃</i>	0.45	0.45		0.5	0.475				0.45
<i>G₁₂ [GPa]</i>	4.8	5.2	5.3	5.6	4.4	5		4.7	5.2
<i>G₁₃ [GPa]</i>	4.8	5.2		5.6					5.2
<i>G₂₃ [GPa]</i>	3.4	3.9		2.8	2.3				3.9
<i>G_{Ic} [kJ/m²]</i>		0.212	0.277	0.277					0.212
<i>G_{IIc} [kJ/m²]</i>		0.774	0.788	0.788					0.774
<i>η</i>		2.1	1.634						2.1
<i>T_g (dry) [°C]</i>			ΔT=155	ΔT=154	177	200	200	208	177⁺⁺
<i>T_g (wet) [°C]</i>					143	154	154	161	143
<i>α₁ [1/°C]</i>	-9 10⁻⁷		-5.5 10 ⁻⁶	-1 10 ⁻⁶					-9 10⁻⁷
<i>α₂ [1/°C]</i>	2.88 10⁻⁵		2.5 10 ⁻⁵	1.8 10 ⁻⁵					2.88 10⁻⁵
<i>α₃ [1/°C]</i>	2.88 10⁻⁵			1.8 10 ⁻⁵					2.88 10⁻⁵
<i>β₁ [1/%M]</i>									0
<i>β₂ [1/%M]</i>									3310 10⁻⁶
<i>ρ [g/cm³]</i>	1.55				1.58	1.58	1.57	1.58	1.55
<i>[g/m²]</i>					190	160		190	

*The material properties are given with reference to the ply coordinate axes where index 11 denotes the ply principal axis that coincides with the direction of maximum in-plane Young's modulus (fiber direction). Index 22 denotes the direction transverse to the fiber in the plane of the lamina and index 33 the direction perpendicular to the plane of the lamina.

TABLE A-II. MATERIAL PROPERTIES FROM DIFFERENT SOURCES

Property	[14]	[15] AS4/8552	[16, 17] grph/epxy	[1] IM6/3501-6	[3] T300/F-155
<i>Fiber Vol. %</i>				57	57
<i>h [mm]</i>			0.127		
<i>E₁₁ [GPa]</i>			135	149.2	127.3
<i>E₂₂ [GPa]</i>			11	8.8	7.9
<i>E₃₃ [GPa]</i>					
<i>ν₁₂</i>			0.301	0.34	0.29
<i>ν₁₃</i>					
<i>ν₂₃</i>				0.42	0.42
<i>G₁₂ [GPa]</i>			5.8	4.5	3.5
<i>G₁₃ [GPa]</i>					
<i>G₂₃ [GPa]</i>				3.1	2.8
<i>G_{Ic} [kJ/m²]</i>					
<i>G_{IIc} [kJ/m²]</i>					
<i>η</i>					
<i>T_g (dry) [°C]</i>		215	177 ⁺⁺	177 ⁺⁺ 171.1 [†]	121 ⁺⁺ 119.3 [†]
<i>T_g (wet) [°C]</i>					
<i>α₁ [1/°C]</i>	0	6 10 ⁻⁷	-0.41 10 ⁻⁶	-0.54 10 ⁻⁶	0.36 10 ⁻⁶
<i>α₂ [1/°C]</i>	3 10 ⁻⁵	2.86 10 ⁻⁵	26.8 10 ⁻⁶	30.6 10 ⁻⁶	27.9 10 ⁻⁶
<i>α₃ [1/°C]</i>	3 10 ⁻⁵				
<i>β₁ [1/%M]</i>			0	0	0
<i>β₂ [1/%M]</i>			5560 10 ⁻⁶	2860 10 ⁻⁶	2530 10 ⁻⁶
<i>ρ [g/cm³]</i>					
<i>[g/m²]</i>					

*The material properties are given with reference to the ply coordinate axes where index 11 denotes the ply principal axis that coincides with the direction of maximum in-plane Young's modulus (fiber direction). Index 22 denotes the direction transverse to the fiber in the plane of the lamina and index 33 the direction perpendicular to the plane of the lamina.

[†]To conform to experimental observations, it is assumed there is no expansion below 0.4% absorbed moisture [15]

⁺⁺cure temperature

^{††}stress-free temperature

TABLE A-III. MATERIAL PROPERTIES FROM DIFFERENT SOURCES

Property	[1] IM7/8551-7	[3] GY70/339	[3] T300/934
<i>Fiber Vol. %</i>	57		
<i>h [mm]</i>			
<i>E₁₁ [GPa]</i>	151.6	290	145
<i>E₂₂ [GPa]</i>	7.9	6.1	10.3
<i>E₃₃ [GPa]</i>			
<i>ν₁₂</i>	0.34	0.31	0.29
<i>ν₁₃</i>			
<i>ν₂₃</i>	0.42		
<i>G₁₂ [GPa]</i>	3.9	4.1	4.8
<i>G₁₃ [GPa]</i>			
<i>G₂₃ [GPa]</i>	2.6		
<i>G_{Ic} [kJ/m²]</i>			
<i>G_{IIc} [kJ/m²]</i>			
<i>η</i>			
<i>T_g (dry) [°C]</i>	177 ⁺⁺ 151.7 [†]		
<i>T_g (wet) [°C]</i>			
<i>α₁ [1/°C]</i>	0.36 10 ⁻⁶	-0.72 10 ⁻⁶	-0.09 10 ⁻⁶
<i>α₂ [1/°C]</i>	28.8 10 ⁻⁶	25.2 10 ⁻⁶	29.7 10 ⁻⁶
<i>α₃ [1/°C]</i>			
<i>β₁ [1/%M]</i>	0		
<i>β₂ [1/%M]</i>	3310 10 ⁻⁶	+5400 10 ⁻⁶	+5400 10 ⁻⁶
<i>ρ [g/cm³]</i>			
<i>[g/m²]</i>			

*The material properties are given with reference to the ply coordinate axes where index 11 denotes the ply principal axis that coincides with the direction of maximum in-plane Young's modulus (fiber direction). Index 22 denotes the direction transverse to the fiber in the plane of the lamina and index 33 the direction perpendicular to the plane of the lamina.

⁺To conform to experimental observations, it is assumed there is no expansion below 0.4% absorbed moisture [15]

⁺⁺cure temperature

[†]stress-free temperature

TABLE A-IV. MATERIAL PROPERTIES FROM DIFFERENT SOURCES

Property	[18, 19] T300/5208	[18, 19] AS4/3501	[20] IM7/8551-7
<i>Fiber Vol. %</i>			
<i>h</i> [mm]			0.127
<i>E</i> ₁₁ [GPa]			165.5
<i>E</i> ₂₂ [GPa]			8.3
<i>E</i> ₃₃ [GPa]			
<i>ν</i> ₁₂			0.18
<i>ν</i> ₁₃			9.3 10 ⁻³
<i>ν</i> ₂₃			
<i>G</i> ₁₂ [GPa]			6.2
<i>G</i> ₁₃ [GPa]			
<i>G</i> ₂₃ [GPa]			
<i>G</i> _{Ic} [kJ/m ²]			
<i>G</i> _{IIc} [kJ/m ²]			
<i>η</i>			
<i>T_g</i> (dry) [°C]		177	
<i>T_g</i> (wet) [°C]			
<i>α</i> ₁ [1/K]	0.02 10 ⁻⁶	-0.3 10 ⁻⁶	-0.04 10 ⁻⁶
<i>α</i> ₂ [1/K]	22.5 10 ⁻⁶	28.1 10 ⁻⁶	18 10 ⁻⁶
<i>α</i> ₃ [1/K]			
<i>β</i> ₁ [1/M]	0.0	0.0	0.01
<i>β</i> ₂ [1/M]	0.6	0.44	0.35
<i>ρ</i> [g/cm ³]		1.6	1.5
[g/m ²]			

*The material properties are given with reference to the ply coordinate axes where index 11 denotes the ply principal axis that coincides with the direction of maximum in-plane Young's modulus (fiber direction). Index 22 denotes the direction transverse to the fiber in the plane of the lamina and index 33 the direction perpendicular to the plane of the lamina.

APPENDIX – B: FINITE ELEMENT MESH GENERATION

Jointmesh - A Fortran based routine to generate Abaqus/Standard® input decks for configurations with overlaps and gaps

A FORTRAN routine (**jointmesh.f**) was developed, which allows the automatic creation of an Abaqus/Standard® [24] input deck (.inp) and thus simplifies quick modifications in specimen dimensions and mesh size. The specimen dimensions and prescribed displacements as well as material data, ply orientation, and stacking sequence are provided by the user in a simple data file that is read by the routine at the beginning of the execution. The user can input up to 100 sections of arbitrary length in the y-direction, as shown in Figure B1, where an example with 15 sections in the y-direction is shown. Please note that in the coordinate system used, x is the through-thickness direction and y is in length direction. For a three-dimensional problem, z is the width direction. The number of sections in the x and z-direction currently remain hard-coded and limited to three, however, the number of elements in all sections may be selected freely by the user. Thus, a multitude of zones along the length (y-direction) and through the thickness (x-direction) may be defined as shown in Figures B1 and B2. The user can assign arbitrary material properties (up to 100) and orientations (up to 9) to each of the zones. The zones extend across the width (z-direction) as shown in Figure B2 for a three-dimensional model. The functions of the main program and the subroutines are briefly described in the following paragraphs together with the data input required from the user. An example data input file (**mesh_input.data**) and a shortened Abaqus/Standard® input deck (**s_multi_gaps_linear.inp**) are provided in the following sections.

Main Program (JOINTMESH)

The main program reads the input data from the file **mesh_input.data**, checks the validity of this data and makes the calls to the appropriate subroutines. As output, a file is created - qus/Standard® format which contains the nodal point coordinates, the element connectivity, material data as well as load and boundary conditions. The file can be used as input directly for a finite element analysis in Abaqus/Standard® [24].

Data Input

The data input file **mesh_input.data** is the only user required input. All variables which are necessary to generate the finite element model including the external loading, the boundary conditions and the material data are defined here.

- **nwrite**: switch to obtain additional informational output to the screen during model generation
- **htext**: problem name header, max. 60 characters
- **utext**: unit header, max. 60 characters
- **abtext**: name of output file to which model data will be written, max. 20 characters
- **eltype**: type of element used in the FE-model, max. eight characters
 - two dimensional four-node element in Abaqus/Standard® [24]
 - Abaqus/Standard® (plane-strain): CPE4, CPE4I, CPE4H, CPE4R, CPE4RH, CPE4IH
 - Abaqus/Standard® (plane-stress): CPS4, CPS4I, CPS4R
 - two dimensional eight-node element

- Abaqus/Standard[®] (plane-strain): CPE8, CPE8R, CPE8H, CPE8RH
 - Abaqus/Standard[®] (plane-stress): CPS8, CPS8R
- three dimensional eight-node brick element
 - Abaqus/Standard[®]: C3D8, C3D8H, C3D8I, C3D8IH, C3D8R, C3D8RH
- three dimensional twenty-node element
 - Abaqus/Standard[®]: C3D20, C3D20H, C3D20R, C3D20RH
- **n**: number of y- segments as shown in Figures B1 (15 here - max. 100)
- **YC (N)** : array defining length (y) segments of specimen as shown in Figure B1
- **NY (N)** : array defining number of elements in corresponding length segment
- **XB (3)** : array defining thickness (x) segments of specimen as shown in Figure B1
- **NX (3)** : array defining number of elements in corresponding thickness segment
- **ZA (3)** : array defining width (z) segments of specimen as shown in Figure B2
- **NZ (3)** : array defining number of elements in corresponding width segment
- **nxyst (3)** : array defining the start values for element zones
- **nxystend (3)** : array defining the end values for element zones
- **zst (3)** : array defining start values for z
- **yst (3)** : array defining start values for y
- **xst (3)** : array defining start values for x
- with the input up to this point, the mesh is generated and the element sets in Abaqus/Standard[®] are defined as shown in Figure B2b.
 - **matnum**: number of materials in the model (a maximum of 100 materials can be defined using the following lines)
- the following block of input has to be repeated **matnum** times (once for each material defined in the model)
 - **mtext**: material name. If the user chooses a value **matnum>100** to act as a switch, a single line with the name of a file needs to be provided here which will be included in the Abaqus/Standard input file **abtext**. This file has to be a Abaqus/Standard input file **.inp** and contain all the necessary data to define a material, orientations and element sections.
 - **naniso**: switch to determine material type
 - naniso=0**: isotropic material, two values E and ν expected (**ianiso=2**)
 - naniso=1**: 2D laminate properties, four values expected (**ianiso=4**)
 - naniso=2**: engineering constants, nine values expected (**ianiso=9**)
 - naniso=3**: orthotropic material, nine values expected (**ianiso=9**)
 - naniso=4**: anisotropic material, 21 values expected (**ianiso=21**)
 - **matdat (ianiso)** : material data, max. 21 values according to Abaqus/Standard[®] [24].
 - **alpha (3)** : coefficients of thermal expansion for the material
 - **beta (3)** : coefficients of moisture expansion for the material
 - **no**: number of orientations for the material (maximum 9)
- the following block of input is repeated for each material
 - **sys (6)** : orientation of the material's x' and y' direction

- **nrot**: axis about which the material layers are rotated
- **orient (no)**: array containing angles of rotation defined for each material layer, max. 9 values
- This ends the input for materials. If the user chooses a value **matnum>100** to act as a switch, a single line with the name of a file needs to be provided here which will be included in the Abaqus/Standard[®] input file **abtext**. This file has to be a Abaqus/Standard[®] input file **.inp** and contain all the necessary data to define a material, orientations and element sections.
- the following line of input has to be repeated **nelx=nx (1) +nx (2) +nx (3)** -times for each element layer in the x-direction
 - **mzone (n)**: array/line with n-values containing the material number and orientation number for each material zone in the model (e.g. 41 is material 4 with orientation 1; 10 is material 1 with orientation 0)
 - **thickn**: thickness value for 2D type elements
 - **nonlin**: switch to perform non-linear analysis in Abaqus/Standard[®] for **nonlin=1**
 - **itnum**: Abaqus/Standard[®]: maximum number of iterations
 - **r (4)**: Abaqus/Standard[®]: increment values
 - **nhtl (3)**: switch to activate analysis for mechanical, temperature and moisture loads
 - **htl (5)**: hygrothermal and mechanical load input
 - initial temperature condition (Abaqus/Standard[®] input shown in Figure B3b)
 - current temperature (Abaqus/Standard[®] input shown in Figure B3b)
 - initial moisture condition (Abaqus/Standard[®] input shown in Figure B3c)
 - current moisture condition (Abaqus/Standard[®] input shown in Figure B3c)
 - applied displacement (Abaqus/Standard[®] input shown in Figure B3a)

An example file is provided in the next section.

Subroutine abelem

This subroutine is used to convert the element names used in Abaqus/Standard[®] to internally used generic type numbers.

call abelem (eltype, nelpt, midnode, ntype, nwrite)

- Input:
 - **eltype**: element name or type in finite element code (maximum eight characters)
 - **nwrite**: switch to obtain additional informational output to the screen during model generation
- Output:
 - **ntype**: internal element number
 - 204: two dimensional four-node element
 - 208: two dimensional eight-node element
 - 308: three dimensional eight-node element
 - 320: three dimensional twenty-node element
 - **nelpt**: number of nodes in this element as stored by the finite element code
 - **midnode**: for elements containing midside nodes **midnode=2**

Subroutine header

This subroutine writes the header line to the Abaqus/Standard[®] input file (**abtext**).

```
call header(ifeicode,htext,utext,iunit)
```

- Input
 - **ifeicode**: switch to determine which FE code will be used (this option is currently not used; **ifeicode=1** hard-coded for Abaqus/Standard[®])
 - **htext**: problem name header, max. 60 characters
 - **utext**: unit header, max. 60 characters
 - **iunit**: fortran unit number to be supplied by the user (this option is currently not used; **iunit=50** hard-coded).

Subroutine genpco

This subroutine computes the nodal point coordinates for a three dimensional rectangular mesh in space. The ***NODE** keyword and the nodal point coordinates are written to the Abaqus/Standard[®] input file (**abtext**).

```
call genpco(XB,YC,NX,NY,M,XST,YST,IUNIT,N,ZA,  
           NZ,ZST,midnode,ifeicode,nwrite,ntype)
```

- Input
 - **XB (3)** : array defining thickness (x) segments of specimen
 - **YC (5)** : array defining length (y) segments of specimen
 - **NX (3)** : array defining number of elements in corresponding thickness segment
 - **NY (5)** : array defining number of elements in corresponding length segment
 - **M**: size of array **XB (M)** , **XST (M)** , **YST (M)** , **NX (M)**
 - **XST (3)** : start value
 - **YST (3)** : start value
 - **IUNIT**: fortran unit number to be supplied by the user (this option is currently not used; **iunit=50** hard-coded).
 - **N**: size of array **yc(n)**, **ny(n)**
 - **ZA (3)** : array defining width (z) segments of specimen
 - **NZ (3)** : array defining number of elements in corresponding width segment
 - **ZST (3)** : start value
 - **midnode**: for elements containing midside nodes **midnode=2**
 - **ifeicode**: switch to determine which FE code will be used (this option is currently not used; **ifeicode=1** hard-coded for Abaqus/Standard[®])
 - **nwrite**: switch to obtain additional output
 - **ntype**: internal element number

Subroutine net2d

This subroutine creates the finite element mesh by assigning nodal point numbers to a rectangular mesh consisting of four or eight-node 2D elements. The ***ELEMENT** keyword and the element connectivity are written to the Abaqus/Standard[®] input file (**abtext**).

```
call net2d(NX,NY,M,N,IUNIT,ELNOD,NELPT,nxyst, nxyend, midnode,  
ntype, eltype,ifecode,nwrite)
```

- Input
 - **NX(3)** : array defining number of elements in corresponding thickness segment
 - **NY(5)** : array defining number of elements in corresponding length segment
 - **M**: size of array xb(m), xst(m),yst(m),nx(m)
 - **N**: size of array yc(n), ny(n)
 - **IUNIT**: fortran unit number to be supplied by the user (this option is currently not used; **iunit=50** hard-coded).
 - **ELNOD**: array of element topology
 - **NELPT**: number of nodal points in element, size of array elnod
 - **nxyst(3)** : array defining the start values for element zones
 - **nxyend(3)** : array defining the end values for element zones
 - **midnode**: for elements containing midside nodes **midnode=2**
 - **ntype**: internal element number
 - **eltype**: type of element used in the FE-model, max. Eight characters
 - **ifecode**: **ifecode**: switch to determine which FE code will be used (this option is currently not used; **ifecode=1** hard-coded for Abaqus/Standard[®])
 - **nwrite**: switch to obtain additional output

Subroutine net3d

This subroutine creates the finite element mesh by assigning nodal point numbers to a rectangular mesh consisting of eight or twenty-node 3D brick elements. The ***ELEMENT** keyword and the element connectivity are written to the Abaqus/Standard[®] input file (**abtext**).

```
call net3d(NX,NY,NZ,M,N,IUNIT,ELNOD,NELPT,nxyst,nxyend  
midnode,ntype,eltype,ifecode,nwrite)
```

- Input
 - **NX(3)** : array defining number of elements in corresponding thickness segment
 - **NY(5)** : array defining number of elements in corresponding length segment
 - **NZ(3)** : array defining number of elements in corresponding width segment
 - **M**: size of array xb(m), xst(m),yst(m),nx(m)
 - **N**: size of array yc(n), ny(n)
 - **IUNIT**: fortran unit number to be supplied by the user (this option is currently not used; **iunit=50** hard-coded).
 - **ELNOD**: array of element topology

- **NELPT**: number of nodal points in element, size of array elnod
- **nxyst(3)**: array defining the start values for element zones
- **nxyend(3)**: array defining the end values for element zones
- **midnode**: for elements containing midside nodes **midnode=2**
- **ntype**: internal element number
- **eltype**: type of element used in the FE-model, max. Eight characters
- **ifecode**: **ifecode**: switch to determine which FE code will be used (this option is currently not used; **ifecode=1** hard-coded for Abaqus/Standard[®])
- **nwrite**: switch to obtain additional output

Subroutine material

This subroutine writes the material data ***MATERIAL**, ***ELASTIC** ... or ***INCLUDE=matfile** keywords to the Abaqus/Standard[®] input file (**abtext**). The ***ORIENTATION** as well as ***SOLID SECTION** keywords are also written to the Abaqus/Standard[®] input file.

```
call material(naniso,matdat,sys,nrot,orient,mm,nx,m,thickn,
iunit,ntype,matfile,alpha,beta,mx,matnum,no,mzone,mtext,nn,N)
```

- Input
 - **naniso**: switch to determine material type
 - **matdat**: material data
 - **sys(6)**: orientation of the material's x' and y' direction
 - **nrot**: axis about which the material layers are rotated
 - **orient(20)**: array containing the angles of rotation of each material layer, max. 20 values
 - **mm**: number of layers or orientations
 - **nx(3)**: array defining number of elements in corresponding thickness segment
 - **m**: size of array xb(m), xst(m),yst(m),nx(m)
 - **thickn**: element thickness for 2D analysis
 - **iunit**: fortran unit number to be supplied by the user (this option is currently not used; **iunit=50** hard-coded).
 - **ntype**: internal element number
 - **matfile**: file name where Abaqus/Standard[®] material data are stored (for naniso=4), max. 20 characters
 - **alpha(3)**: coefficients of thermal expansion
 - **beta(3)**: coefficients of moisture expansion
 - **mx**: length of material array
 - **matnum**: number of materials used
 - **no**: number orientations defined for a material
 - **mzone(n)**: array/line with n-values containing the material number and orientation number for each material zone in the model

- **mtext**: material name
- **nn**: maximum size of array yc(n), ny(n). Hard-coded n=100
- **N**: actual size of array yc(n), ny(n)

Subroutine abhist

This subroutine sets up the Abaqus/Standard[®] “history” part of the input file (**abtext**).

The ***STEP**, ***END STEP** as well as ***STATIC** keywords are written to the input file together with keywords that specify the hygro-thermal and mechanical loads. Keywords that specify the requested output are also written to the input file.

```
call abhist(NX,NY,NZ,ZA,M,N,R,NFRD,IUNIT,nonlin,htl,
           nodef,itnum,ntype,midnode,ifecode,nwrite,nhtl)
```

- Input
 - **NX (3)** : array defining number of elements in corresponding thickness segment
 - **NY (5)** : array defining number of elements in corresponding length segment
 - **NZ (3)** : array defining number of elements in corresponding width segment
 - **ZA (3)** : array defining width (z) segments of specimen
 - **M**: size of array xb(m), xst(m), yst(m), nx(m)
 - **N**: size of array yc(n), ny(n)
 - **R (4)** : Abaqus/Standard[®]: increment values
 - **NFRD**: number of degrees of freedom
 - **IUNIT**: fortran unit number to be supplied by the user (this option is currently not used; **iunit=50** hard-coded).
 - **nonlin**: switch to non-linear analysis for **nonlin=1**
 - **htl (5)** : hygrothermal and mechanical load input
 - **nodef**: **array**
 - **itnum**: Abaqus/Standard[®]: maximum number of iterations
 - **ntype**: internal element number
 - **midnode**: for elements containing midside nodes **midnode=2**
 - **ifecode**: switch to determine which FE code will be used
 - **nwrite**: switch to obtain additional output
 - **nhtl (3)** : switch to activate analysis for mechanical, temperature and moisture loads .

Example user input file: mesh_input.data

This example file refers to the problem shown in Figure B1. The input shown is for generating a model that contains 15 y-segments ($N=15$) and a total of 28 element layers ($NX(3)=(2, 24, 2)$) across the thickness (x-direction). Four materials are defined for this example ($MATNUM=4$). Three material definitions are used to define the 0° , $\pm 45^\circ$ and 90° orientations of the IM-7/8552 tape and one material for the 8552 resin. For the definition of the IM-7/8552 tape plies, laminate properties are supplied ($NANISO=1$). The 8552 resin material is isotropic ($NANISO=0$). Only for the IM-7/8552 tape plies, one orientation each has been defined ($no=1$). For each of the 28 element layers across the thickness (x-direction), input is provided to assign a material and orientation to each of the y-segements along the length. The first digit represents the material and the second digit the orientation. Therefore, 31 denotes that material data from material 3 (IM7/8552) and orientation 1 ($\pm 45^\circ$) are assigned to that particular section. Since material 4 (8552 resin) is isotropic, no orientations have been assigned, and the sequence 40 is used.

```
'NWRITE: WRITE SWITCH FOR OUTPUT COMMENT'      3
'HEADER-TEXT: max 60 characters'                'section - delta=6.35 mm, c=2.54 mm, multi gaps'
'UNIT-TEXT: max 60 characters'                  'units: mm, N, MPa'
'name of output file max 20 characters'         's_multi_gaps_linear.inp'
'Element Type C3D20,CPE4, etc'                 'CPS8'
'N: number of Y-SEGMENTS'                      15
'YC: LENGTH of Y-SEGMENTS'                    14.605  2.54  6.35  2.54  3.81  2.54  2.54  6.35
2.54  2.54  3.81  2.54  6.35  2.54  14.605
'NY: NUMBER OF ELEMENTS IN Y-SEGMENTS'        146  25  63  25  144  96  96  240  96  96  144  25
63  25  146
'XB: length of x-segments'                    0.3  0.6  0.3
'NX: NUMBER OF ELEMENTS IN X-SEGMENTS'        2  24  2
'ZA: LENGTH of z-segments'                    5.0  15.4  5.0
'NZ: NUMBER OF ELEMENTS IN Z-SEGMENTS'        10  15  10
'NXYST: first y-segment with elements'        1  1  1
'NXYEND: last y-segment with elements'        15  15  15
'ZST: start value'                            0.  0.  0.
'YST: start value'                            76.2  0.  0.
'XST: start value'                            0.  0.  0.
'MATNUM: number of materials in the model'     4
'material name'                                'IM7/8552-0'
'NANISO: =0:iso,=1:lam,=2:eng,=3:ort,=4:ani'  1
'Material Input E11, ... max. 21 values'       160523.  14386.  0.467  5171.
'alpha: coefficients of thermal expansion'      -9.E-7  2.88E-5  2.88E-5
'beta: coefficients of moisture expansion'      0.  3310.E-6  3310.E-6
'number of orientations'                       1
'SYS: material system, 6 values'               0.0  -1.0  0.0  1.0  0.0  0.0
'nrot: axis about which material is rotated'    3
'orient: orientation of material in layers'     0.
'material name'                                'IM7/8552-90'
'NANISO: =0:iso,=1:lam,=2:eng,=3:ort,=4:ani'  1
'Material Input E11, ... max. 21 values'       9809.  12422.  0.461  3923.
'alpha: coefficients of thermal expansion'      2.88E-5  2.88E-5  -9.E-7
'beta: coefficients of moisture expansion'      3310.E-6  3310.E-6  0.
'number of orientations'                       1
'SYS: material system, 6 values'               0.0  -1.0  0.0  1.0  0.0  0.0
'nrot: axis about which material is rotated'    3
'orient: orientation of material in layers'     0.
'material name'                                'IM7/8552-45'
'NANISO: =0:iso,=1:lam,=2:eng,=3:ort,=4:ani'  1
'Material Input E11, ... max. 21 values'       32381.  13810.  0.464  4547.
'alpha: coefficients of thermal expansion'      1.39E-5  2.88E-5  1.39E-5
'beta: coefficients of moisture expansion'      1655.E-6  3310.E-6  1655.E-6
'number of orientations'                       1
'SYS: material system, 6 values'               0.0  -1.0  0.0  1.0  0.0  0.0
'nrot: axis about which material is rotated'    3
```



```

'orient: orientation of material in layers'      0.
'material name'                                'R8552'
'NANISO: =0:iso,=1:lam,=2:eng,=3:ort,=4:ani'   0
'Material Input E11, ... max. 21 values'       11380. 0.3
'alpha: coefficients of thermal expansion'      2.88E-5
'beta: coefficients of moisture expansion'      3310.E-6
'number of orientations'                       0
'material zones x(1) '                        31 31 31 31 31 31 31 31 31 31 31 31 31 31 31
'material zones x(2) '                        21 21 21 21 21 21 21 21 21 21 21 21 21 40 21
'material zones x(3) '                        31 31 31 31 31 31 31 31 31 31 31 40 31 31 31
'material zones x(4) '                        31 31 31 31 31 31 31 31 31 31 31 40 31 31 31
'material zones x(5) '                        31 31 31 31 31 31 31 31 31 31 31 40 31 31 31
'material zones x(6) '                        31 31 31 31 31 31 31 31 31 31 31 40 31 31 31
'material zones x(7) '                        31 31 31 31 31 31 31 31 31 31 31 40 31 31 31
'material zones x(8) '                        31 31 31 31 31 31 31 31 31 31 31 40 31 31 31
'material zones x(9) '                        11 11 11 11 11 11 11 11 40 31 31 31 31 31 31
'material zones x(10) '                      11 11 11 11 11 11 11 11 40 31 31 31 31 31 31
'material zones x(11) '                      11 11 11 11 11 11 11 11 40 31 31 31 31 31 31
'material zones x(12) '                      11 11 11 11 11 11 11 11 40 31 31 31 31 31 31
'material zones x(13) '                      11 11 11 11 11 11 11 11 40 31 31 31 31 31 31
'material zones x(14) '                      11 11 11 11 11 11 11 11 40 31 31 31 31 31 31
'material zones x(15) '                      31 31 31 31 31 31 40 11 11 11 11 11 11 11 11
'material zones x(16) '                      31 31 31 31 31 31 40 11 11 11 11 11 11 11 11
'material zones x(17) '                      31 31 31 31 31 31 40 11 11 11 11 11 11 11 11
'material zones x(18) '                      31 31 31 31 31 31 40 11 11 11 11 11 11 11 11
'material zones x(19) '                      31 31 31 31 31 31 40 11 11 11 11 11 11 11 11
'material zones x(20) '                      31 31 31 31 31 31 40 11 11 11 11 11 11 11 11
'material zones x(21) '                      21 21 21 40 31 31 31 31 31 31 31 31 31 31 31
'material zones x(22) '                      21 21 21 40 31 31 31 31 31 31 31 31 31 31 31
'material zones x(23) '                      21 21 21 40 31 31 31 31 31 31 31 31 31 31 31
'material zones x(24) '                      21 21 21 40 31 31 31 31 31 31 31 31 31 31 31
'material zones x(25) '                      21 21 21 40 31 31 31 31 31 31 31 31 31 31 31
'material zones x(26) '                      21 21 21 40 31 31 31 31 31 31 31 31 31 31 31
'material zones x(27) '                      31 40 21 21 21 21 21 21 21 21 21 21 21 21 21
'material zones x(28) '                      31 31 31 31 31 31 31 31 31 31 31 31 31 31 31
'thickness for 2d elements, specimen width'   25.4
'NONLIN: =1 for non-linear analysis'          0
'itnum: maximum number of iterations'         500
'R: 4 increment values'                       0.1 1. 0.001 1.
'nhtl: mechanical, temp, hygro - on(1),off(0)' 1 0 0
'htl: intl cond, temp, intl cond, hygro, disp' 450. 293. 0. 1.0 0.762

```

Example Abaqus/Standard[®] input file: `s_multi_gaps_linear.inp`

The FORTRAN routine *Jointmesh* discussed above generates Abaqus/Standard[®] input file (.inp) which can be used directly to perform a finite element analysis in Abaqus/Standard[®]. It is assumed that the reader is familiar with Abaqus/Standard[®] and the syntax used in the input file. The example input file is given to provide an overview of an entire analysis and assist the readers in creating their own analyses.

```

*HEADING
section - delta=6.35 mm, c=2.54 mm, multi gaps
units: mm, N, MPa
*NODE, NSET=NALL
    1 , 0.0000000E+00 , 76.20000 , 0.0000000E+00
    2 , 7.5000003E-02 , 76.20000 , 0.0000000E+00
    3 , 0.1500000 , 76.20000 , 0.0000000E+00
...
*NSET, NSET=NFORCE, GENERATE
    1 , 57 , 1
*NSET, NSET=NBOUNDL, GENERATE
    1 , 57 , 1
*NSET, NSET=NBOUNDR, GENERATE
    163021 , 163077 , 1
*ELEMENT, TYPE=CPS8 , ELSET=EALL
    1 , 1 , 115 , 117 , 3 ,
    58 , 116 , 60 , 2

```

```

      2 ,      115 ,      229 ,      231 ,      117 ,
    172 ,      230 ,      174 ,      116
...
...
*ELSET, ELSET=LY01, GENERATE
      1 ,      1430 ,      1
*ELSET, ELSET=LY01-01, GENERATE
      1 ,      146 ,      1
*ELSET, ELSET=LY01-02, GENERATE
     147 ,      171 ,      1
*ELSET, ELSET=LY01-03, GENERATE
     172 ,      234 ,      1
*ELSET, ELSET=LY01-04, GENERATE
     235 ,      259 ,      1
*ELSET, ELSET=LY01-05, GENERATE
     260 ,      403 ,      1
*ELSET, ELSET=LY01-06, GENERATE
     404 ,      499 ,      1
*ELSET, ELSET=LY01-07, GENERATE
     500 ,      595 ,      1
*ELSET, ELSET=LY01-08, GENERATE
     596 ,      835 ,      1
*ELSET, ELSET=LY01-09, GENERATE
     836 ,      931 ,      1
*ELSET, ELSET=LY01-10, GENERATE
     932 ,      1027 ,      1
*ELSET, ELSET=LY01-11, GENERATE
    1028 ,      1171 ,      1
*ELSET, ELSET=LY01-12, GENERATE
    1172 ,      1196 ,      1
*ELSET, ELSET=LY01-13, GENERATE
    1197 ,      1259 ,      1
*ELSET, ELSET=LY01-14, GENERATE
    1260 ,      1284 ,      1
*ELSET, ELSET=LY01-15, GENERATE
    1285 ,      1430 ,      1
*ELSET, ELSET=LY02, GENERATE
    1431 ,      2860 ,      1
*ELSET, ELSET=LY02-01, GENERATE
    1431 ,      1576 ,      1
*ELSET, ELSET=LY02-02, GENERATE
    1577 ,      1601 ,      1
*ELSET, ELSET=LY02-03, GENERATE
    1602 ,      1664 ,      1
*ELSET, ELSET=LY02-04, GENERATE
    1665 ,      1689 ,      1
*ELSET, ELSET=LY02-05, GENERATE
    1690 ,      1833 ,      1
*ELSET, ELSET=LY02-06, GENERATE
    1834 ,      1929 ,      1
*ELSET, ELSET=LY02-07, GENERATE
    1930 ,      2025 ,      1
*ELSET, ELSET=LY02-08, GENERATE
    2026 ,      2265 ,      1
*ELSET, ELSET=LY02-09, GENERATE
    2266 ,      2361 ,      1
*ELSET, ELSET=LY02-10, GENERATE
    2362 ,      2457 ,      1
*ELSET, ELSET=LY02-11, GENERATE
    2458 ,      2601 ,      1
*ELSET, ELSET=LY02-12, GENERATE
    2602 ,      2626 ,      1
*ELSET, ELSET=LY02-13, GENERATE
    2627 ,      2689 ,      1
*ELSET, ELSET=LY02-14, GENERATE
    2690 ,      2714 ,      1
*ELSET, ELSET=LY02-15, GENERATE
    2715 ,      2860 ,      1
...
...
*ELSET, ELSET=LY28-15, GENERATE

```

```

39895 ,      40040 ,      1
*BOUNDARY
NBOUNDR, 1, 2
NBOUNDL, 1, 1
*Initial Conditions, type=TEMPERATURE
NALL, 450.00000
*Initial conditions, type=field, variable=1
NALL, 0.00000
*MATERIAL, NAME=IM7/8552-0
*ELASTIC, TYPE=LAMINA
0.16052E+06, 14386. , 0.46700 , 5171.0 ,
*Expansion, type=ortho
-8.9999997E-07 , 2.8799999E-05 , 2.8799999E-05
*Expansion, type=ortho, field=1
0.0000000E+00 , 3.3100001E-03 , 3.3100001E-03
*ORIENTATION, NAME=LY0011, SYSTEM=RECTANGULAR, DEFINITION=COORDINATES
0.0000 , -1.00000 , 0.0000 , 1.00000 , 0.0000 , 0.0000 ,
3, 0.000
*MATERIAL, NAME=IM7/8552-90
*ELASTIC, TYPE=LAMINA
9809.0 , 12422. , 0.46100 , 3923.0 ,
*Expansion, type=ortho
2.8799999E-05 , 2.8799999E-05 , -8.9999997E-07
*Expansion, type=ortho, field=1
3.3100001E-03 , 3.3100001E-03 , 0.0000000E+00
*ORIENTATION, NAME=LY0021, SYSTEM=RECTANGULAR, DEFINITION=COORDINATES
0.0000 , -1.00000 , 0.0000 , 1.00000 , 0.0000 , 0.0000 ,
3, 0.000
*MATERIAL, NAME=IM7/8552-45
*ELASTIC, TYPE=LAMINA
32381. , 13810. , 0.46400 , 4547.0 ,
*Expansion, type=ortho
1.3900000E-05 , 2.8799999E-05 , 1.3900000E-05
*Expansion, type=ortho, field=1
1.6550000E-03 , 3.3100001E-03 , 1.6550000E-03
*ORIENTATION, NAME=LY0031, SYSTEM=RECTANGULAR, DEFINITION=COORDINATES
0.0000 , -1.00000 , 0.0000 , 1.00000 , 0.0000 , 0.0000 ,
3, 0.000
*MATERIAL, NAME=R8552
*ELASTIC, TYPE=ISOTROPIC
11380.00 , 0.3000000
*Expansion, type=iso
2.8799999E-05
*Expansion, type=iso, field=1
3.3100001E-03
*SOLID SECTION, ELSET=LY01-01, ORIENTATION=LY0031, MATERIAL=IM7/8552-45
25.40000 ,
*SOLID SECTION, ELSET=LY01-02, ORIENTATION=LY0031, MATERIAL=IM7/8552-45
25.40000 ,
*SOLID SECTION, ELSET=LY01-03, ORIENTATION=LY0031, MATERIAL=IM7/8552-45
25.40000 ,
*SOLID SECTION, ELSET=LY01-04, ORIENTATION=LY0031, MATERIAL=IM7/8552-45
25.40000 ,
*SOLID SECTION, ELSET=LY01-05, ORIENTATION=LY0031, MATERIAL=IM7/8552-45
25.40000 ,
*SOLID SECTION, ELSET=LY01-06, ORIENTATION=LY0031, MATERIAL=IM7/8552-45
25.40000 ,
*SOLID SECTION, ELSET=LY01-07, ORIENTATION=LY0031, MATERIAL=IM7/8552-45
25.40000 ,
*SOLID SECTION, ELSET=LY01-08, ORIENTATION=LY0031, MATERIAL=IM7/8552-45
25.40000 ,
*SOLID SECTION, ELSET=LY01-09, ORIENTATION=LY0031, MATERIAL=IM7/8552-45
25.40000 ,
*SOLID SECTION, ELSET=LY01-10, ORIENTATION=LY0031, MATERIAL=IM7/8552-45
25.40000 ,
*SOLID SECTION, ELSET=LY01-11, ORIENTATION=LY0031, MATERIAL=IM7/8552-45
25.40000 ,
*SOLID SECTION, ELSET=LY01-12, ORIENTATION=LY0031, MATERIAL=IM7/8552-45
25.40000 ,
*SOLID SECTION, ELSET=LY01-13, ORIENTATION=LY0031, MATERIAL=IM7/8552-45
25.40000 ,

```

```

*SOLID SECTION, ELSET=LY01-14, ORIENTATION=LY0031, MATERIAL=IM7/8552-45
 25.40000
,SOLID SECTION, ELSET=LY01-15, ORIENTATION=LY0031, MATERIAL=IM7/8552-45
 25.40000
,SOLID SECTION, ELSET=LY02-01, ORIENTATION=LY0021, MATERIAL=IM7/8552-90
 25.40000
,SOLID SECTION, ELSET=LY02-02, ORIENTATION=LY0021, MATERIAL=IM7/8552-90
 25.40000
,SOLID SECTION, ELSET=LY02-03, ORIENTATION=LY0021, MATERIAL=IM7/8552-90
 25.40000
,SOLID SECTION, ELSET=LY02-04, ORIENTATION=LY0021, MATERIAL=IM7/8552-90
 25.40000
,SOLID SECTION, ELSET=LY02-05, ORIENTATION=LY0021, MATERIAL=IM7/8552-90
 25.40000
,SOLID SECTION, ELSET=LY02-06, ORIENTATION=LY0021, MATERIAL=IM7/8552-90
 25.40000
,SOLID SECTION, ELSET=LY02-07, ORIENTATION=LY0021, MATERIAL=IM7/8552-90
 25.40000
,SOLID SECTION, ELSET=LY02-08, ORIENTATION=LY0021, MATERIAL=IM7/8552-90
 25.40000
,SOLID SECTION, ELSET=LY02-09, ORIENTATION=LY0021, MATERIAL=IM7/8552-90
 25.40000
,SOLID SECTION, ELSET=LY02-10, ORIENTATION=LY0021, MATERIAL=IM7/8552-90
 25.40000
,SOLID SECTION, ELSET=LY02-11, ORIENTATION=LY0021, MATERIAL=IM7/8552-90
 25.40000
,SOLID SECTION, ELSET=LY02-12, ORIENTATION=LY0021, MATERIAL=IM7/8552-90
 25.40000
,SOLID SECTION, ELSET=LY02-13, ORIENTATION=LY0021, MATERIAL=IM7/8552-90
 25.40000
,SOLID SECTION, ELSET=LY02-14, MATERIAL=R8552
 25.40000
,SOLID SECTION, ELSET=LY02-15, ORIENTATION=LY0021, MATERIAL=IM7/8552-90
 25.40000
,
...
...
*SOLID SECTION, ELSET=LY28-15, ORIENTATION=LY0031, MATERIAL=IM7/8552-45
 25.40000
,
*STEP
*STATIC
1.0000, 1.0000,
*BOUNDARY
NFORCE, 2, 2, 0.76200
*OUTPUT, FIELD, VARIABLE=PRESELECT, FREQ=1
*ELEMENT OUTPUT, ELSET=EALL
TEMP, FV1
*Output, history, VARIABLE=PRESELECT, freq=1
*NODE output, NSET=NBOUNDR
RF2
*NODE output, NSET=NFORCE
RF2
*NODE output, NSET=NBOUNDR
U2
*NODE output, NSET=NFORCE
U2
*END STEP

```

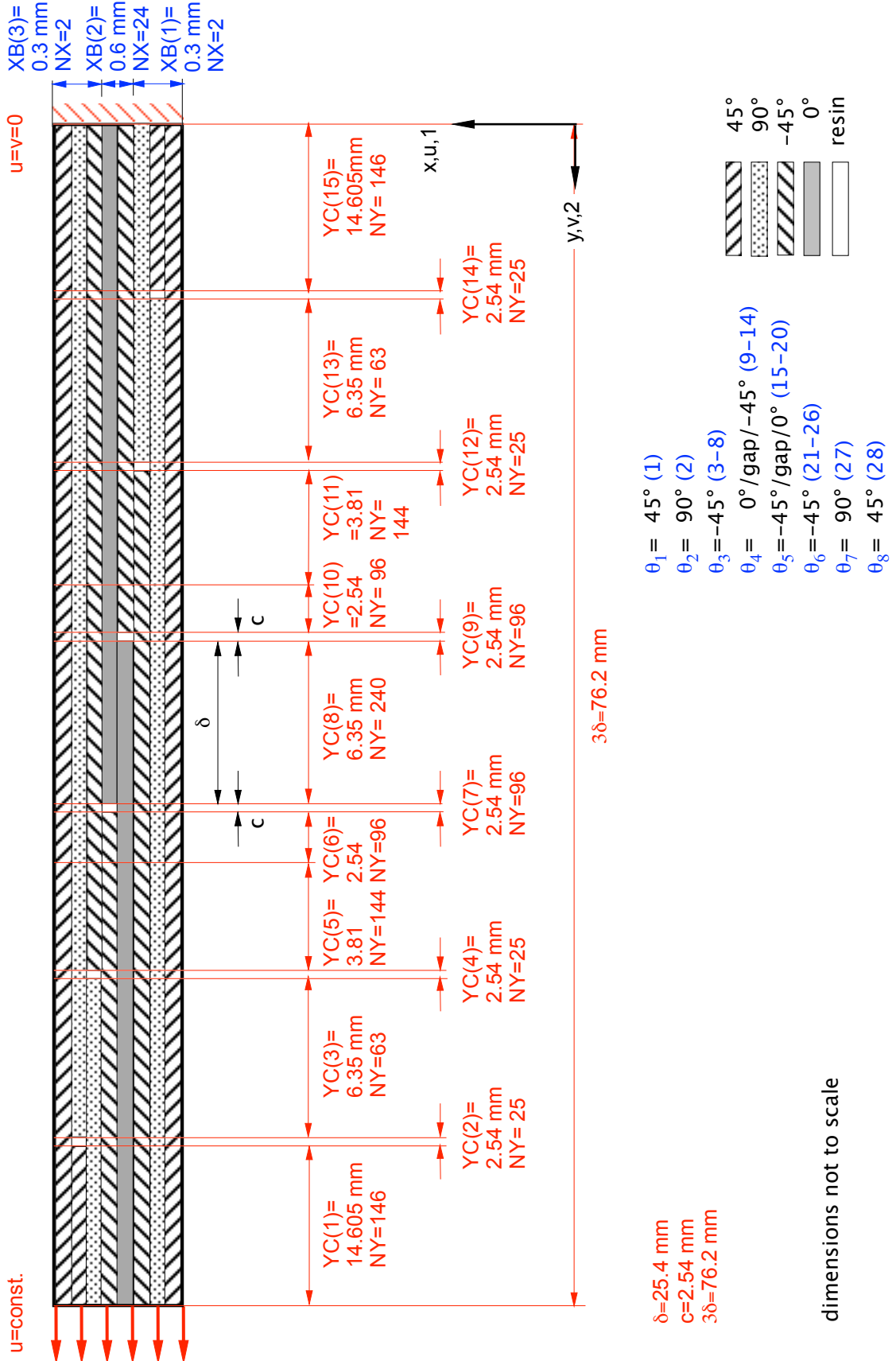
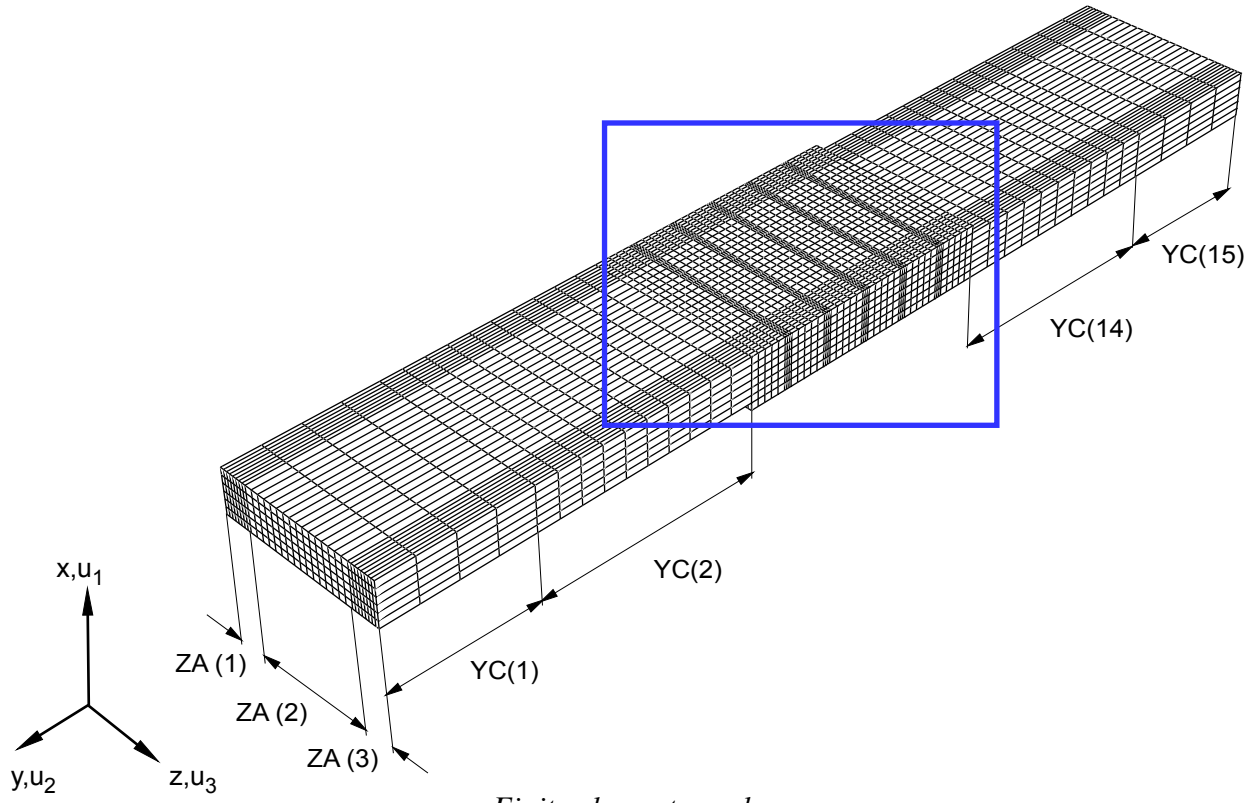
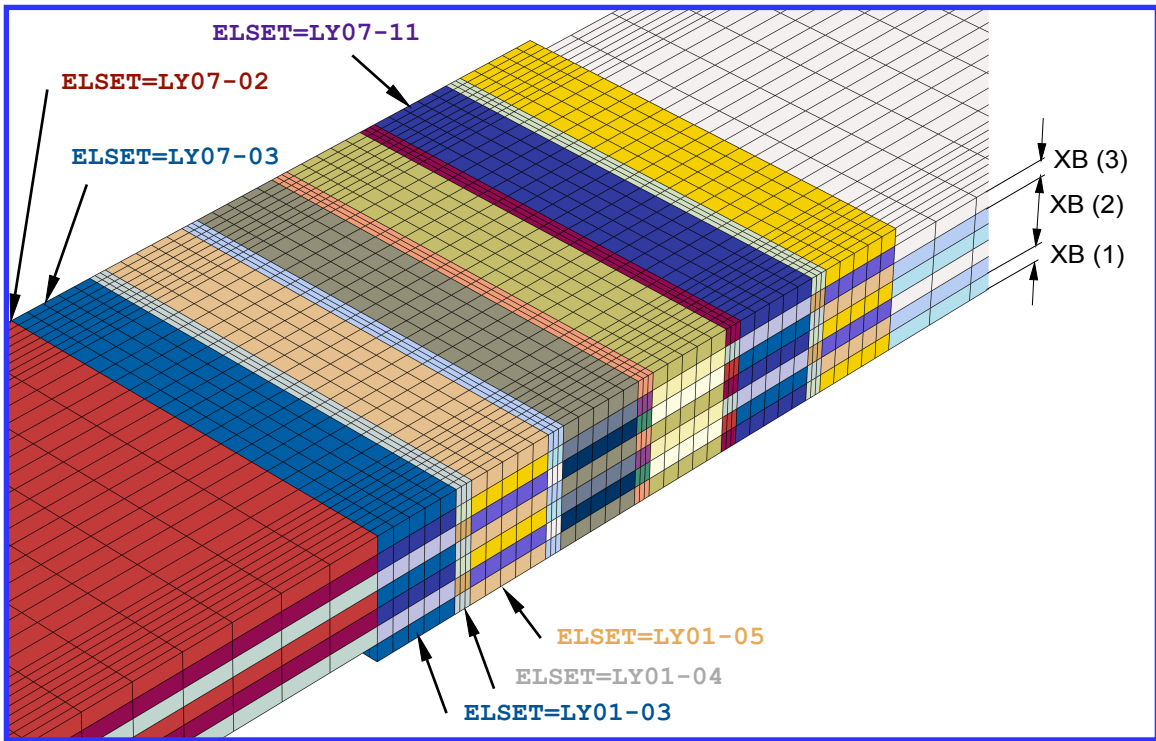


Figure B1. Example of input to user data file mesh_input.data.



a. Finite element mesh.



b. Detail of local zones.

Figure B2. Example of a three-dimensional model with element sets to define material properties.

REPORT DOCUMENTATION PAGE

*Form Approved
OMB No. 0704-0188*

The public reporting burden for this collection of information is estimated to average 1 hour per response, including the time for reviewing instructions, searching existing data sources, gathering and maintaining the data needed, and completing and reviewing the collection of information. Send comments regarding this burden estimate or any other aspect of this collection of information, including suggestions for reducing this burden, to Department of Defense, Washington Headquarters Services, Directorate for Information Operations and Reports (0704-0188), 1215 Jefferson Davis Highway, Suite 1204, Arlington, VA 22202-4302. Respondents should be aware that notwithstanding any other provision of law, no person shall be subject to any penalty for failing to comply with a collection of information if it does not display a currently valid OMB control number.
PLEASE DO NOT RETURN YOUR FORM TO THE ABOVE ADDRESS.

1. REPORT DATE (DD-MM-YYYY) 01-06-2014		2. REPORT TYPE Contractor Report		3. DATES COVERED (From - To)	
4. TITLE AND SUBTITLE Finite Element Analysis of Composite Joint Configurations With Gaps and Overlaps				5a. CONTRACT NUMBER NNL09AA00A	
				5b. GRANT NUMBER	
				5c. PROGRAM ELEMENT NUMBER	
6. AUTHOR(S) Krueger, Ronald				5d. PROJECT NUMBER	
				5e. TASK NUMBER	
				5f. WORK UNIT NUMBER 031102.02.07.05.9D67.13	
7. PERFORMING ORGANIZATION NAME(S) AND ADDRESS(ES) NASA Langley Research Center Hampton, VA 23681-2199				8. PERFORMING ORGANIZATION REPORT NUMBER NIA Report No. 2014-0619	
9. SPONSORING/MONITORING AGENCY NAME(S) AND ADDRESS(ES) National Aeronautics and Space Administration Washington, DC 20546-0001				10. SPONSOR/MONITOR'S ACRONYM(S) NASA	
				11. SPONSOR/MONITOR'S REPORT NUMBER(S) NASA/CR-2014-218284	
12. DISTRIBUTION/AVAILABILITY STATEMENT Unclassified - Unlimited Subject Category 24 Availability: NASA CASI (443) 757-5802					
13. SUPPLEMENTARY NOTES Langley Technical Monitor: Jonathan B. Ransom					
14. ABSTRACT The goal of the current study is to identify scenarios for which thermal and moisture effects become significant in the loading of a composite structure. In the current work, a simple configuration was defined, and material properties were selected. A Fortran routine was created to automate the mesh generation process. The routine was used to create the models for the initial mesh refinement study. A combination of element length and width suitable for further studies was identified. Also, the effect of the overlap length and gap length on computed shear and through-thickness stresses along the bondline of the joints was studied for the mechanical load case. Further, the influence of neighboring gaps and overlaps on these joint stresses was studied and was found to be negligible. The results suggest that for an initial study it is sufficient to focus on one configuration with fixed overlap and gap lengths to study the effects of mechanical, thermal and moisture loading and combinations thereof on computed joint stresses.					
15. SUBJECT TERMS Composites; Finite element analysis; Joints; Ply overlaps					
16. SECURITY CLASSIFICATION OF:			17. LIMITATION OF ABSTRACT	18. NUMBER OF PAGES	19a. NAME OF RESPONSIBLE PERSON
a. REPORT	b. ABSTRACT	c. THIS PAGE			STI Help Desk (email: help@sti.nasa.gov)
U	U	U	UU	60	19b. TELEPHONE NUMBER (Include area code) (443) 757-5802